

21  
August 1983  
Final Report  
Phase II

DOT HS 806 656



U.S. Department  
of Transportation  
National Highway  
Traffic Safety  
Administration

---

Test Device and Test Procedure to Assess Side Structures  
Volume III -- Appendices A - D

Dynamic Science, Inc.  
1850 West Pinnacle Peak Road  
Phoenix, Arizona 85027

Contract No. DOT HS-8-01933 (II)

**TECHNICAL REPORT STANDARD TITLE PAGE**

1. Report No. DOT HS 806 656		2. Government Accession No.		3. Recipient's Catalog No.	
4. Title and Subtitle TEST DEVICE AND TEST PROCEDURE TO ASSESS SIDE STRUCTURES - PHASE II FINAL REPORT. VOLUME III - APPENDICES A - D				5. Report Date August 1983	
				6. Performing Orgn Code	
7. Author(s) R. Garn, S. Davis, M. Rodack, N. Johnson				8. Performing Orgn Rpt No. 8327-83-032/2090	
9. Performing Organization Name and Address Dynamic Science, Inc. An Exodyne Company 1850 West Pinnacle Peak Road Phoenix, Arizona 85027				10. Work Unit No.	
				11. Contract or Grant No. DOT-HS-8-01933(II)	
				13. Type of Report and Period Covered FINAL REPORT September 1979 - August 1983	
12. Sponsoring Agency Name and Address U.S. Department of Transportation National Highway Traffic Safety Administration 400 Seventh Street, S.W. Washington, D.C. 20590				14. Sponsoring Agency Code	
15. Supplementary Notes Carl L. Ragland, NHTSA Contract Technical Manager (NRD-12)					
16. Abstract  A deformable moving barrier (Side Impactor) was developed to evaluate passenger vehicle side structures in front-to-side collisions. Force-deflection properties were determined for production vehicles in 0° and 30° frontal impacts and used to establish the design stiffness of the side impactor's deformable face. Verification of side impactor stiffness was accomplished through load cell barrier testing and side impactor-to-car testing, using two prototype side impact dummies. Data obtained from Side Impactor-to-car and car-to-car side impacts were used for comparative analyses, and it was concluded that the Side Impactor reasonably duplicated the target vehicle damage and dummy response in reference car-to-car impacts.					
17. Key Words Side Impactor, Side Structure, Crash Tests			18. Distribution Statement Document is available to the public through the National Highway Technical Information Service, Springfield, Virginia 22161		
19. Security Classif. (of this report) Unclassified		20. Security Classif. (of this page) Unclassified		21. No. Pages 149	22. Price

# METRIC CONVERSION FACTORS

## Approximate Conversions to Metric Measures

Symbol	When You Know	Multiply by	To Find	Symbol
L F N G I H				
in	inches	2.5	centimeters	cm
ft	feet	30	centimeters	cm
yd	yards	0.9	meters	m
mi	miles	1.6	kilometers	km
AREA				
m <sup>2</sup>	square inches	6.5	square centimeters	cm <sup>2</sup>
ft <sup>2</sup>	square feet	0.09	square meters	m <sup>2</sup>
yd <sup>2</sup>	square yards	0.8	square meters	m <sup>2</sup>
mi <sup>2</sup>	square miles	2.6	square kilometers	km <sup>2</sup>
	acres	0.4	hectares	ha
MASS (weight)				
oz	ounces	28	grams	g
lb	pounds	0.45	kilograms	kg
	short tons (2000 lb)	0.9	metric ton	t
VOLUME				
tsp	teaspoons	5	milliliters	ml
Tbsp	tablespoons	15	milliliters	ml
in <sup>3</sup>	cubic inches	16	milliliters	ml
fl oz	fluid ounces	30	milliliters	ml
c	cups	0.24	liters	L
pt	pints	0.47	liters	L
qt	quarts	0.95	liters	L
gal	gallons	3.8	liters	L
ft <sup>3</sup>	cubic feet	0.03	cubic meters	m <sup>3</sup>
yd <sup>3</sup>	cubic yards	0.76	cubic meters	m <sup>3</sup>
TEMPERATURE (exact)				
°F	degrees Fahrenheit	5/9 (after subtracting 32)	degrees Celsius	°C

## Approximate Conversions from Metric Measures

Symbol	When You Know	Multiply by	To Find	Symbol
L F N G I H				
mm	millimeters	0.04	inches	in
cm	centimeters	0.4	inches	in
m	meters	3.3	feet	ft
m	meters	1.1	yards	yd
km	kilometers	0.6	miles	mi
AREA				
cm <sup>2</sup>	square centimeters	0.16	square inches	in <sup>2</sup>
m <sup>2</sup>	square meters	1.2	square yards	yd <sup>2</sup>
km <sup>2</sup>	square kilometers	0.4	square miles	mi <sup>2</sup>
ha (10,000 m <sup>2</sup> )	hectares	2.5	acres	
MASS (weight)				
g	grams	0.035	ounces	oz
kg	kilograms	2.2	pounds	lb
t (1000 kg)	metric ton	1.1	short tons	
VOLUME				
ml	milliliters	0.03	fluid ounces	fl oz
mL	milliliters	0.06	cubic inches	in <sup>3</sup>
l	liters	2.1	pints	pt
L	liters	1.06	quarts	qt
l	liters	0.26	gallons	gal
m <sup>3</sup>	cubic meters	35	cubic feet	ft <sup>3</sup>
m <sup>3</sup>	cubic meters	1.3	cubic yards	yd <sup>3</sup>
TEMPERATURE (exact)				
°C	degrees Celsius	9/5 (then add 32)	degrees Fahrenheit	°F

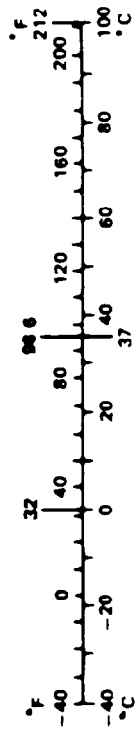


**TABLE OF CONTENTS**  
**VOLUME III**

	<u>Page</u>
APPENDIX A - ANALYSIS OF 30-DEGREE ANGLE IMPACT TEST DATA . . . . .	A-1
APPENDIX B - NHTSA METHOD FOR SIMULATING TWO-VEHICLES- MOVING COLLISIONS . . . . .	B-1
APPENDIX C - MGA BARRIER WEIGHT ANALYSIS REPORT . . . . .	C-1
APPENDIX D - MGA OCCUPANT INJURY ANALYSIS REPORT . . . . .	D-1

## APPENDIX A

### Analysis of 30-Degree Angle Impact Test Data

#### A.1 INTRODUCTION

Because of the angular configuration of the test vehicles during a 30-degree angle frontal impact, the accelerometers mounted on the vehicles are not aligned in a common coordinate system. All displacement (crush) and force data must therefore be resolved either in the initial direction of the Test Device or of the target vehicle. The following sections describe the techniques used to resolve the force/displacement data in the direction of either vehicle.

#### A.2 STATIC CRUSH OF TARGET VEHICLE

##### A.2.1 Crush in Direction of Target Vehicle

A pre-test profile of the target vehicle was obtained by measuring from a fixed referenced plane in front of the vehicle to pre-determined reference points on the front face of the vehicle. All measurements were made parallel to the target vehicle centerline. The post-test profile was determined by measuring from the same reference plane through the pre-test reference points to the front face of the vehicle. All measurements are, again, parallel to the target vehicle centerline. The static crush at each point is the axial difference between pre- and post-test measurements.

The pre- and post-test profiles of the Side Impactor in Test 8321-4.04 (conducted during Phase I of the program) are shown in Figure A-1. These profiles were generated from the pre- and post-test measurements described above.

The maximum static crush in the direction of the target vehicle was determined graphically. A straight line was drawn on the post-test profile from the centerline post-test position to the post-test position of the impact point (as shown in Figure A-1, Bumper Level). This line represents the crush plane of the vehicle. A line, parallel to the vehicle centerline, was drawn

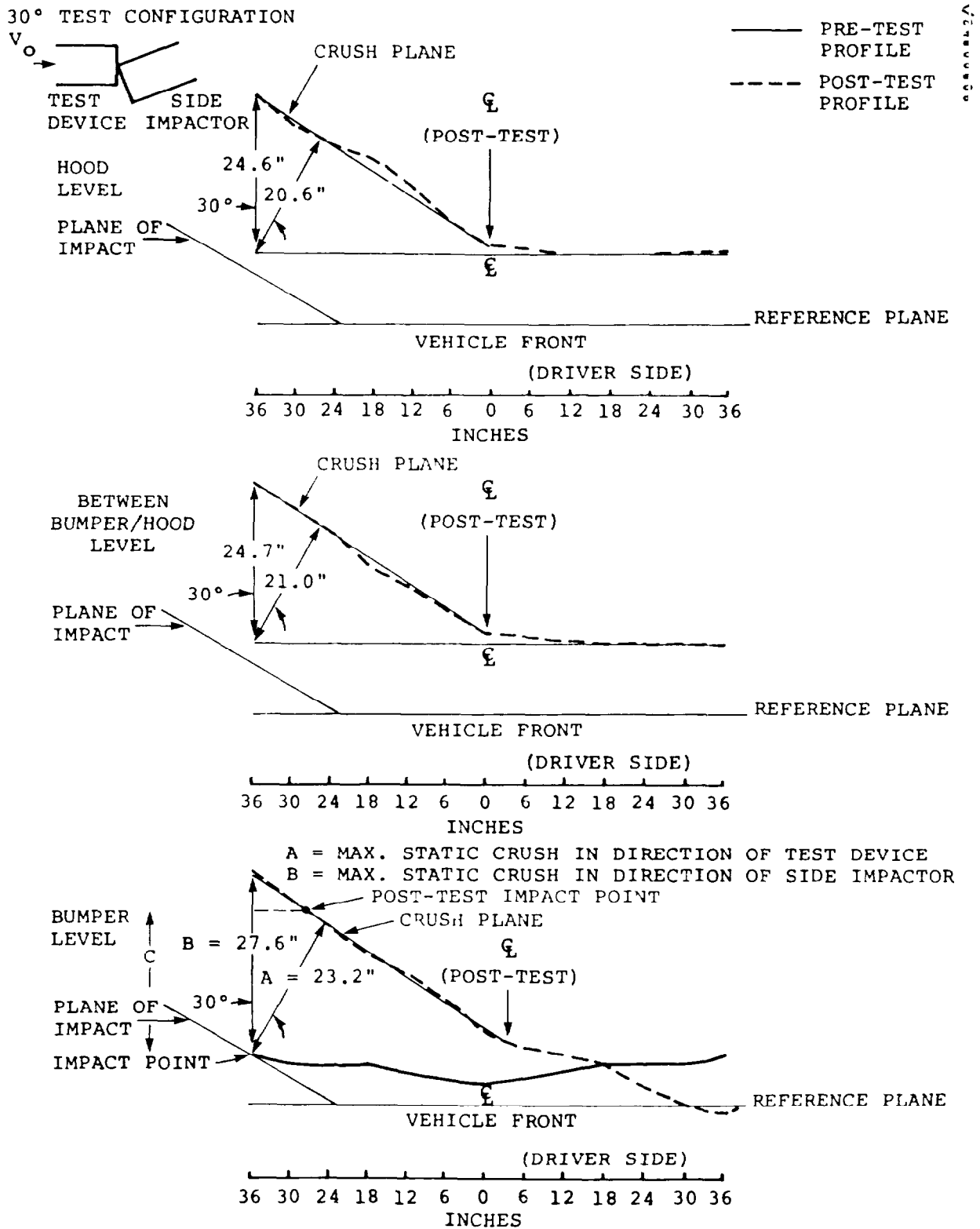


FIGURE A-1. PRE- AND POST-TEST PROFILES AT HOOD, MID, AND BUMPER LEVELS OF SIDE IMPACTOR (TEST 8321-4.04).

from the pre-test impact point to the crush plane. The dimension corresponding to this line (B) is considered the maximum static crush along the edge of the target vehicle.

The maximum static crush of the Side Impactor in Test 4.04 was determined graphically as 27.6 inches. This corresponds to a post-test measured value of 28.1 inches.

#### **A.2.2 Crush in Direction of Test Device (LCMB)**

The maximum post-test crush in the direction of the Test Device (LCMB) was also determined graphically. A 30-degree line from the initial impact point was drawn to the line representing the crush plane of the target vehicle (see Figure A-1). The dimension represented by this line (A) is considered as the maximum static crush in the direction of the Test Device. The crush was thus determined to be 23.2 inches in Test 4.04.

As might be expected, the impact point on the Side Impactor moved rearward along a line nearly parallel to the 30-degree line of the Test Device initial impact direction. The measured distance between the pre- and post-test positions of the impact point on the Side Impactor was 24.5 inches as compared to the 23.2 inches of static crush determined graphically in the direction of the Test Device.

#### **A.2.3 Longitudinal Displacement of Impact Point**

Another measure of crush in the direction of the target vehicle can be defined as being equal to the displacement of the impact point parallel to the target vehicle longitudinal axis. This dimension was also determined graphically, as shown by line C in Figure A-1.

### **A.3 MUTUAL DISPLACEMENT (CRUSH)**

#### **A.3.1 Displacement From Accelerometer Data**

##### **A.3.1.1 Displacement In Direction of Test Device**

The configuration of the two test vehicles in a 30-degree left front impact is shown in Figure A-2. The relative geometry

$A_x$  = LONGITUDINAL ACCELERATION OF TARGET VEHICLE  
 $A_y$  = LATERAL ACCELERATION OF TARGET VEHICLE  
 $A_R$  = RESULTANT ACCELERATION OF TARGET VEHICLE  
 $A_{R'}$  = COMPONENT OF RESULTANT ACCELERATION IN DIRECTION OF TEST TRACK

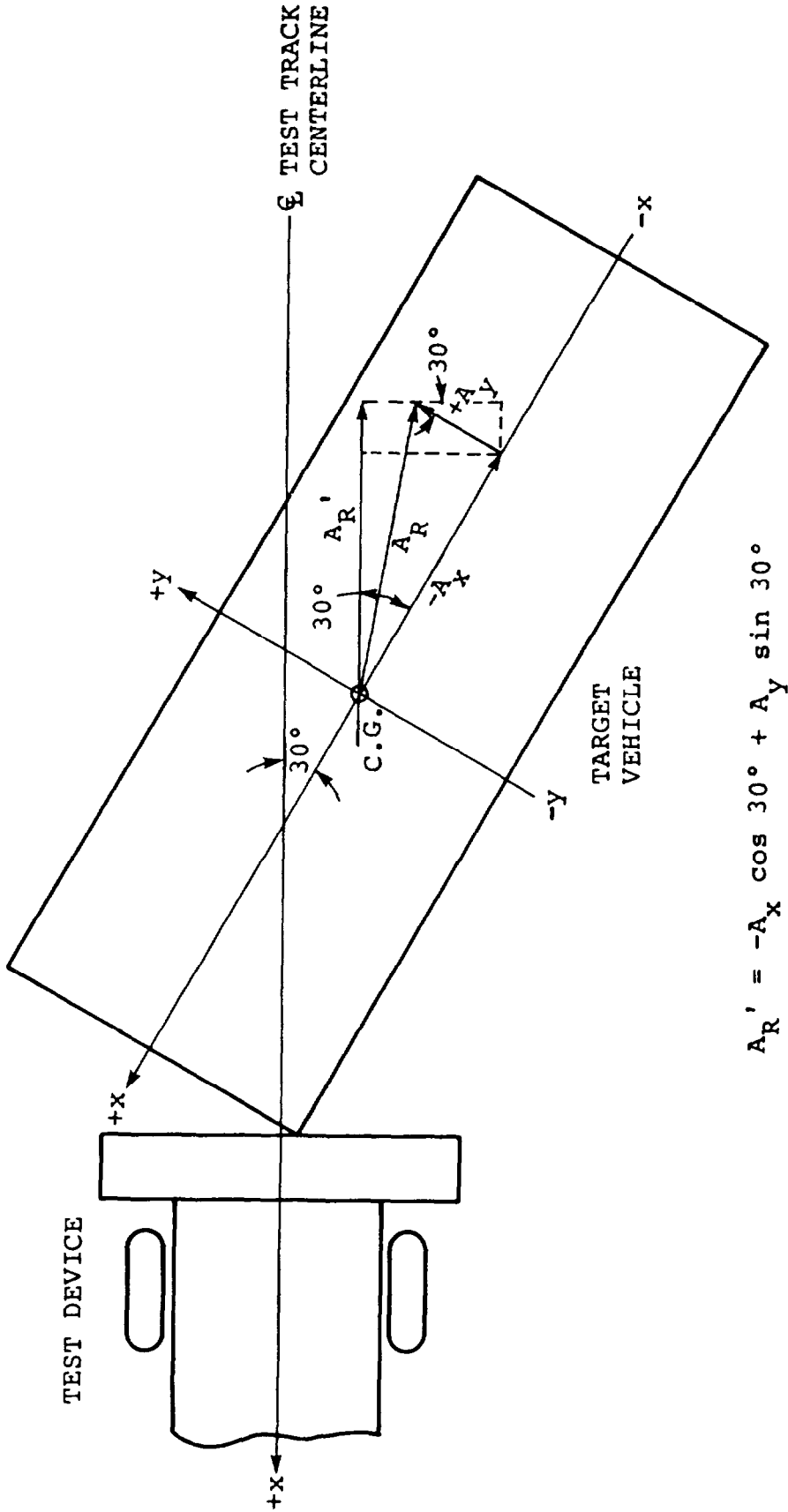


FIGURE A-2. RELATIVE GEOMETRY OF TARGET VEHICLE ACCELERATION COMPONENTS AND TEST TRACK.

of the longitudinal and lateral accelerations measured on the target vehicle with respect to the test track (i.e., the direction of the initial velocity of the Test Device) is also shown in Figure A-2. This is the direction in which the target vehicle acceleration and crush was to be calculated.

The component of the target vehicle resultant acceleration in the direction of the test track is shown as the vector  $A_R'$  in Figure A-2. From this figure it can be seen that

$$A_R' = -A_x \cos 30^\circ + A_y \sin 30^\circ \quad (A.1)$$

The relationship in A.1 will be valid throughout the entire impact sequence if the vehicles do not rotate around their centers of gravity. Thus, at any time, the displacement of the target vehicle along the test track may be found by treating the displacements obtained from the accelerometer data according to Equation A.1. Subtracting the target vehicle displacement from the Test Device displacement will yield the mutual relative displacement (i.e., crush). Thus

$$\text{Crush}_{TD} = S_{xTD} + S_{xTV} \cos 30^\circ - S_{yTV} \sin 30^\circ \quad (A.2)$$

where  $\text{Crush}_{TD}$  = crush in direction of Test Device

$S_{xTD}$  = longitudinal displacement of Test Device

$S_{xTV}$  = longitudinal displacement of target vehicle

$S_{yTV}$  = lateral displacement of target vehicle

The same relationship holds for a 30-degree right front corner impact except that the lateral acceleration of the target vehicle will be negative instead of positive. Thus, for a right front impact, the crush is given by

$$\text{Crush}_{TD} = S_{xTD} + S_{xTV} \cos 30^\circ + S_{yTV} \sin 30^\circ \quad (A.3)$$

### A.3.1.2 Displacement In Direction of Target Vehicle

The maximum crush in the direction of the target vehicle is obtained by dividing the crush in the direction of the Test Device by  $\cos 30^\circ$ . Thus, for a left front impact,

$$\text{Crush}_{TV} = S_{xTD}/\cos 30^\circ + S_{xTV} - S_{yTV} \tan 30^\circ \quad (\text{A.4})$$

and for a right front impact,

$$\text{Crush}_{TV} = S_{xTD}/\cos 30^\circ + S_{xTV} + S_{yTV} \tan 30^\circ \quad (\text{A.5})$$

### **A.3.2 Displacement From Film Data**

#### **A.3.2.1 Displacement Not Corrected for Rotation**

Displacement data was obtained from two cameras, one on each side of the test track, and averaged to obtain the mutual relative displacement in the direction of the Test Device. The average was divided by  $\cos 30^\circ$  to obtain the maximum displacement in the direction of the target vehicle.

#### **A.3.2.2 Displacement Corrected for Rotation**

The film data can be corrected for the rotation of the vehicles. However, the rotation is small during the impact event, as shown by the film analysis presented in Figure A-3. Therefore, rotation corrections are not usually necessary. For this analysis, however, rotation corrections were applied to determine their effect on the data. Comparison of curves 1 and 2 in Figure A-4 shows that there is little difference in the data up to the point of maximum crush.

### **A.3.3 Correction to Static Crush Level**

The mutual crush values were corrected to the measured post-test static crush level by the following method:

1. Determine the time of vehicle separation from film analysis.
2. Determine the correction factor by dividing the maximum static crush by the dynamic crush at the time of separation.
3. Multiply all dynamic crush values by this correction factor.

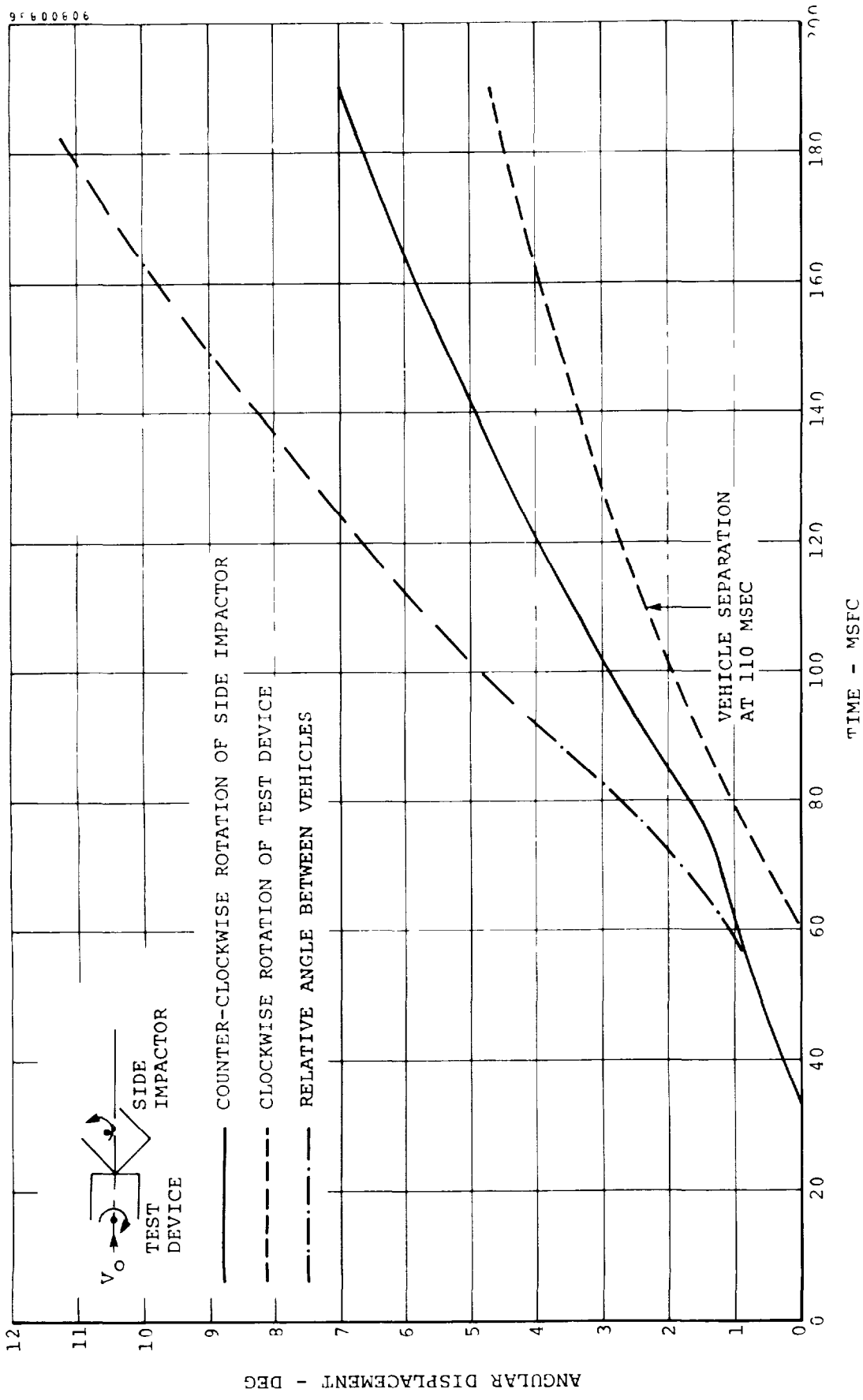


FIGURE A-3. ANGULAR DISPLACEMENT VERSUS TIME FROM FILM DATA - NHTSA MOVING TEST DEVICE AND SIDE IMPACTOR (TEST 8321-4.04).

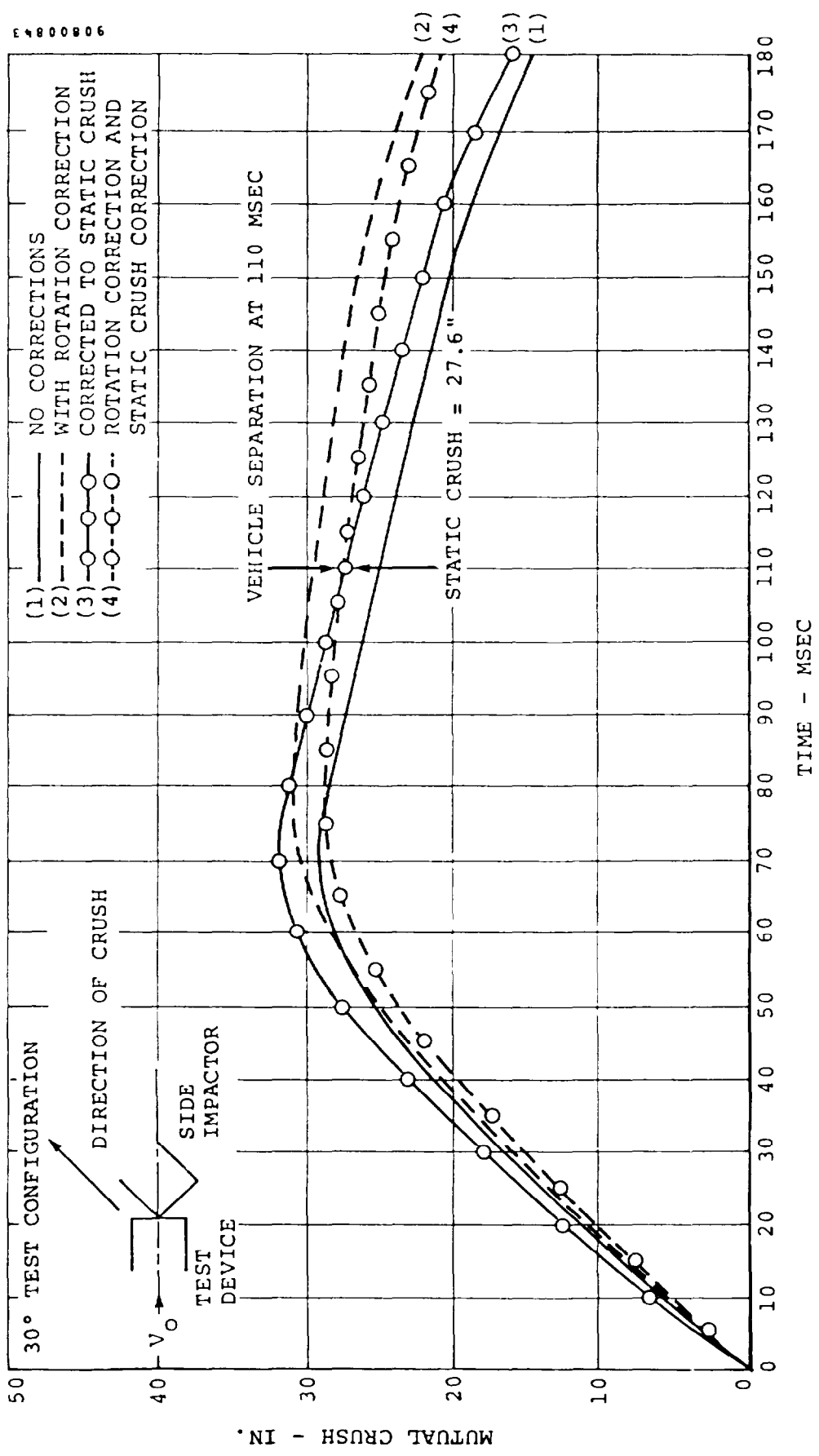


FIGURE A-4. MUTUAL CRUSH FROM FILM DATA IN DIRECTION OF SIDE IMPACTOR (TEST 8321-4.04).

This method was applied to the dynamic mutual displacements in the Test Device direction and the target vehicle direction. The effects of the static crush corrections on the film data may be seen in curves 3 and 4 of Figure A-4.

The effects of the static crush corrections, as well as rotation corrections, on the dynamic crush obtained from the accelerometer data are shown in Figure A-5. It can be seen from this figure that the rotation corrections have less effect on accelerometer data than do the static crush corrections. This might be expected since the accelerometer crush values are obtained from two accelerometers which are mutually perpendicular. As the vehicle rotates, the lessening acceleration vector of one accelerometer is partially compensated for by an increase in the acceleration vector of the other. Thus, the relationships derived in Section A.2.1 are reasonably valid and rotation corrections need not be applied to the accelerometer data.

#### **A.4 FORCE/DEFLECTION DATA**

Force/deflection data may also be determined in the direction of either the Test Device or the target vehicle. The forces may be those registered by the Test Device load cells or the inertial forces calculated from the accelerometers on the Test Device or on the target vehicle. When determining forces in the direction of the target vehicle, the load cell readings must be multiplied by  $\cos 30^\circ$ . Figure A-6 presents these curves in the direction of the target vehicle for Test 4.04.

The total force is the sum of all load cells on the Test Device. The lower region load is obtained by summing the loads in rows A and B, while the upper region load is obtained by summing rows C and D. The loads thus obtained for Test 4.04, in the direction of the Side Impactor, are shown in Figure A-7.

Force/deflection curves were obtained by cross-plotting the force and deflection data. The deflection data is that obtained from the accelerometers with the static crush correction applied. These curves may be generated in the direction of the Test Device or in the direction of the target vehicle, as shown in Figure A-8.

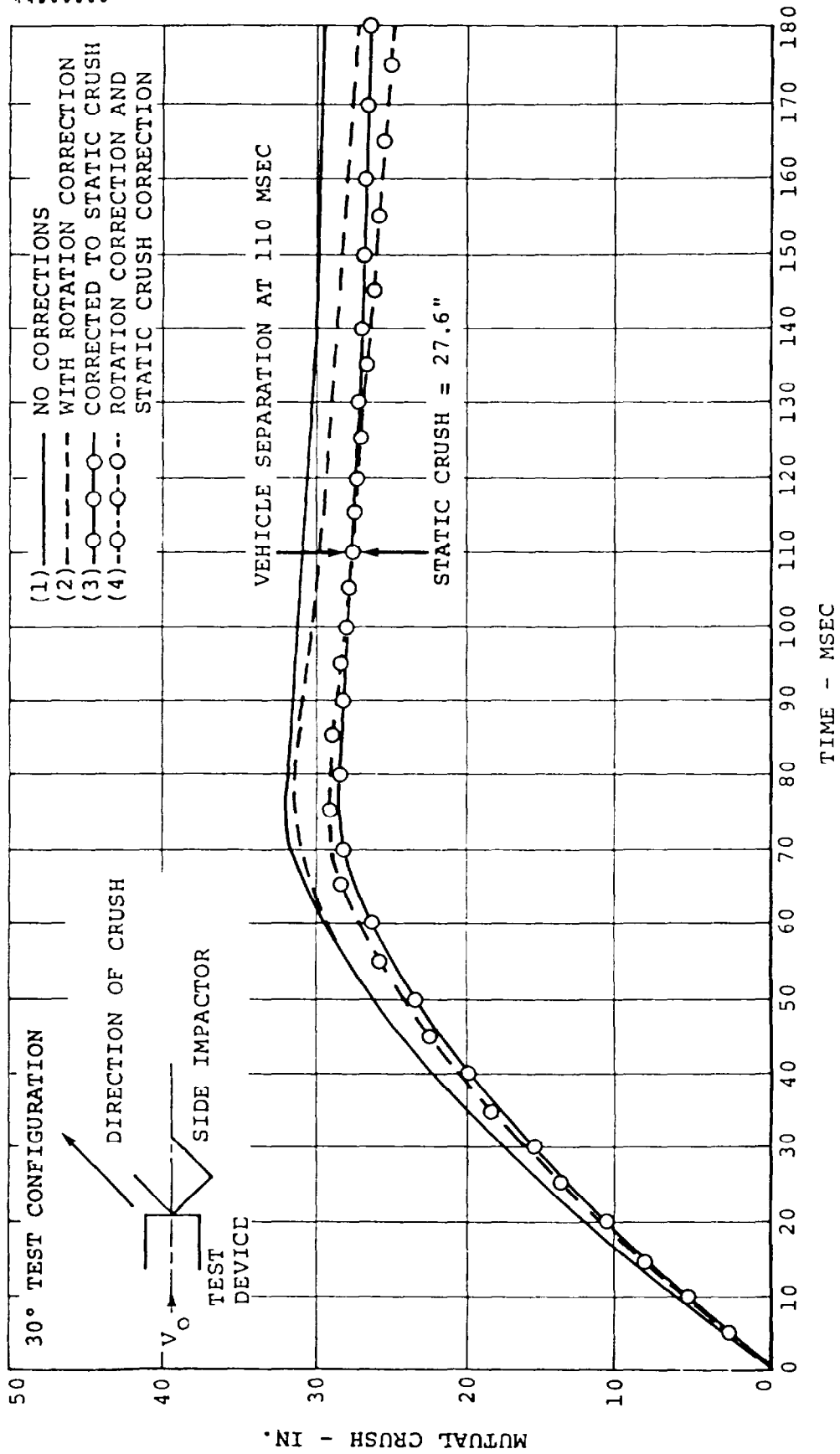


FIGURE A-5. MUTUAL CRUSH FROM ACCELEROMETER DATA IN DIRECTION OF SIDE IMPACTOR (TEST 8321-4.04).

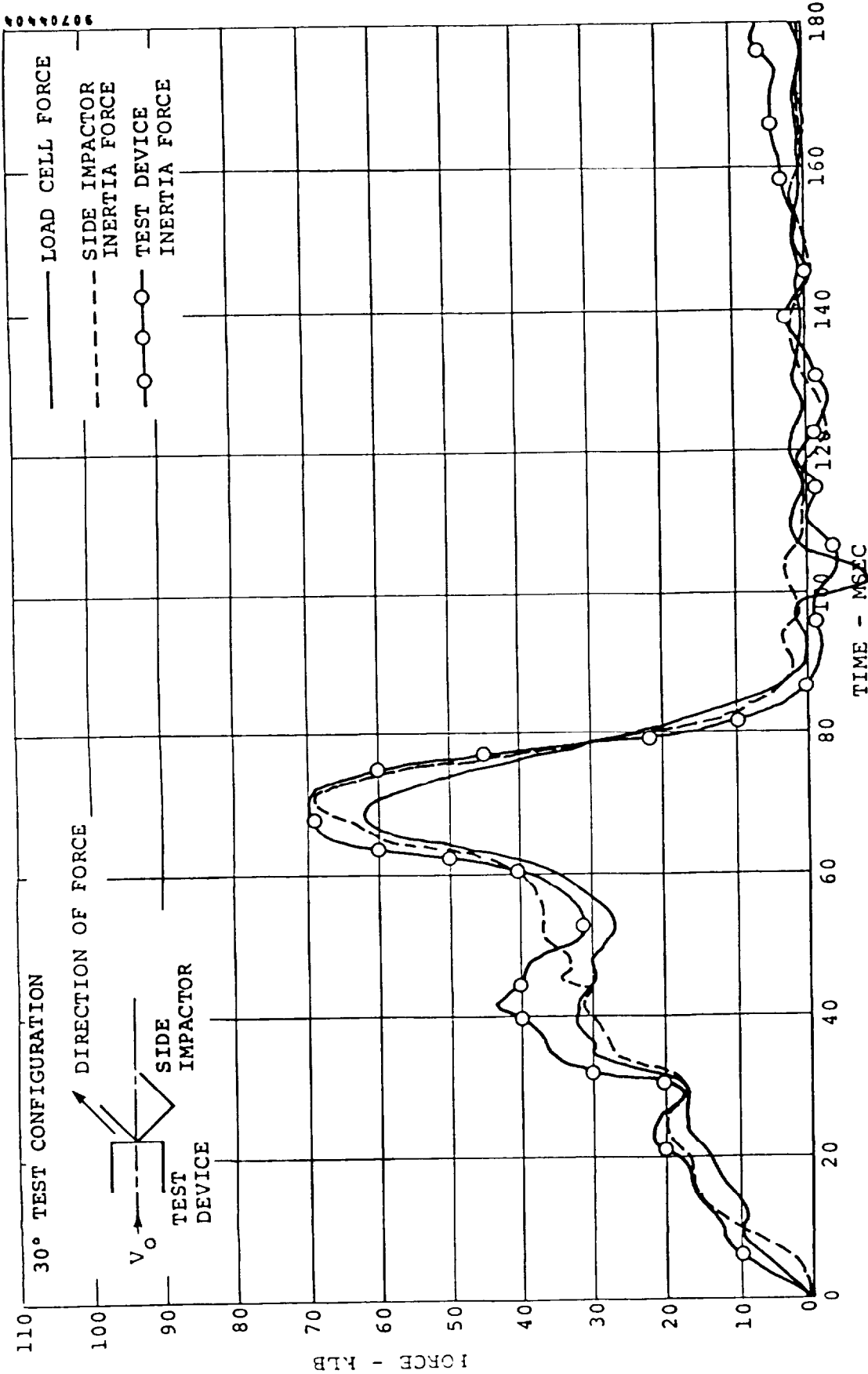


FIGURE A-6. COMPARISON OF TOTAL FORCE FROM LOAD CELL AND VEHICLE ACCELEROMETER DATA IN THE DIRECTION OF THE SIDE IMPACTOR (TEST 8321-4.04).

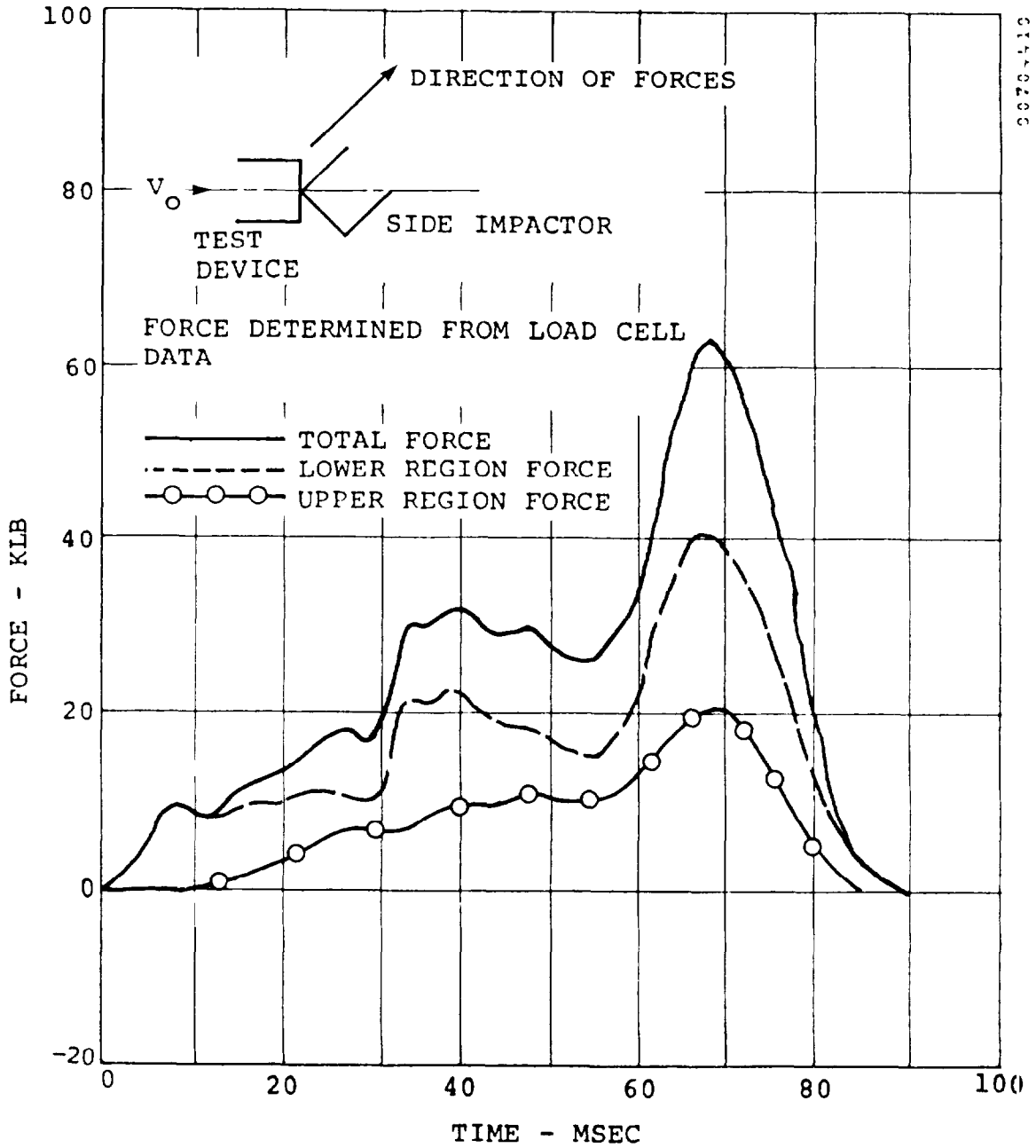


FIGURE A-7. LOWER REGION, UPPER REGION, AND TOTAL FORCE VERSUS TIME IN DIRECTION OF SIDE IMPACTOR (TEST 8321-4.04).

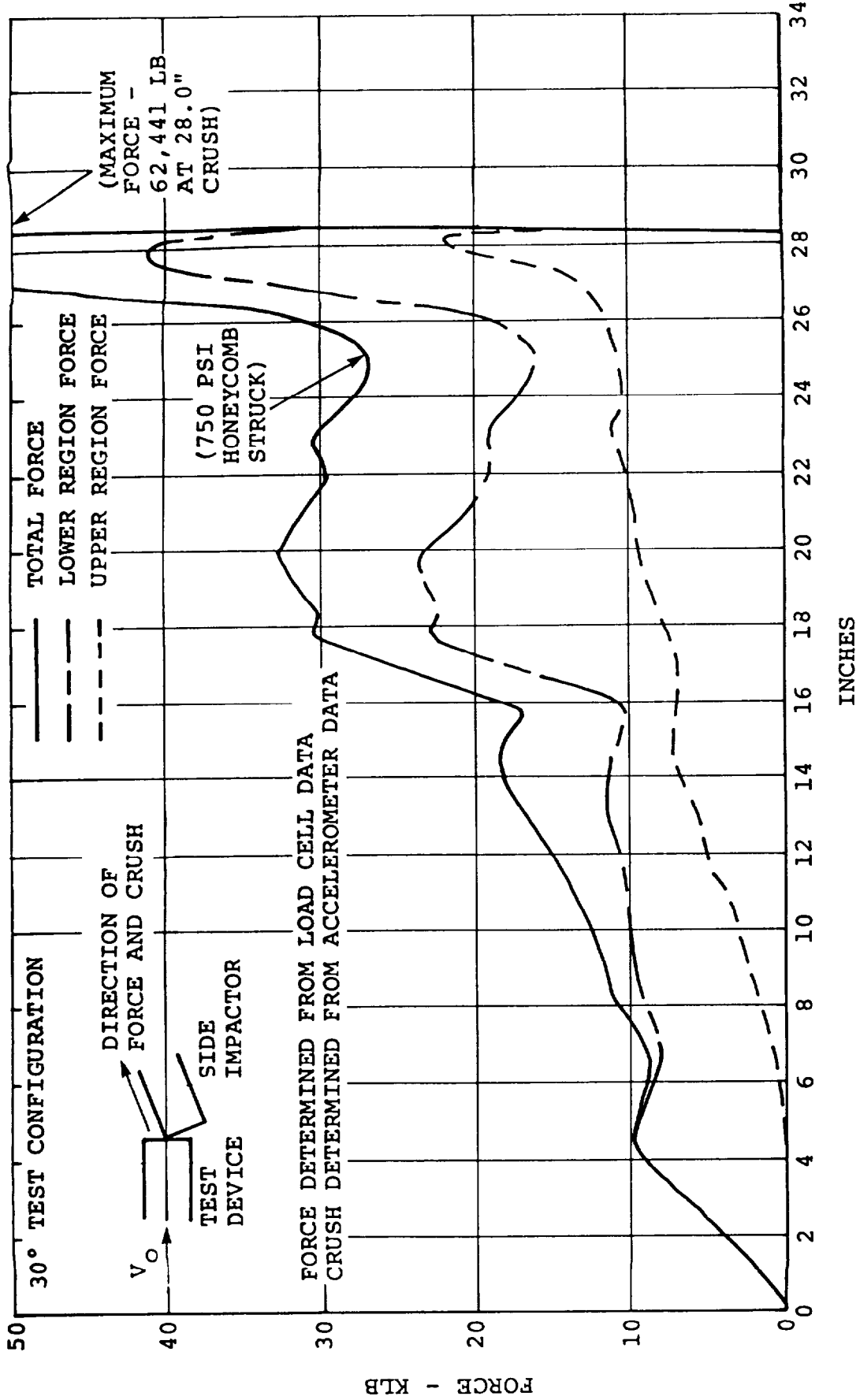


FIGURE A-8. LOWER REGION, UPPER REGION, AND TOTAL FORCE VERSUS CRUSH IN DIRECTION OF SIDE IMPACTOR (TEST 8321-4.04).

**APPENDIX B**  
NHTSA METHOD FOR SIMULATING  
TWO-VEHICLES-MOVING COLLISIONS

**B.1 INTRODUCTION**

This appendix presents an analysis of the method proposed by the NHTSA for simulating a two-vehicle collision in which both are moving by means of a crash test in which one vehicle (the target) is held stationary (see Reference, Section B.4). In this method the bullet vehicle is mounted on a set of auxiliary wheels and towed into the target vehicle. The longitudinal axis of the bullet vehicle is held at an angle ( $\alpha$ ) to the direction of the tow track. This is shown in Figure B-1. The purpose of this analysis was to supply a set of curves which could be used to choose the required orientation ( $\alpha, \phi$ ) of the bullet and target vehicles with respect to the tow track and the required tow velocity ( $V_R$ ).

**B.2 MATHEMATICAL ANALYSIS**

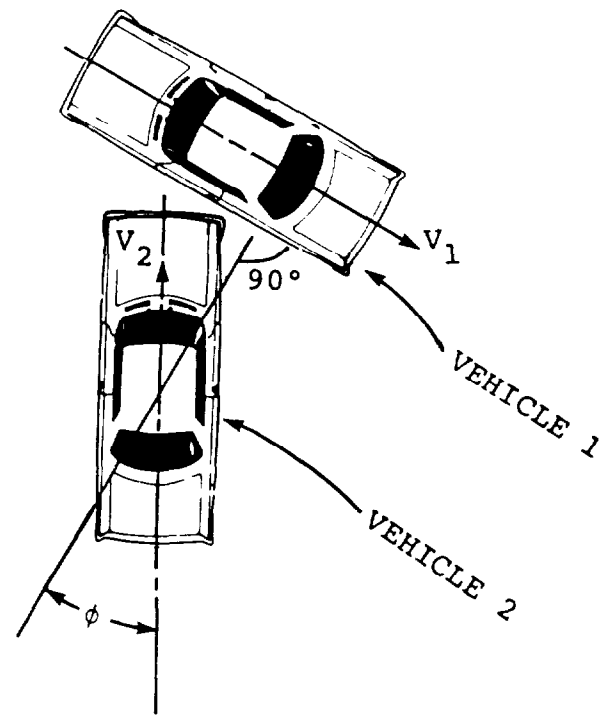
The fundamental requirements of this simulation method are that the principal directions of force with respect to the bullet and target vehicles be unchanged, and that the magnitude of the relative velocity of the two vehicles remains the same as in the two-car-moving case.

Figure B-2 shows the relevant geometry, using the nomenclature indicated in Figure B-1. Using the law of sines for the triangle OAB is evident that

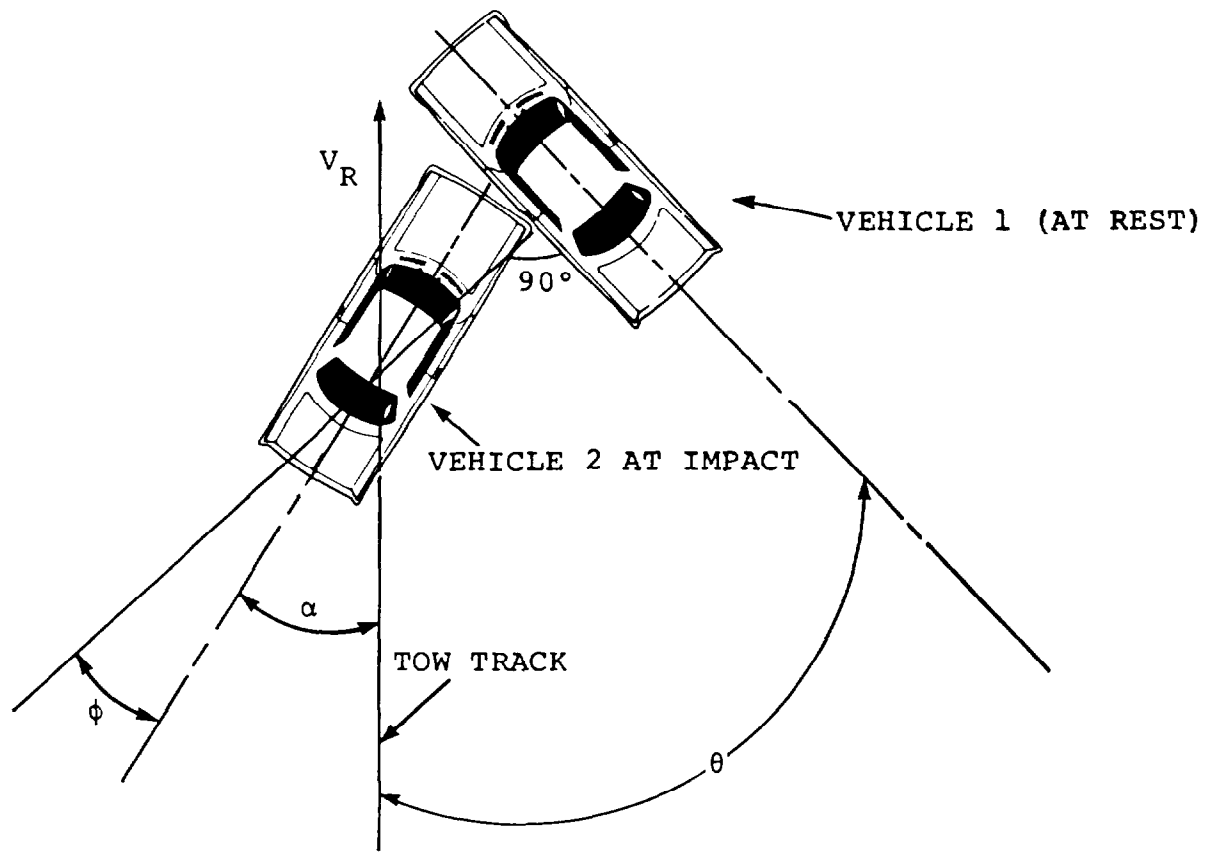
$$\frac{V_1}{\sin \alpha} = \frac{V_2}{\sin \theta} \quad (1)$$

Since the angles are related by:

$$\begin{aligned} \psi &= 90 + \phi \\ \delta &= \psi + \alpha \\ \theta &= 180 - \delta \\ \alpha &= 90 - (\phi + \theta) \end{aligned}$$



a) Collision to be Simulated

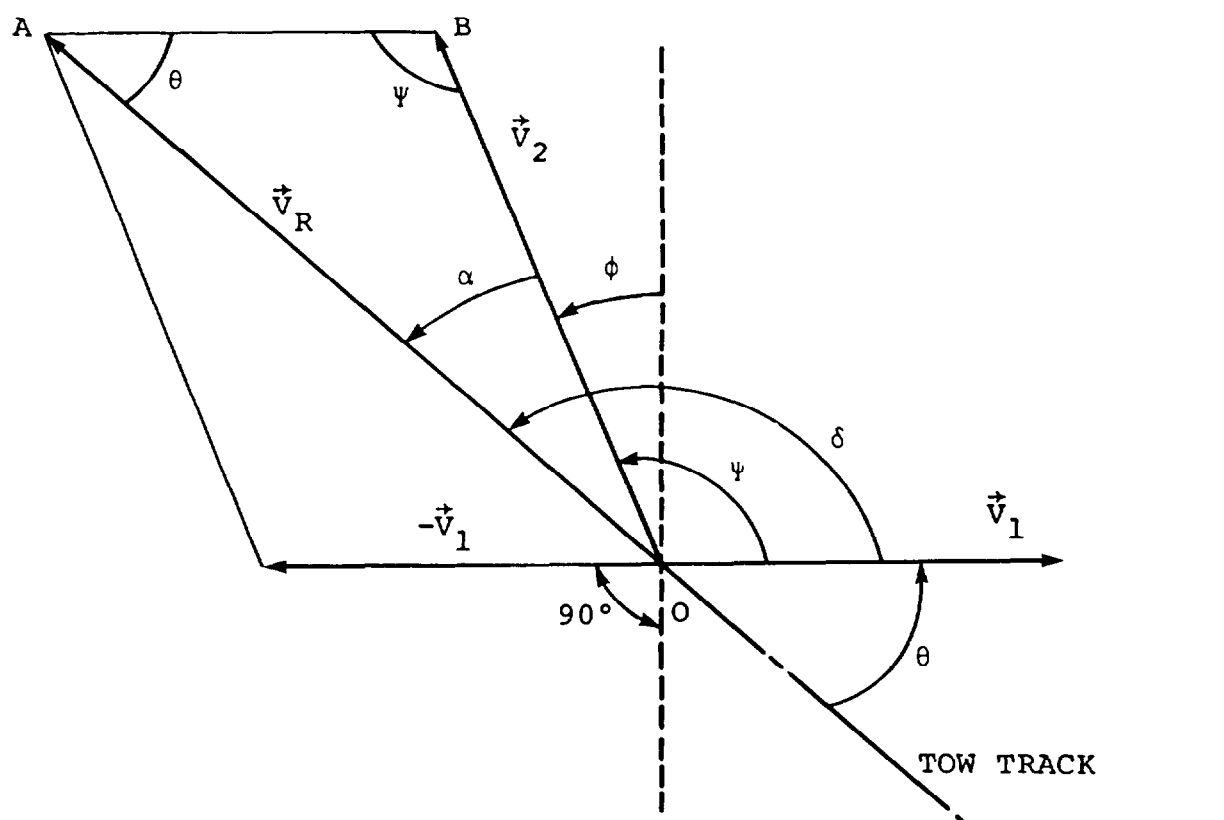


b) Corresponding Test Configuration

FIGURE B-1. EXPLANATION OF TECHNIQUE TO SIMULATE COLLISION.

$\vec{V}_1$  = TARGET VEHICLE VELOCITY  
 $\vec{V}_2$  = BULLET VEHICLE VELOCITY  
 $\vec{V}_R$  = REQUIRED TOWING VELOCITY

} TWO-VEHICLE MOVING COLLISION



$\Psi$  = ANGLE BETWEEN BULLET VELOCITY VECTOR AND TARGET VELOCITY VECTOR ( $\Psi = 90 + \phi$ )  
 $\phi$  = ANGLE BETWEEN BULLET VEHICLE AXIS AND THE PERPENDICULAR TO THE TARGET VEHICLE AXIS (FIXED)  
 $\theta$  = REQUIRED ORIENTATION OF TARGET VEHICLE WITH RESPECT TO TOW TRACK  
 $\alpha$  = REQUIRED ANGLE BETWEEN BULLET VEHICLE AXIS AND TOW TRACK  
 $\delta = \Psi + \alpha$

FIGURE B-2. VEHICLE/TOW TRACK GEOMETRY.

We obtain from (1):

$$\frac{V_1}{V_2} = \frac{\cos (\phi + \theta)}{\sin \theta} \quad (2)$$

Solving Eqn (2) for the angle  $\theta$  gives:

$$\cot \theta = \frac{V_1}{V_2} \cdot \frac{1}{\cos \phi} + \tan \phi \quad (3)$$

The angle  $\alpha$  is then determined from the relation:

$$\alpha = 90 - (\phi + \theta) \quad (4)$$

The required towing speed  $V_R$  is determined by either the law of cosines:

$$V_R^2 = V_1^2 + V_2^2 - 2V_1V_2 \cos \psi \quad (5)$$

or from the law of sines:

$$\frac{V_R}{V_2} = \frac{\cos \phi}{\sin \theta} \quad (6)$$

Since  $\theta$  is a function of  $\phi$  and the velocity ratio  $V_1/V_2$ , the ratio  $V_R/V_2$  (or  $V_R/V_1$  if desired) can be plotted as a function of these two variables.

It should be noted that in using the foregoing equations, the angle  $\phi$  is to be counted negative when the angle  $\psi$  is acute. This is the case when the bullet vehicle approaches the target vehicle from behind.  $\phi = 0$  corresponds to perpendicular impact.

### **B.3 PRESENTATION OF RESULTS**

Generalized curves showing the parameters required to set up the simulated test configuration in which only one vehicle (bullet) is moving have been derived using Equations (3), (4), and (6).

Figure B-3 presents a set of curves giving the angle  $\theta$  (the required orientation angle of the stationary target vehicle with respect to the tow track) as a function of the collision angle  $\phi$ , with the velocity ratio  $V_1/V_2$  as a parameter. As is evident from the figure these curves are divided into two subsets by the  $V_1/V_2 = 1$  line. The line marked  $\phi = 0$  corresponds to a two-vehicle moving collision in which the longitudinal axes of target and bullet vehicles are at right angles.

Figure B-4 presents a set of curves giving the angle  $\alpha$  (the required angle between the "crabbed" bullet vehicle longitudinal axis and the tow track) versus the impact angle  $\phi$ , with the velocity ratio  $V_1/V_2$  as a parameter. Again the set of curves is divided into two subsets by the  $V_1/V_2 = 1$  line. In this case, however, the values for  $V_1/V_2$  greater than 1 (target vehicle speed greater than bullet vehicle speed) are in the upper part of the figure, while in Figure B-3 these were in the lower part.

Figure B-5 presents a set of curves for the velocity ratio  $V_R/V_2$ , given as a function of the velocity ratio  $V_1/V_2$ , with the collision angle as a parameter. The results are plotted in this format in order to avoid intersecting curves. This figure shows that for all values of the angle  $\phi \geq 0$ , the ratio  $V_R/V_2$  is  $\geq 1$ . As noted above  $\phi \geq 0$  corresponds to the case of the bullet vehicle approaching the target from the front.

An example of the use of the curves to determine the required test conditions is illustrated below:

$$\begin{aligned} V_1 \text{ (Target)} &= 15 \text{ mph} \\ V_2 \text{ (Bullet)} &= 30 \text{ mph} \\ \phi \text{ (Collision)} &= 30^\circ \end{aligned}$$

Therefore

$$\begin{aligned} V_1/V_2 &= 0.5 \\ \theta &= 41^\circ \text{ (Figure B-3)} \\ \alpha &= 19^\circ \text{ (Figure B-4)} \end{aligned}$$

and

$$\frac{V_R}{V_2} = 1.32 \text{ (Figure B-5)}$$

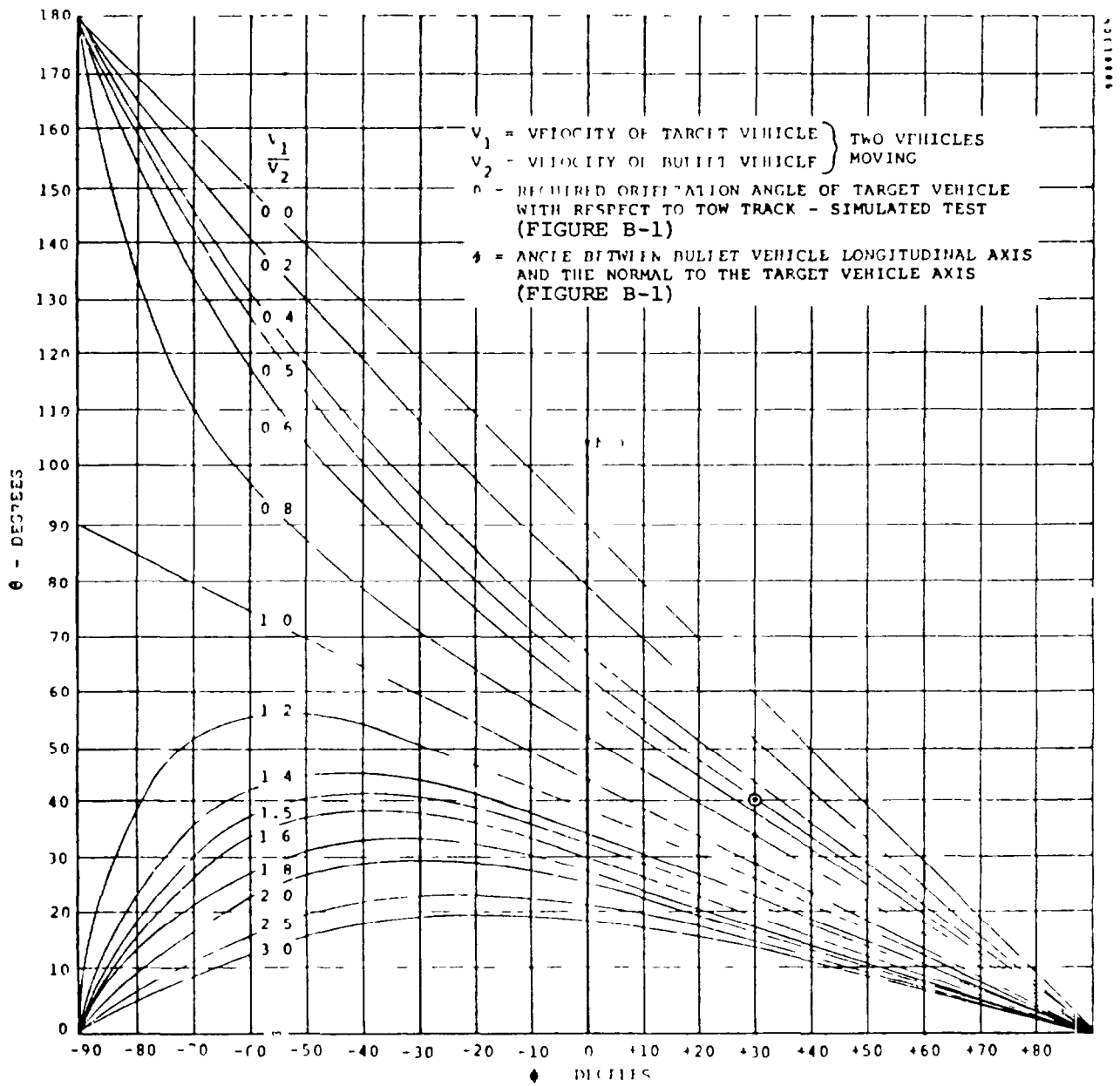


FIGURE B-3. TARGET CAR ANGLE  $\theta$  VERSUS COLLISION ANGLE  $\phi$ .

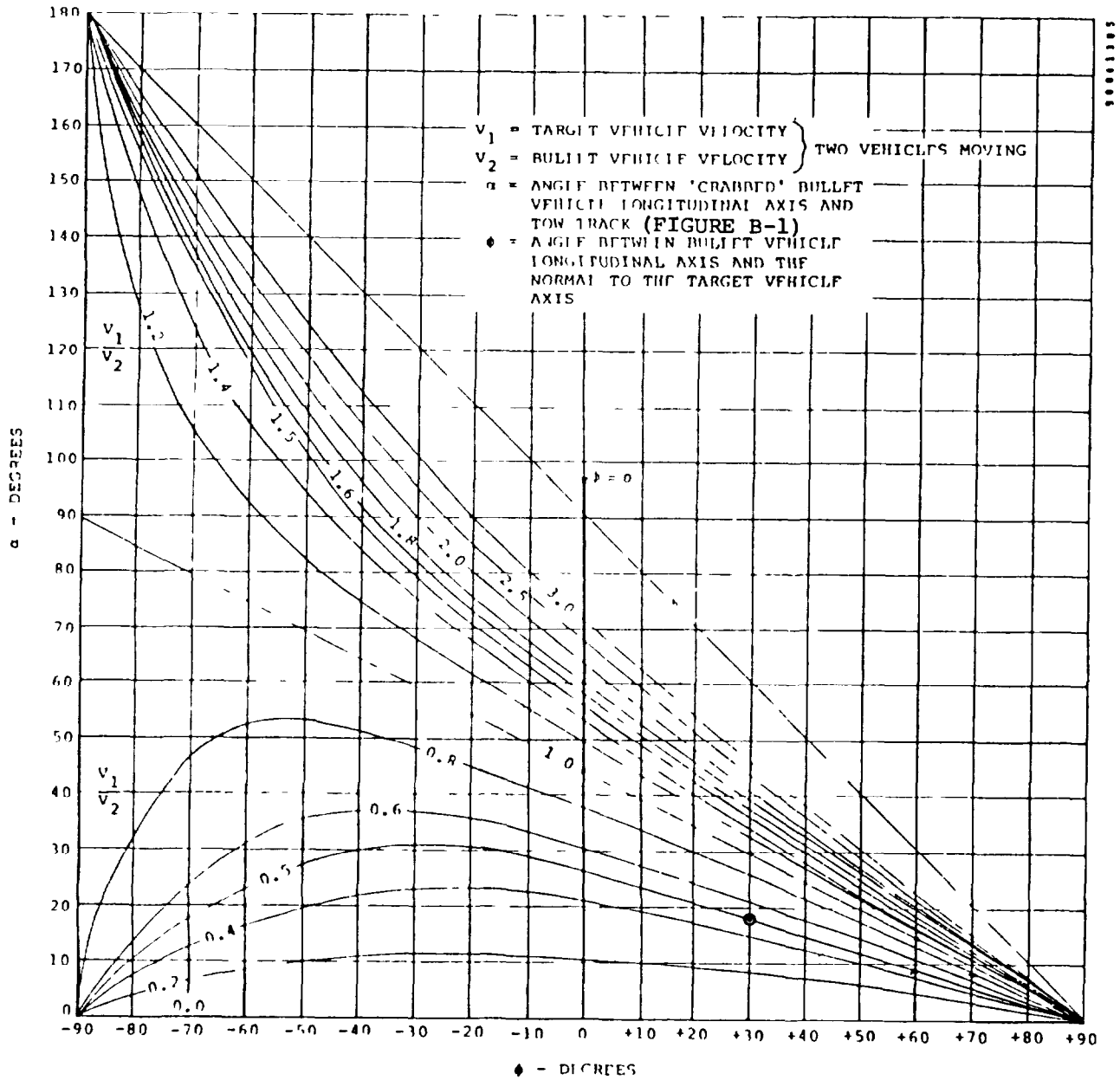


FIGURE B-4. BULLET CAR ANGLE  $\alpha$  VERSUS COLLISION ANGLE  $\phi$ .

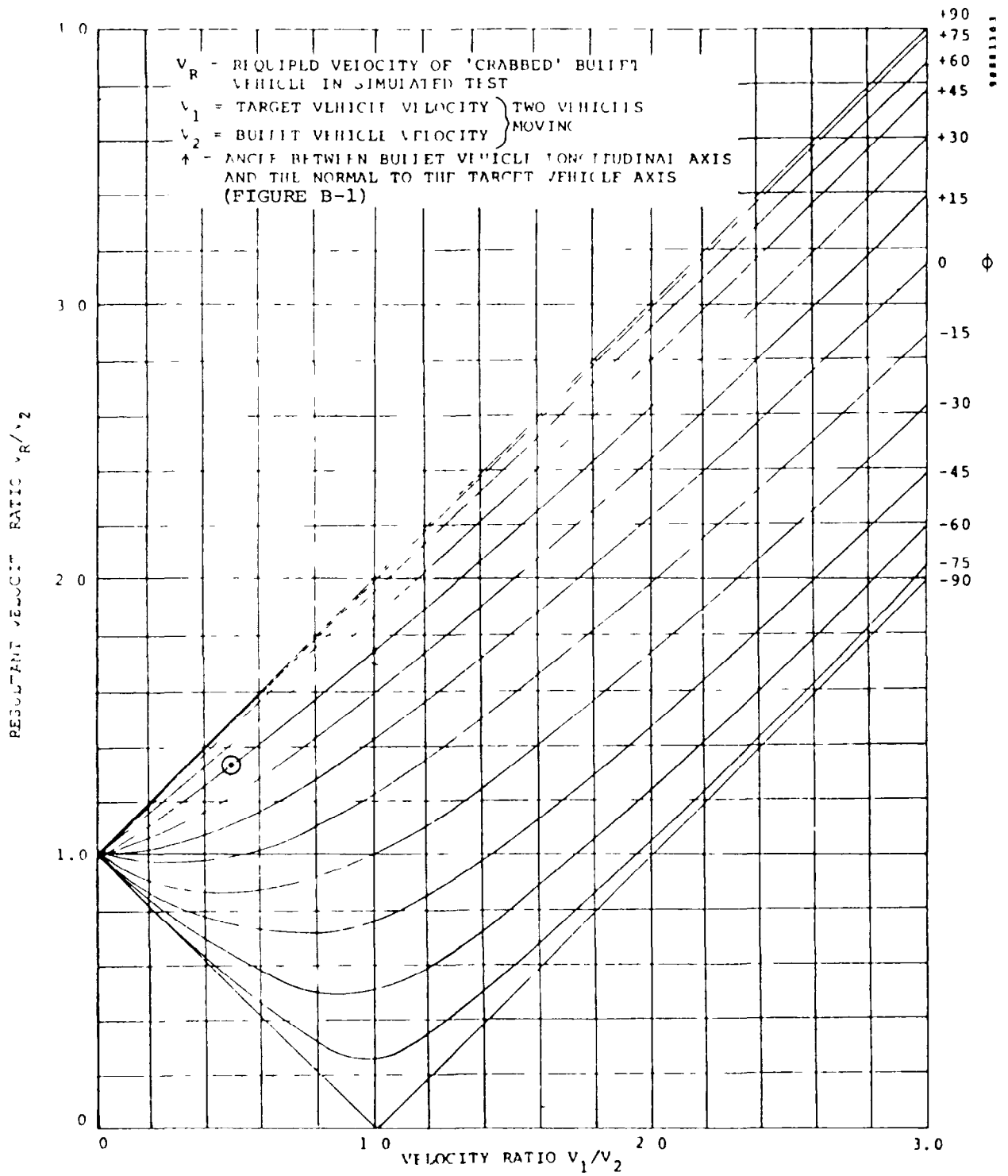


FIGURE B-5. VELOCITY RATIO  $v_R/v_2$  VERSUS VELOCITY RATIO  $v_1/v_2$ .

The points corresponding to the example are shown as ⊙ on Figures B-3, B-4, and B-5. Therefore, the required towing velocity is  $V_R = (1.32) (30) = 39.6$  mph.

#### **B.4 REFERENCE**

NHTSA Statement of Work for RFP, "Occupant Survivability in Lateral Collision," as reported in Greene, J.E., "Occupant Survivability in Lateral Collisions," Calspan Report No. ZS-5562-V-2, October 1975.

APPENDIX C  
MGA BARRIER WEIGHT ANALYSIS REPORT

MGA RESEARCH CORPORATION  
58 Sonwil Drive  
Buffalo, New York 14225  
(716) 683-5855

METHODOLOGY FOR RECOMMENDING SIDE IMPACT  
MOVING BARRIER WEIGHT

DAVID J. SEGAL AND PATRICK M. MILLER

NOVEMBER 1981

FINAL REPORT  
MGA Report No. G9-003-V-1

Dynamic Science Purchase Order No. 02668  
Contract No. DOT-HS-8-01933

Prepared for:  
DYNAMIC SCIENCE, INC.  
1850 West Pinnacle Peak Road  
Phoenix, Arizona 85027

## TABLE OF CONTENTS

		<u>Page no.</u>
1	INTRODUCTION	1
2.	METHODOLOGY	4
	2.1 Data Available	5
	2.2 Procedure Used to Recommend Barrier Weight	11
	2.3 Procedure for Estimating Benefit	22
3.	DISCUSSION OF RESULTS	25
4	REFERENCES	32

## LIST OF FIGURES

<u>FIGURE NO.</u>	<u>TITLE</u>	<u>PAGE NO.</u>
1	Cumulative Frequency Distributions of Passenger Car Populations by Weight	8
2	Cumulative Relative Frequency Distributions of Fatalities and Severe Injuries by Weight Difference	10
3	Cumulative Relative Frequency Distribution of Serious Injuries by Lateral Change in Velocity	12
4	Weight Difference Probability for 1976 and NCSS Passenger Car Populations	16
5	Fatality Rates vs. Weight Difference	17
6	Curve Fit to Fatality Rate Data Points	19
7	Predicted vs. Actual 1976 Fatalities	20
8	Predicted vs. Actual 1978 Fatalities	21
9	Probability of Weight Difference for NCSS Vehicle Sample	26
10	Cumulative Relative Fatality Frequency by Weight Difference for 1978 Vehicle Population	26
11	Injury Reduction Benefit for 1978 Vehicle Population vs. Barrier Weight	27
12	Cumulative Relative Fatality Frequency by Weight Difference for 1985 Vehicle Population	28
13	Injury Reduction Benefit for 1985 Vehicle Sales Population vs. Barrier Weight	30

LIST OF TABLES

<u>TABLE NO.</u>	<u>TITLE</u>	<u>PAGE NO.</u>
1	Frequency Distributions of Car Populations by Weight	9
2	Frequency Distribution of FARS Fatalities by Weight Difference	14

## 1. INTRODUCTION

Accident studies, particularly the National Crash Severity Study (NCSS), have provided information indicating the serious nature of the current side impact problem. For example, Reference 1 indicates that the side impact accidents contained in the NCSS file constitute 26% of the vehicles, 27% of the occupants, 33% of the serious (AIS  $\geq$  4) injuries, and 36% of the fatalities

In response to this problem, the National Highway Traffic Safety Administration (NHTSA) has placed a high priority on reducing the injuries resulting from side impacts. A major effort to upgrade FMVSS 214, "Side Impact Protection" is currently underway. As part of this overall effort, Dynamic Science, Inc., under Contract No. DOT-HS-8-01933, is developing for NHTSA a side impact test device (i.e., impacting barrier) and demonstrating a compliance test procedure. MGA Research Corporation is supporting the Dynamic Science project under a subcontract arrangement.

Our activities involve analyses which will provide background information which may be used by NHTSA in the selection of a barrier weight and a test impact speed. The test condition is intended to be "reasonably" representative of real world car-to-car side impact accidents. In this sense, accident data must be somehow related to the limited configuration of a single side impact crash test. The effort described in this report attempts to provide a rational means for selecting the moving barrier test weight based upon accident data and automobile fleet population.

The process of selecting the test condition must take into consideration several factors. The more notable ones are.

- a) possible benefit
- b) realism to real world accident conditions
- c) feasibility and practicality (i.e., costs)

It is understood that NHTSA will take these factors into consideration. Our effort was somewhat more limited in that consideration was given only to items a. and b. That is, an analysis was conducted to estimate possible benefit as a function of test severity (both in terms of barrier weight and impact speed). A secondary part of the analysis relates weight difference (between striking and struck vehicles) to the frequency of occurrence of the more severe injuries. The potential problem of designing motor vehicles to meet a given test condition has not been addressed. Hence, the results of this limited study do not provide a complete basis for setting desirable compliance test conditions.

Although the selection of a barrier weight may appear to be straightforward, it is complicated by a number of factors. First, the barrier weight must be reasonably "representative" of the weight range for automobiles operating on the Nation's highways. Second, because elimination of the more severe injuries is the goal of the standard upgrading, the barrier weight must attempt to approximate conditions associated with the more severe injuries. Third, it must be recognized that the automotive fleet weight distribution is undergoing substantial changes as a result of a major effort to improve fuel economy. Hence, a barrier weight believed to be a reasonable compromise for present highway conditions, would likely be totally unrealistic for the automotive fleet conditions of the mid-1980's. Each of these factors has been considered in the study.

The estimate of benefits (injury reduction) was based upon a methodology proposed by Burgett (Ref. 2). In this method, a change in velocity imposed on a population of vehicles is calculated based on the assumption of a plastic impact between a barrier of given weight (and speed) and a stationary automobile. An estimation of the number of injuries occurring in the struck car population is then made based on a relative cumulative frequency curve of the percent of the number of near-side occupant serious injuries as a function of lateral  $\Delta V$ , developed from NCSS data. The calculations are repeated for a

number of barrier weights and speeds. The results of these calculations are a series of curves relating the number (or percent) of injuries sustained to barrier weight, parametric in barrier velocity. The analysis considered a number of different automobile fleet weight distributions.

The approach to factor in weight (or more specifically, weight difference between striking and struck vehicles) makes use of information extracted from the FARS data base together with a frequency distribution of passenger cars by weight and is a modification of a technique suggested by Ragland (Ref. 4). In this approach, the passenger car weight distribution is employed to calculate the probability that a given weight difference between two cars involved in a collision will exist. This probability is then divided into the frequency of fatalities for the corresponding weight difference extracted from FARS data. The result is fatality rate as a function of weight difference. This fatality rate is then assumed to remain relatively constant over time and is used to project the number of fatalities in the future from a projected distribution of passenger cars by weight.

Computer programs were developed for each of these analytical techniques, permitting evaluation of the effect of several different variables. In both instances, vehicle population believed to be representative of the latter 1970 automobile fleet and projected 1985 conditions were analyzed. Based on the complete study, it is our recommendation that a barrier weight of about 3450 lbs. be selected as a reasonable compromise for the multitude of influencing conditions. Once the barrier weight is selected, it is then necessary to select a test impact speed. Results obtained in the study allow a direct determination of estimated benefits for a range of impact speeds. However, selection of a precise impact speed must take into consideration feasible and practical automobile side impact safety systems.

In the next section, the methodology utilized in the study is presented. This is followed by a presentation of the results generated for the various hypotheses and a general discussion of the results.

## 2. METHODOLOGY

As noted in the Introduction, the basic objectives of this study were to provide NHTSA with information that would aid in choosing a moving barrier weight for side impact compliance testing, to document a methodology for evaluating the benefits associated with a moving barrier side impact test procedure, and to evaluate the effects of the chosen test conditions with respect to an ever changing vehicle population.

Accident study results indicate that injuries to the occupants of vehicles involved in collisions are strongly associated with the change in velocity experienced by the vehicle. This fact suggests that the most straightforward approach to producing a known level of benefit (i.e., reduction of injuries) through setting performance criteria in a test procedure would be to require all vehicles tested to experience a given change in velocity associated with the desired level of injury reduction. However, assuming a collision between the test vehicle and moving barrier can be considered to be a problem in plastic, central impact mechanics, the change in velocity experienced by the test vehicle is a function of two variables, the barrier weight and the closing speed. Hence, imposing a test procedure that would require all vehicles to undergo a fixed change in velocity would, in fact, require that one or both of these variables be changed as a function of the test vehicle weight. The current feeling is that this requirement would lead to a test procedure of limited practicality.

Consequently, it becomes necessary to choose a specific set of test conditions, i.e., barrier weight and speed, that can be considered to be representative of accident exposure experience.

This study has attempted to accomplish this objective by means of a logical methodology making use of vehicle population and occupant injury data. Vehicle population data that were available included current (NCSS) and previous (1976) passenger car frequency distributions by weight and a projection

of 1985 new car sales by weight. Injury measure information available included a count of near side fatalities and severe injuries in car-to-car crashes as a function of striking car weight and weight difference between striking and struck cars, both from the FARS data file and the NCSS data file. Also available was a cumulative distribution of serious ( $AIS \geq 4$ ) injuries to near side occupants of passenger cars struck in the compartment as a function of lateral change in velocity, developed from reconstructed NCSS accident cases.

The general approach used in this study was to use FARS (and NCSS) cumulative injury data as a function of weight difference between striking and struck cars to provide a reasonable test barrier weight in relation to either the current or a projected vehicle population weight distribution. Then, given a level of benefit, the other test variable, closing velocity, can be determined.

The following three subsections describe the data used in this study and the procedures used to recommend a barrier weight and to evaluate the benefits expected to be achieved by a side impact test procedure.

## 2.1 Data Available

Frequency distributions of passenger cars by weight were required for the procedures that are described in the subsequent sections. Four such distributions were employed in this study. These were:

- Frequency distribution of passenger cars by weight as of July 1, 1976 (from Ref. 3)
- Frequency distribution of passenger car weight contained in the NCSS sample (Ref. 4)
- Projected distribution of 1985 new car sales by weight (Ref. 4)

- Projected distribution of 1985 total car population by weight

The information contained in Ref. 3 was developed from a count of vehicles by make, model, and model year for each state. Vehicle curb weight was obtained from Ref. 5. Data were provided separately, for domestic and foreign cars for the model years 1966 through 1976. Combining these data yielded a total vehicle count of approximately 96.6 million cars, of which approximately 14.9% were either pre-1966 or otherwise unidentified. Since this count was based on curb weight, three hundred pounds were added for use in the study in order to approximate on the road, or inertia, weight. The mean weight of the population (inertia weight) was approximately 3840 lbs.

The vehicle count by weight for all passenger cars in the NCSS file was provided by the National Center for Statistics and Analysis. At the time the information was obtained, the weighted file contained 72,242 cars. The mean weight of this sample was approximately 3730 lbs., which also included a 300 lb. increment to reflect an approximate on-the-road weight.

The projection of vehicle sales by inertia weight for 1985 was provided by NHTSA. The mean weight of this sample was approximately 2950 lbs. Also provided were sales by weight for the years 1970 through 1979. In order to project the total car population for 1985, estimates of sales by weight were made for the years 1980 through 1984 by linear interpolation between values for 1979 and 1985. This admittedly crude attempt at estimating vehicle sales for these years was necessary because NHTSA projections were not available at the time of this study. An estimate of the percentage of cars remaining in service, as a function of age was then obtained from Ref. 6 and applied to the new car sales data for 1970 through 1985 resulting in a projected 1985 vehicle population. The mean weight of this population was approximately 3240 lbs. This projection resulted in an estimated 104.1 million passenger cars in service in 1985, an increase of about 8% over 1976.

A cumulative relative frequency distribution of passenger cars by weight for each of these vehicle populations is shown in Figure 1 and frequency distributions are compared in Table 1.

Occupant injury data available included counts of the number of fatalities by weight and weight difference between striking and struck cars from the NCSS data base and from the FARS data base for the years 1975 through 1978. Cumulative near side fatality frequency (expressed as a percent of the total) from FARS for the years 1976 and 1978 as a function of weight difference are shown in Figure 2. Also indicated on the figure, is the cumulative frequency of severe injuries ( $AIS \geq 4$ ) extracted from the NCSS file as a function of weight difference between the striking and struck vehicle.

The two FARS distributions agree very closely with a slight tendency for a greater frequency of fatality at large weight differences in the 1978 data. The median point of both distributions are close to a 500 lb. weight difference in favor of the striking car. It is interesting to note that the NCSS cumulative distribution of near side injuries with  $AIS \geq 4$  also agrees quite well with the two FARS curves considering the limited number of data points (25). As a result of this general agreement, it was decided that the FARS data would be used for selection of a barrier weight since many more data points comprise the cumulative distribution.

It is also interesting to note that data supplied in Ref. 7 indicates that the median weight for the 1976 FARS striking car weight was 4080 lbs. (including an increment of 300 lbs. to reflect the same assumption as was used to develop the 1976 weight distribution) and the median weight for the 1976 population from Figure 1 is about 3960 lbs. Similarly the median NCSS striking car weight for all side impacts was 3950 (including an added 300 lbs.) while the median from the NCSS cumulative weight distribution curve of Figure 1 is about 3800 lbs. Hence, the median striking car weight for the more serious side collisions tends to be somewhat greater than the median of the vehicle population.

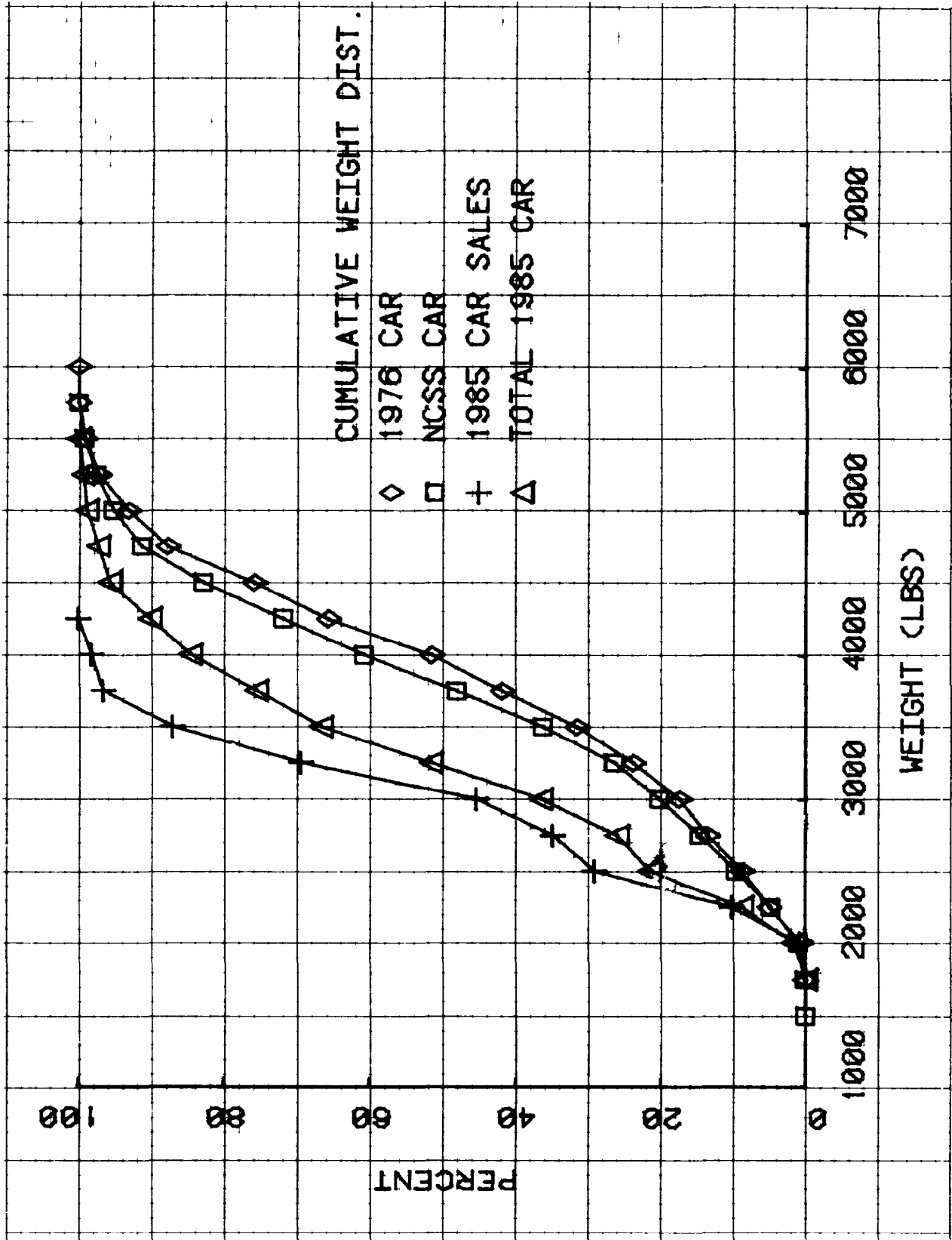


Figure 1 CUMULATIVE FREQUENCY DISTRIBUTIONS OF PASSENGER CAR POPULATION BY WEIGHT

TABLE 1  
 FREQUENCY DISTRIBUTIONS OF CAR POPULATIONS BY WEIGHT

INERTIA WEIGHT INCREMENTS (LBS.)	RELATIVE FREQUENCY (PERCENT)			
	1976 POPULATION	NCSS SAMPLE	1985 NEW CAR SALES PROJECTION	1985 TOTAL POPULATION PROJECTION
< 1750	---	0.1	---	---
1750 - 1999	0.6	0.9	0.8	1.6
2000 - 2249	4.4	3.8	9.4	7.2
2250 - 2499	3.7	4.8	18.9	12.7
2500 - 2749	4.8	5.0	5.8	4.5
2750 - 2999	3.9	5.6	10.5	10.5
3000 - 3249	6.4	6.2	24.1	15.1
3250 - 3499	7.8	9.9	17.5	15.1
3500 - 3749	10.3	11.8	9.6	8.9
3750 - 3999	9.5	12.6	1.7	8.9
4000 - 4249	14.2	11.1	1.7	5.6
4250 - 4499	10.2	11.0	---	5.6
4500 - 4749	11.9	8.5	---	1.6
4750 - 4999	5.4	3.9	---	1.6
5000 - 5249	4.1	2.4	---	0.6
5250 - 5499	2.0	1.7	---	0.5
5500 - 5749	0.8	0.7	---	---
5750 - 5999	---	---	---	---

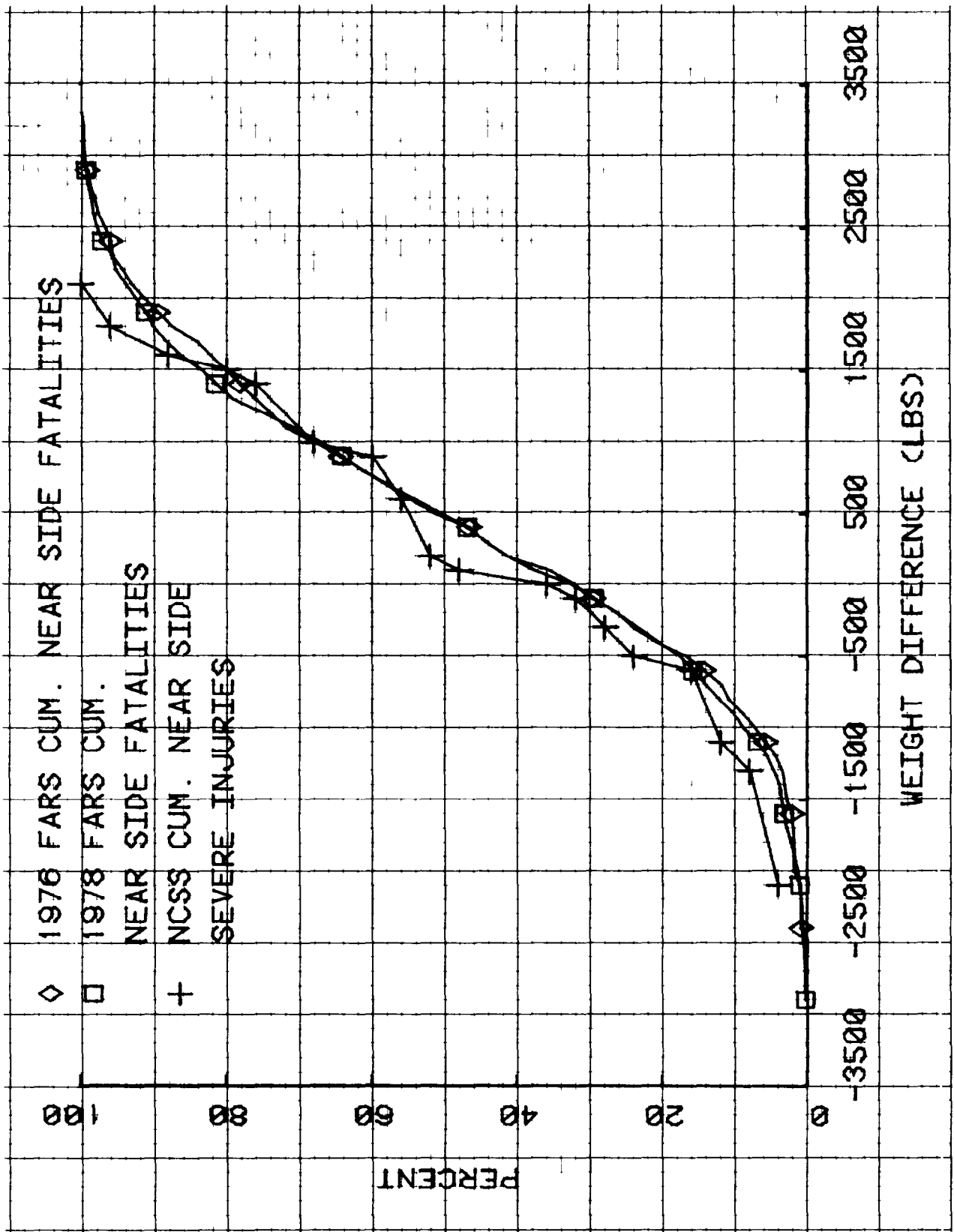


Figure 2 CUMULATIVE RELATIVE FREQUENCY DISTRIBUTIONS OF FATALITIES AND SEVERE INJURIES BY WEIGHT DIFFERENCE

Figure 3 shows the cumulative relative distribution of serious (AIS  $\geq$  4) injuries incurred to near side occupants of automobiles struck in the passenger compartment as a function of lateral change in velocity. This information was provided by NHTSA (Ref. 4) as determined from the most recent NCSS file update. Note that the lateral change in velocity is determined by CRASH reconstructions of the subject accidents.

## 2.2 Procedure Used to Recommend Barrier Weight

As indicated in the previous section, a cumulative distribution of fatalities (or serious injuries) by weight difference is believed to provide a reasonable means of selecting a weight difference for application to a test procedure. Two difficulties exist, however. First, this distribution exists only through the year 1978 for the FARS data base. Thus, a projection of a cumulative fatality distribution to the 1985 vehicle population is necessary. And second, while this fatality distribution provides a means of establishing a reasonable weight difference that is characteristic of the more severe side impacts, it in and of itself, does not directly indicate a barrier weight to be used. Each of these points is discussed below.

In order to project a cumulative fatality distribution to the future, a procedure employing information extracted from the FARS data base and a distribution of passenger car weights was used. In this procedure, the passenger car weight distribution is used to calculate the probability that a given weight difference between two cars involved in a collision will exist. This probability is then divided into the frequency of fatalities for the corresponding weight difference extracted from FARS data. The result is fatality rate as a function of weight difference. This fatality rate is then assumed to remain constant over time and is used to project the number of fatalities in the future from a projected weight distribution.

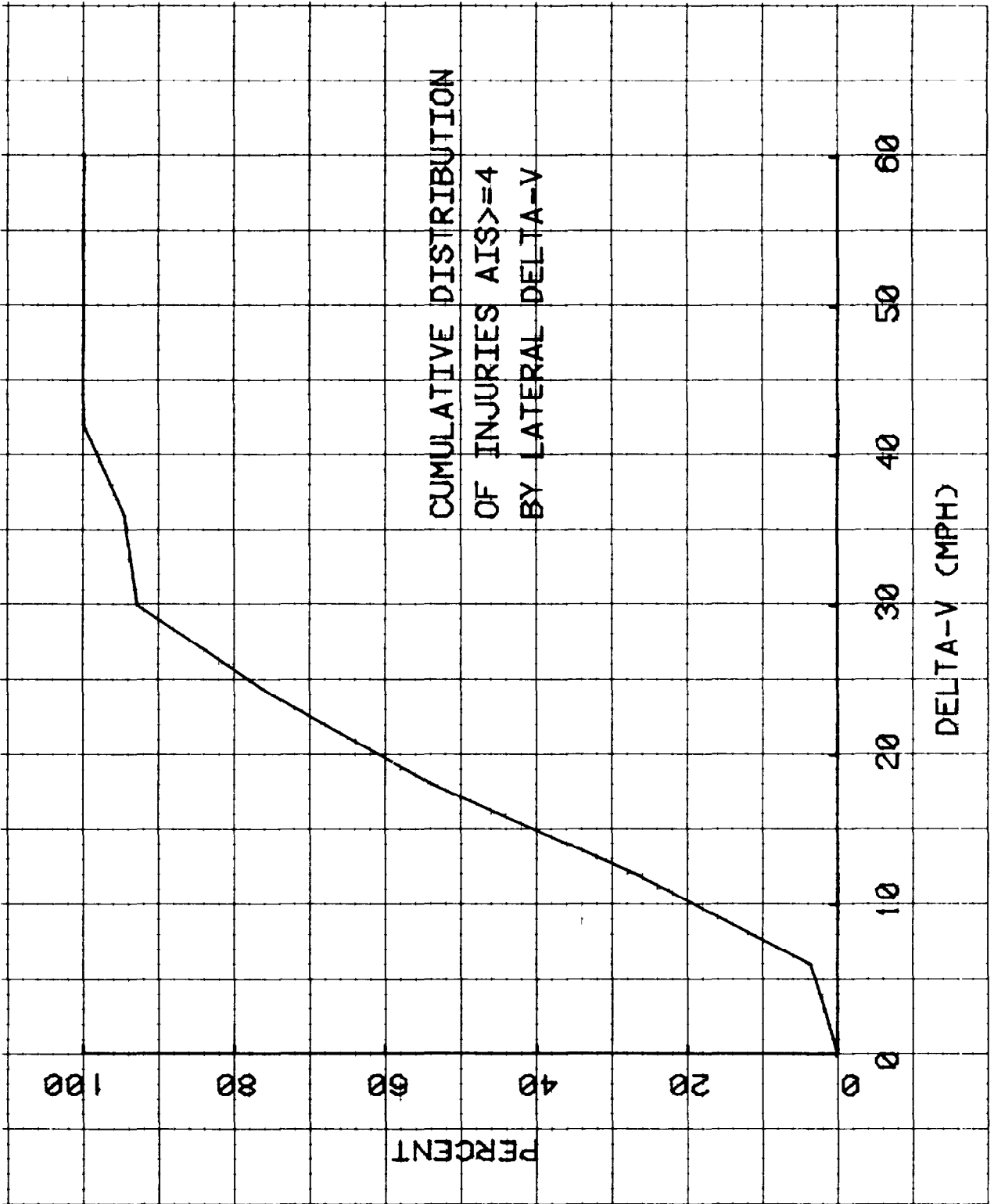


Figure 3 CUMULATIVE RELATIVE FREQUENCY DISTRIBUTION OF SERIOUS INJURIES BY LATERAL CHANGE IN VELOCITY

Data required for this procedure are:

- distribution of passenger car population by weight for a given time period
- frequency of near side fatalities as a function of the weight difference between striking and struck vehicles, for the same time period as the above distribution
- projected distribution of passenger car population by weight at some future period of time.

Tabulations of the number of near side fatalities as a function of weight difference (striking minus struck) obtained from FARS data (Ref. 7) are given in Table 2. The distributions of passenger car population by weight used were discussed in Section 2.1.

The computational steps for this procedure are as follows:

1. Divide the vehicle population weight distribution into  $n$  discrete weight cells of constant cell width. The total number of vehicles in the population is then normalized to 1.0. Compute the probability that, taking two vehicles at a time, all possible weight differences will occur, i.e.,  $P_{i,j} = P_i P_j$ . Note that  $i$  and  $j$  are both varied over the  $n$  cells in the weight distribution. Then, the probability that a given weight difference will occur and that weight differences are computed:

$$P_k = \sum P_{i,j}$$

$$W_k = W_i - W_j$$

where  $k = i - j$

TABLE 2  
 FREQUENCY DISTRIBUTIONS OF FARS FATALITIES\*  
 BY WEIGHT DIFFERENCE

Weight Difference (Striking Minus Struck) LBS.	NUMBER OF FATALITIES			
	1975	1976	1977	1978
-3200 to -2800	0	0	0	3
-2700 to -2300	3	2	2	3
-2200 to -1800	0	4	8	16
-1700 to -1300	13	7	12	21
-1200 to - 800	24	28	40	51
- 700 to - 300	22	44	78	77
- 200 to 200	44	65	99	129
300 to 700	43	67	100	123
800 to 1200	57	66	107	119
1300 to 1700	20	38	54	99
1800 to 2200	18	39	46	49
2300 to 2700	11	15	19	25
2800 to 3200	3	9	5	9
3300 to 3700	0	0	0	2

\* Taken from Reference 7

The result of this step is a probability,  $P_k$ , that a weight difference,  $W_k$ , will occur when vehicles in the population are taken two at a time.

2. Divide the frequency distribution of fatalities as a function of weight difference into weight difference cell widths equal to that used in Step 1. Obtain a rate of fatality as a function of weight difference by dividing the number of fatalities occurring within a given cell by the probability that the corresponding weight difference will occur within the distribution of vehicle weights.
3. Step 1 is then repeated for a projected weight distribution and the resulting weight difference probabilities are multiplied by the corresponding fatality rates obtained in Step 2. The result is a projected frequency of fatality distribution by weight difference for the future vehicle population.

As developed from the above described procedure, the probability of a given weight difference existing for the 1976 vehicle population and the NCSS sample described in Section 2.1 are shown in Figure 4. Note that the NCSS sample is assumed to be representative of the 1978 vehicle population.

Fatality rates derived from using the 1976 FARS fatality frequency distribution by weight difference together with the 1976 passenger car weight distribution, and from the 1977 and 1978 FARS fatality frequencies both with the total NCSS weight distribution are shown in Figure 5. Very good agreement exists in the rates derived from these three data sets, particularly in the region where fatality frequencies were relatively high. The fatality rate actually used to project fatality frequency to a future vehicle population was

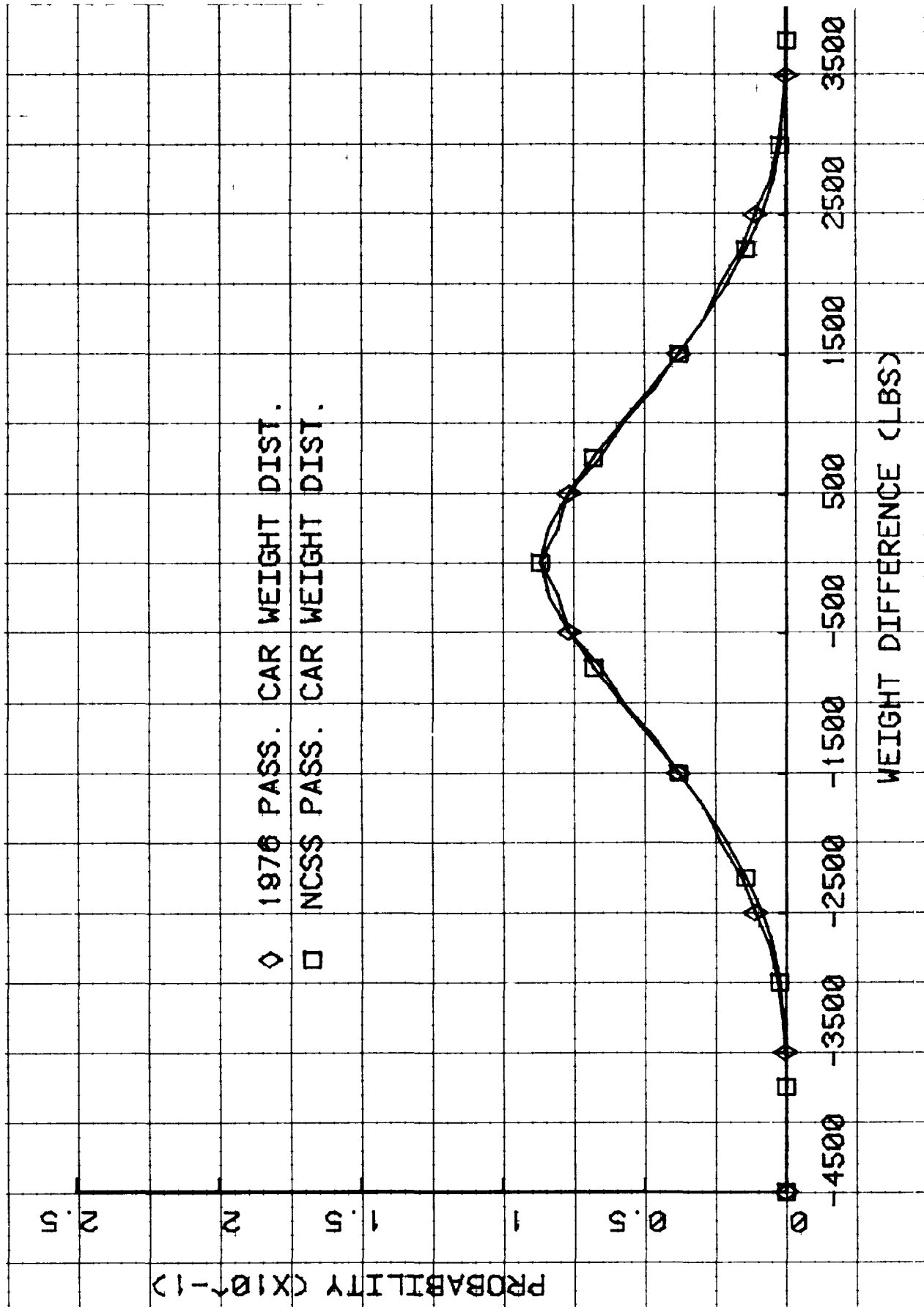


Figure 4 WEIGHT DIFFERENCE PROBABILITY FOR 1976 AND NCSS PASSENGER CAR POPULATIONS

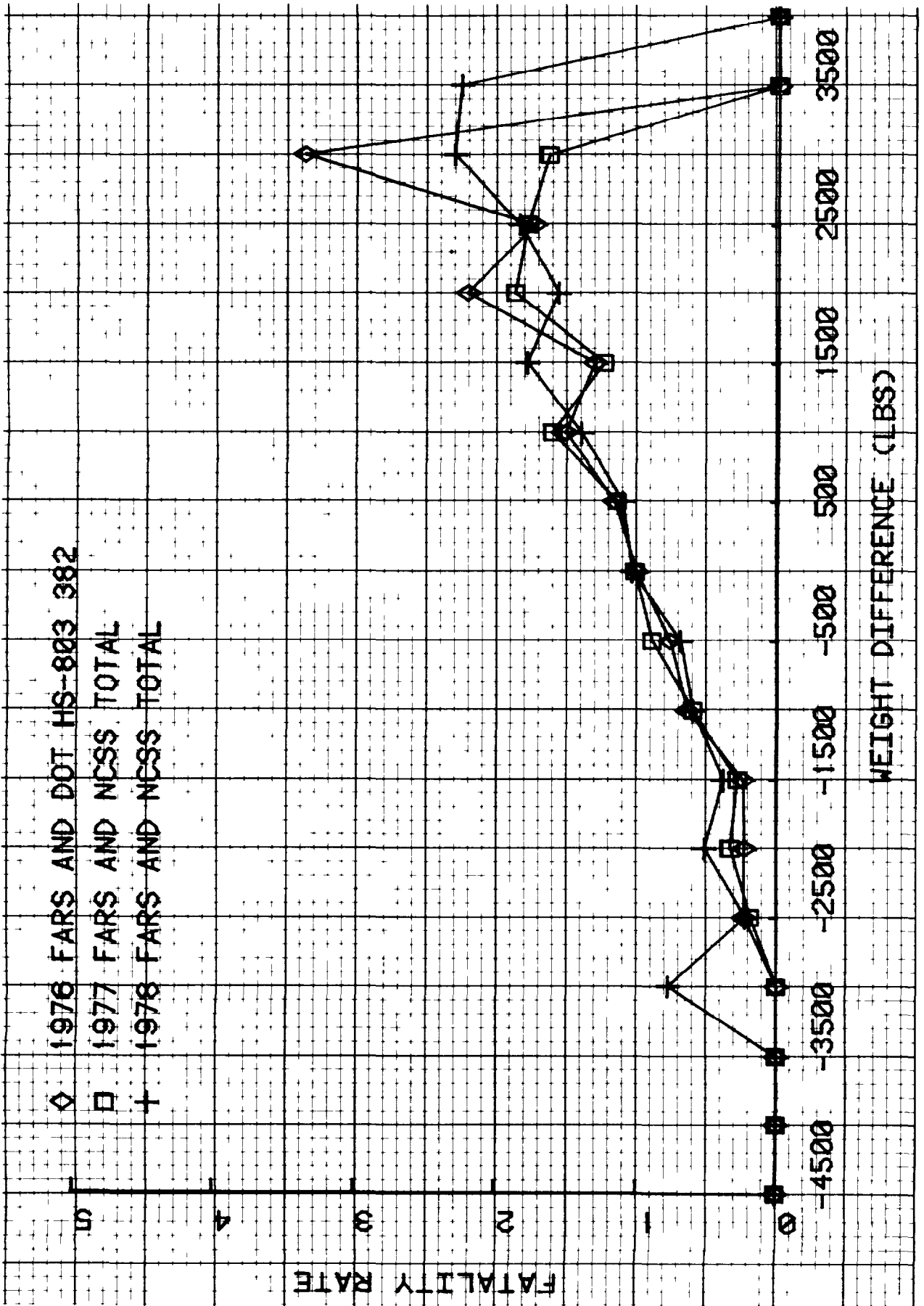


Figure 5 FATALITY RATES VS. WEIGHT DIFFERENCE

obtained by fitting a least squares, second order curve to the three years of data points shown in Figure 5. This fit, superimposed on the derived fatality rate data points are shown in Figure 6.

Using this curve fit fatality rate, a "prediction" of the cumulative fatality frequency can be made using the 1976 and NCSS passenger car weight distributions for comparison with the observed results from FARS data. These comparisons are shown in Figures 7 and 8 illustrating a generally good predictive capability. Given the assumption that the fatality rate remains constant over time in a changing vehicle population, it is then possible to predict the fatality frequency distribution by weight difference between striking and struck cars if a future vehicle population weight distribution is known.

As noted above, this procedure helps to provide a weight difference between striking and struck cars based on a chosen fatality percentile. From Figure 2, it is seen that 50 percent of the near side fatalities within the current population occur with a weight difference of 500 lbs. or less. Also, since the rather limited number of data points in the NCSS cumulative severe injury distribution by weight difference follow quite closely the FARS data, it is reasonable to assume that approximately 50 percent of the severe near side injuries will also occur at a weight difference of about 500 lbs. or less. Thus, a 500 lb. weight difference is believed to be a reasonable condition that is representative of more severe side collisions within the current vehicle population. It then remains to choose a specific moving barrier test weight that would provide a reasonable approximation of this weight difference over the entire struck vehicle population. This can be accomplished by adding the chosen weight difference to the mode of the vehicle population weight distribution on the basis that this will result in the highest probability of this weight difference occurring.

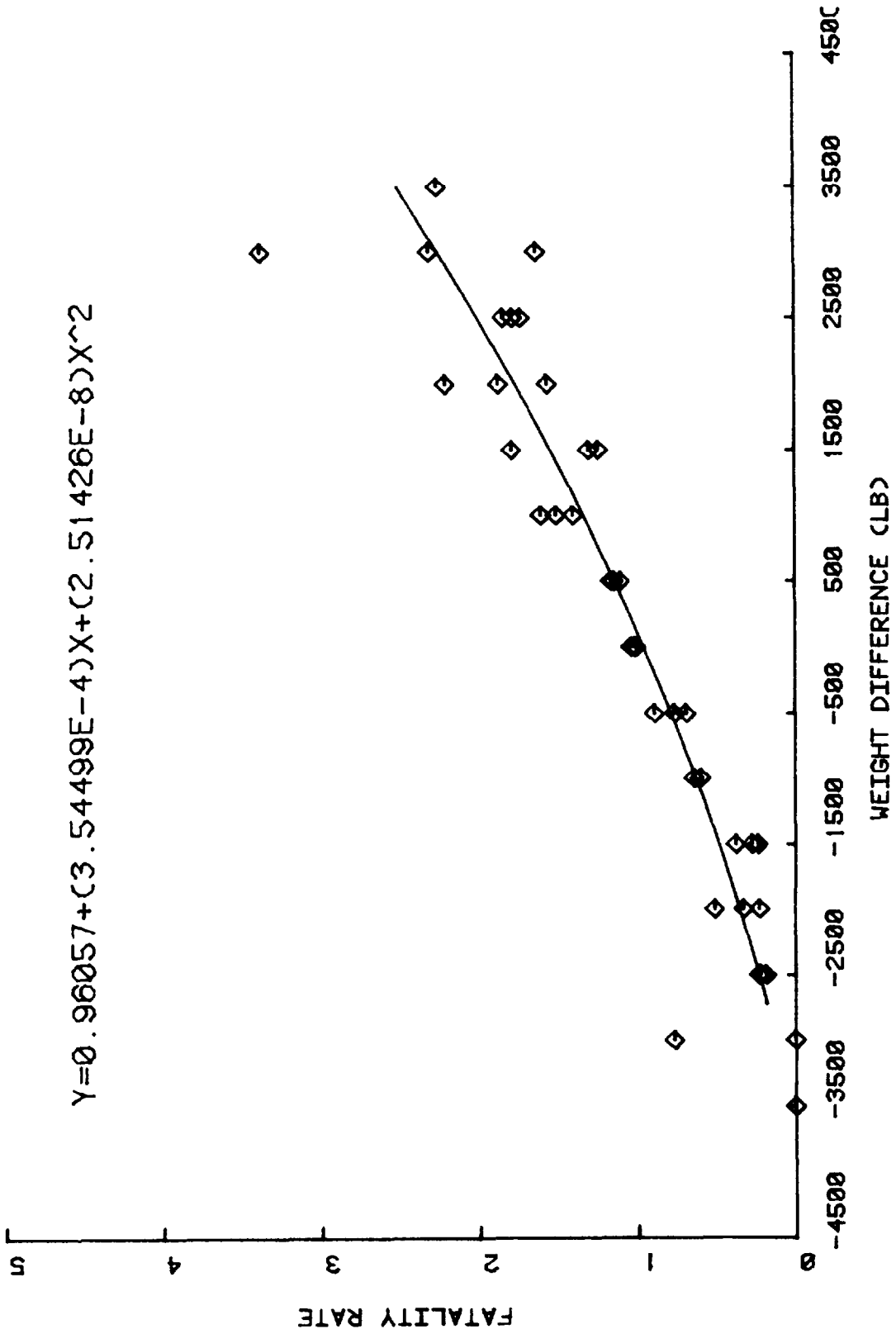


Figure 6 CURVE FIT TO FATALITY RATE DATA POINTS

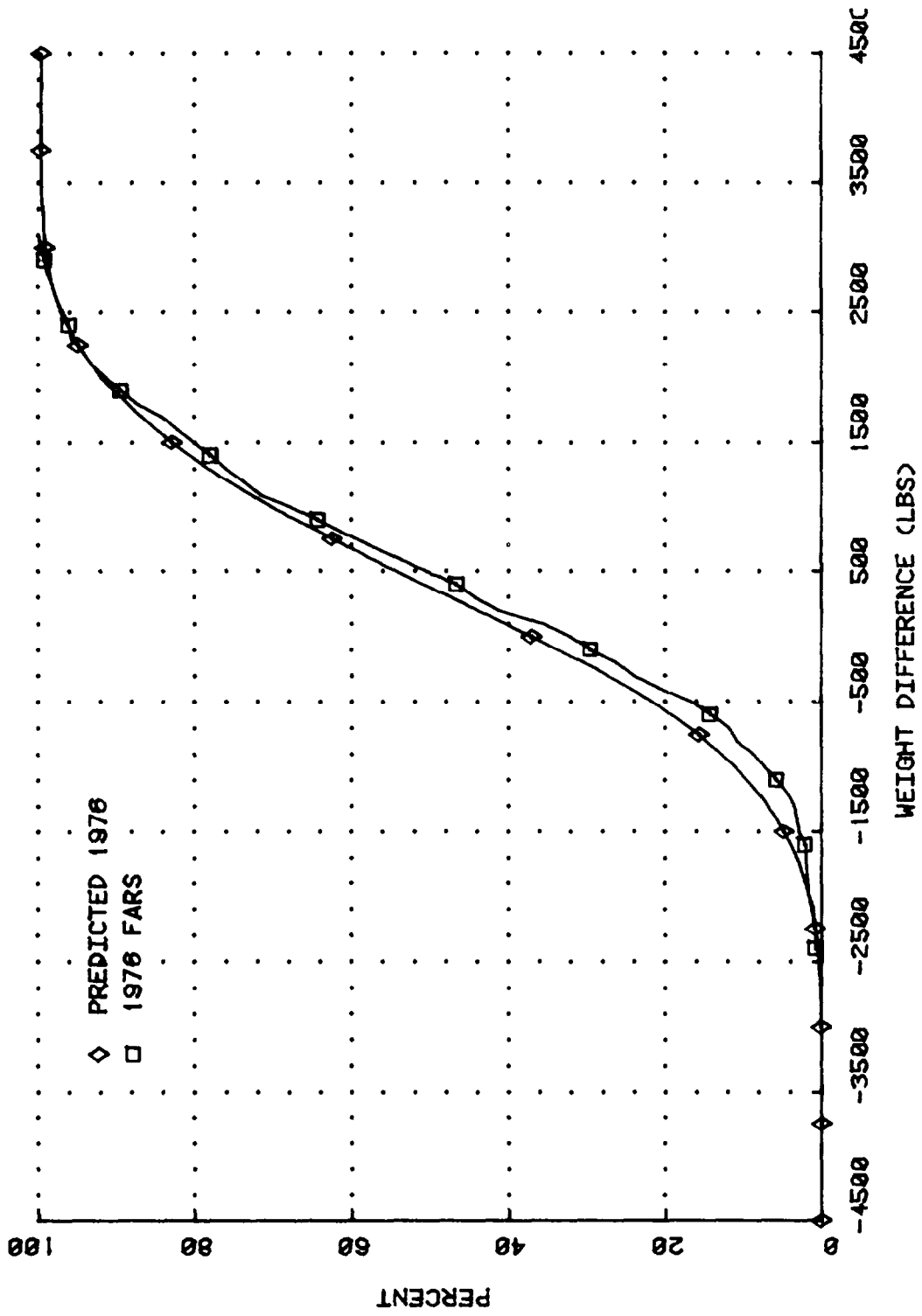


Figure 7 PREDICTED VS. ACTUAL 1976 FATALITIES

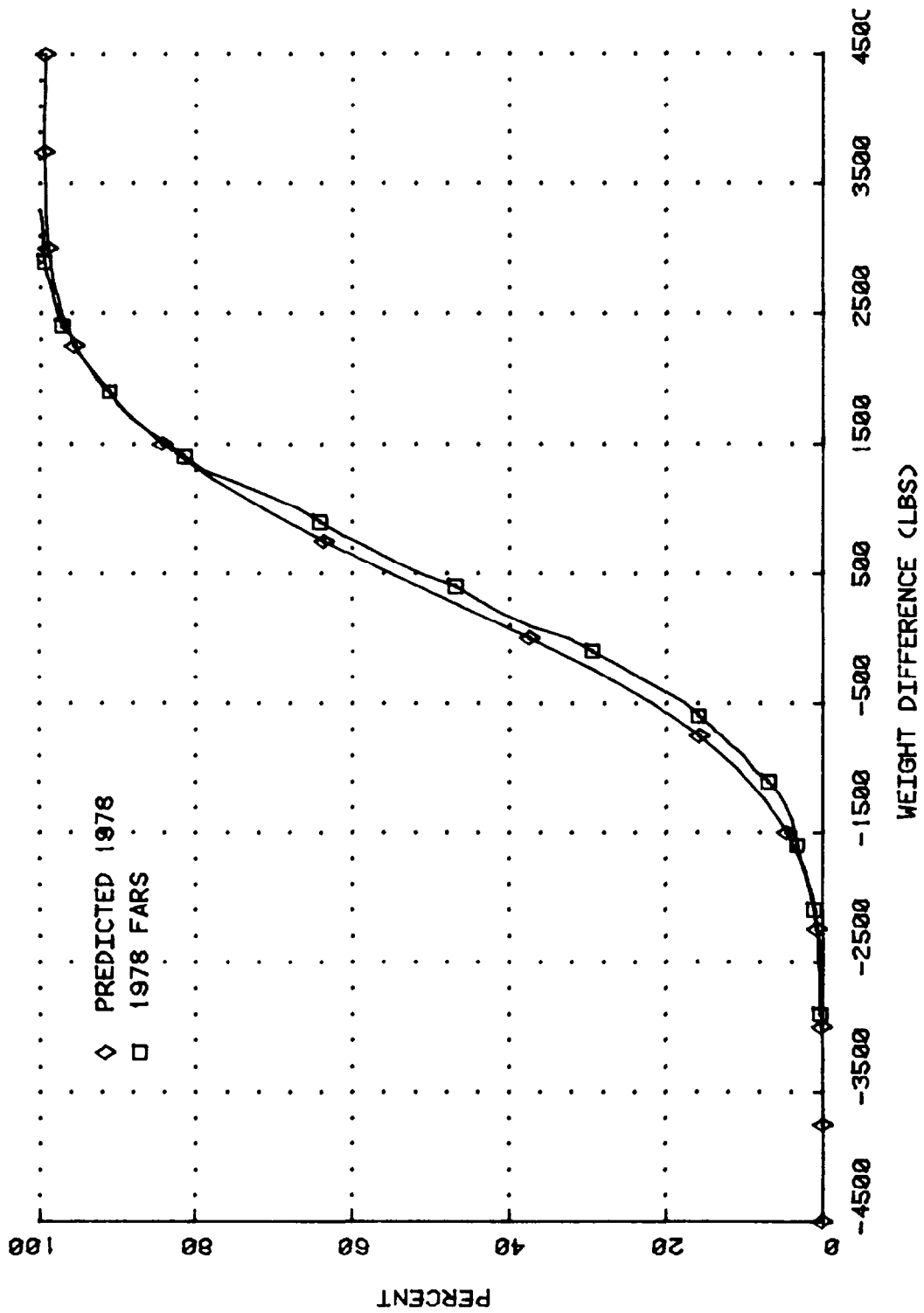


Figure 8 PREDICTED VS. ACTUAL 1978 FATALITIES

### 2.3 Procedure for Estimating Benefit

The previous section has described a means of determining a barrier weight which might be expected to provide a given level of reduction in serious injuries or fatalities. The procedure described in this section attempts to quantify to a greater degree, the level of benefit associated with the chosen barrier weight and a closing velocity or, alternately, recommends a barrier test velocity which, in conjunction with the barrier weight will result in a given level of benefit.

The approach is based on a calculation of  $\Delta V$  imposed on a population of vehicles as a result of impact with a moving barrier of a given weight and speed based on plastic, central collision mechanics. An estimation of injuries incurred by near side occupants is then made from a cumulative frequency curve of injuries as a function of  $\Delta V$ . Calculations are repeated for a number of barrier weights and speeds, resulting in a series of curves relating injury to barrier weight, parametric in barrier velocity.

Data required for this procedure are

- passenger car frequency distribution as a function of weight
- cumulative distribution of severe injuries ( $AIS \geq 4$ ) incurred by near side passengers of cars struck on the side of the passenger compartment, as a function of lateral  $\Delta V$

The computational steps are outlined below

1. The frequency distribution of vehicle weights is divided into  $n$  discrete weight cells of constant cell width. The total number of vehicles in the

population is normalized to 1.0, thus the fraction of vehicles in each cell represents the probability of single vehicle being within that cell. The probability for each cell is assigned the symbol  $P_m$ , where the subscript  $m$  refers to the  $m$ th cell in the weight distribution. The corresponding value of weight,  $W_m$ , is taken as the midpoint value of weight cell  $m$ .

2. Choose a moving barrier speed,  $V_1$ .
3. For a moving barrier weight  $W_{Bj}$  (where  $W_{Bj} = W_m$  for  $m = j$ ), calculate a change in velocity ( $\Delta V$ ) for the entire distribution of struck car weights,  $W_{Sk} = W_m$  for  $m = k$ ). That is

$$\Delta V_{k,1} = \frac{W_{Bj} V_1}{(W_{Bj} + W_{Sk})} \quad \text{for } k = 1 \text{ to } n$$

4. For each computed  $\Delta V_{k,1}$  determine the fraction of serious injuries ( $AIS \geq 4$ ) that would occur from the NCSS developed cumulative distribution of injury versus lateral  $\Delta V$ . Assign this injury value to the symbol  $I_{k,1}$ . Sum the injury values weighted by the probability that the struck car is of weight  $W_{Sk}$ , i.e.,

$$B_{j,1} = \sum_{k=1}^n I_{k,1} P_k$$

$B_{j,1}$  thus represents the fraction of serious injuries incurred by near side occupants in the entire population of struck cars when impacted by a vehicle of weight  $W_{Bj}$  traveling at speed  $V_1$ .

- 5 Repeat Steps 3 and 4 for all barrier weights  $W_{BJ}$  considered in the analysis
6. Repeat Steps 3, 4 and 5 for all barrier velocities,  $V_1$ , considered in the analysis.

The application of this procedure results in a set of curves relating an expected benefit (or reduction in injuries) to barrier weight parametric in closing velocity. The benefit results from the assumption that vehicles will satisfy a no severe injury requirement (i.e.,  $AIS \geq 4$ ) when impact tested in a specified manner. Given a barrier weight, as determined from the procedure described in the previous section, the resulting curves can then be used to choose a test velocity once a desired level of benefit is established, or a level of benefit can be expressed as a function of test velocity

This information can then be used together with cost information in order to maximize a cost/benefit relationship to choose the test speed and level of benefit expected.

### 3. DISCUSSION OF RESULTS

In order to give some perspective to a total analysis of barrier weight and benefits for the 1985 time period, the procedure is first carried out for the current vehicle population. The vehicle weight distribution for the current population is assumed to be represented by the NCSS vehicle sample. Using this distribution, the probability of weight differences occurring, taking two vehicles at a time was calculated and is shown in Figure 9. Applying the fatality rate information developed in Section 2.2 to this distribution results in the cumulative fatality distribution shown in Figure 10. On this figure, the 50th percentile fatality level occurs at a weight difference of about 400 lbs. Applying the weight difference to the mode of the frequency distribution by weight yields a suggested barrier weight of 4275 lbs. From a cumulative weight distribution for this population, it is noted that some 73% of the cars are of weight less than or equal to 4275 lbs.

Application of the procedure described in Section 2.3 to this vehicle population yields the benefit curves shown in Figure 11. From this figure, it can be seen that with a barrier weight of 4275 lbs., 50% of the serious near side injuries could have been eliminated if all cars in the population had been required to comply with an AIS  $\leq$  4 specification when tested at a closing speed of approximately 32 MPH\*.

Projecting current side impact experience in combination with estimates of the vehicle population to the 1985 time period results in a cumulative fatality distribution as shown in Figure 12. From this figure, it is seen that 50 percent of all fatalities are expected to occur with a weight difference between striking and struck cars of about 300 lbs. or less. Applying this weight difference, which is representative of the more serious side collisions expected for this population, to the mode of the 1985 vehicle sales frequency by weight yields a suggested barrier weight of approximately 3425 lbs.

---

\* Actually barrier speed as analysis assumes barrier impact with a stationary vehicle.

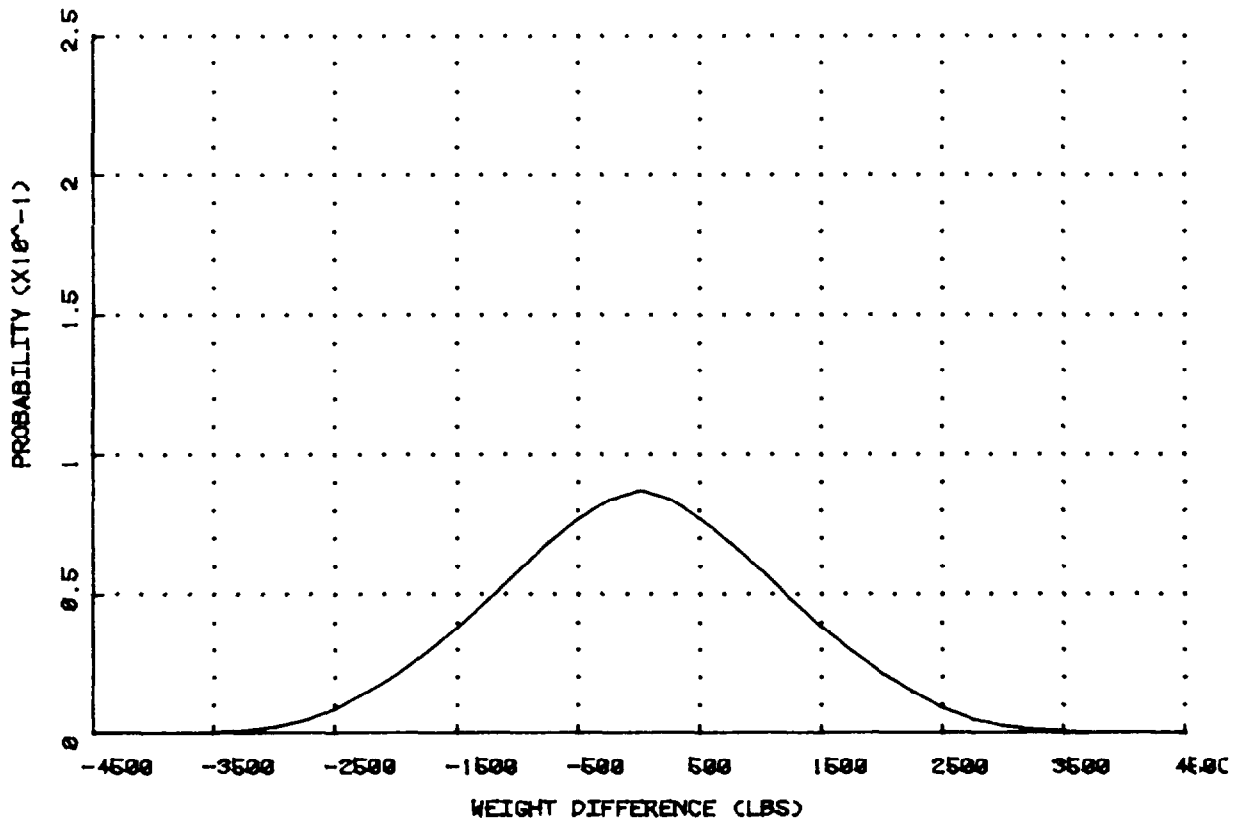


Figure 9 PROBABILITY OF WEIGHT DIFFERENCE FOR NCSS VEHICLE SAMPLE

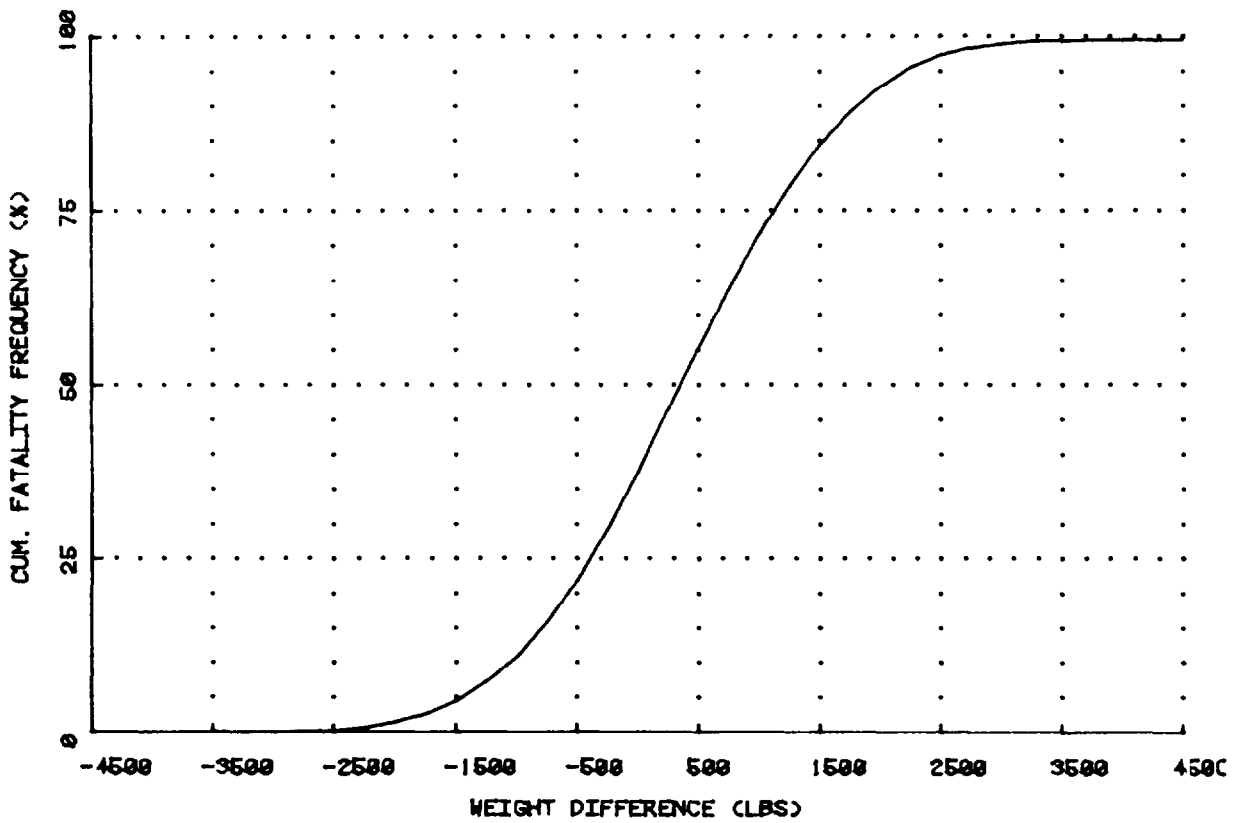


Figure 10 CUMULATIVE RELATIVE FATALITY FREQUENCY BY WEIGHT DIFFERENCE FOR 1978 VEHICLE POPULATION

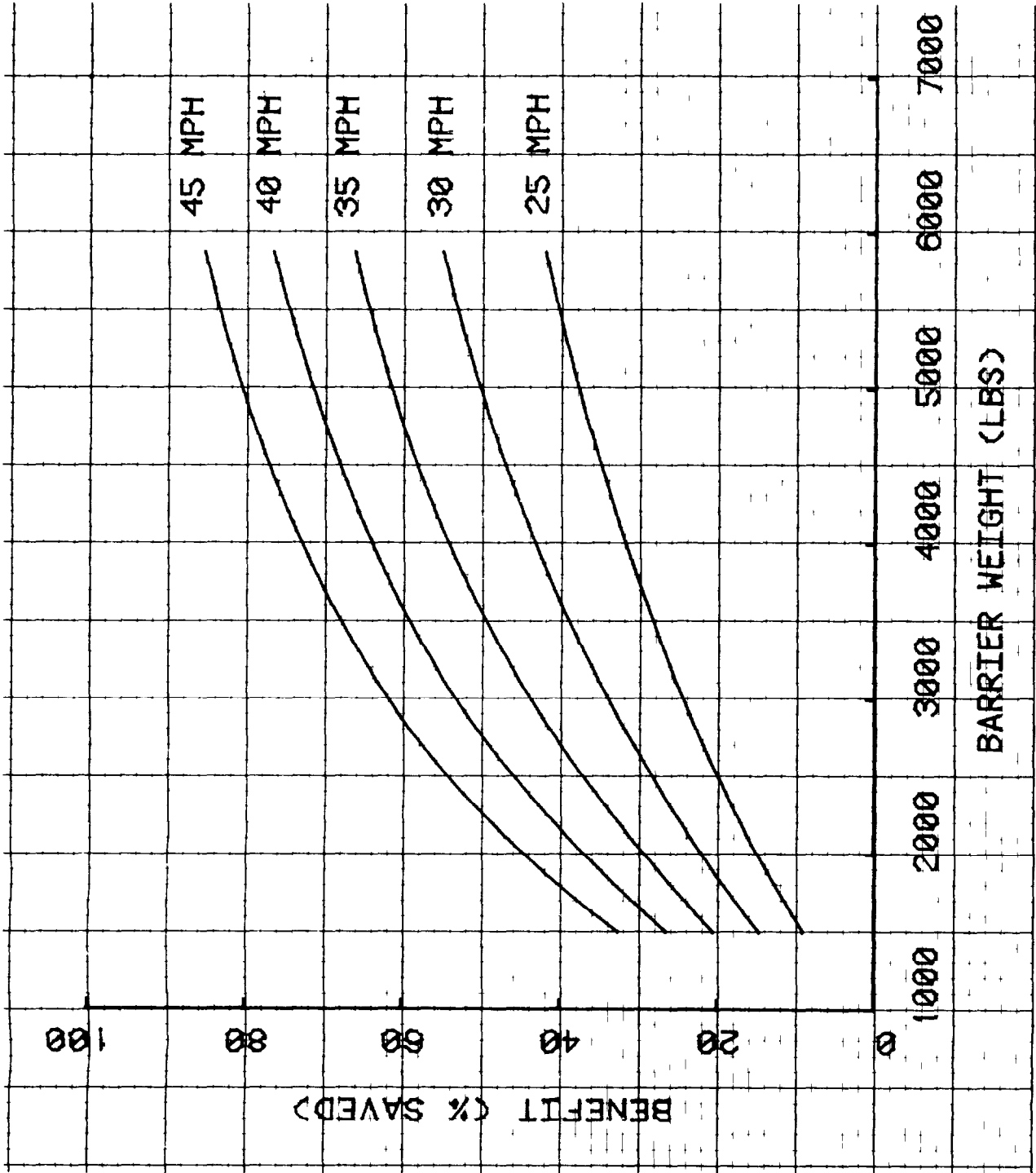


Figure 11 INJURY REDUCTION BENEFIT FOR 1978 VEHICLE POPULATION VS. BARRIER WEIGHT

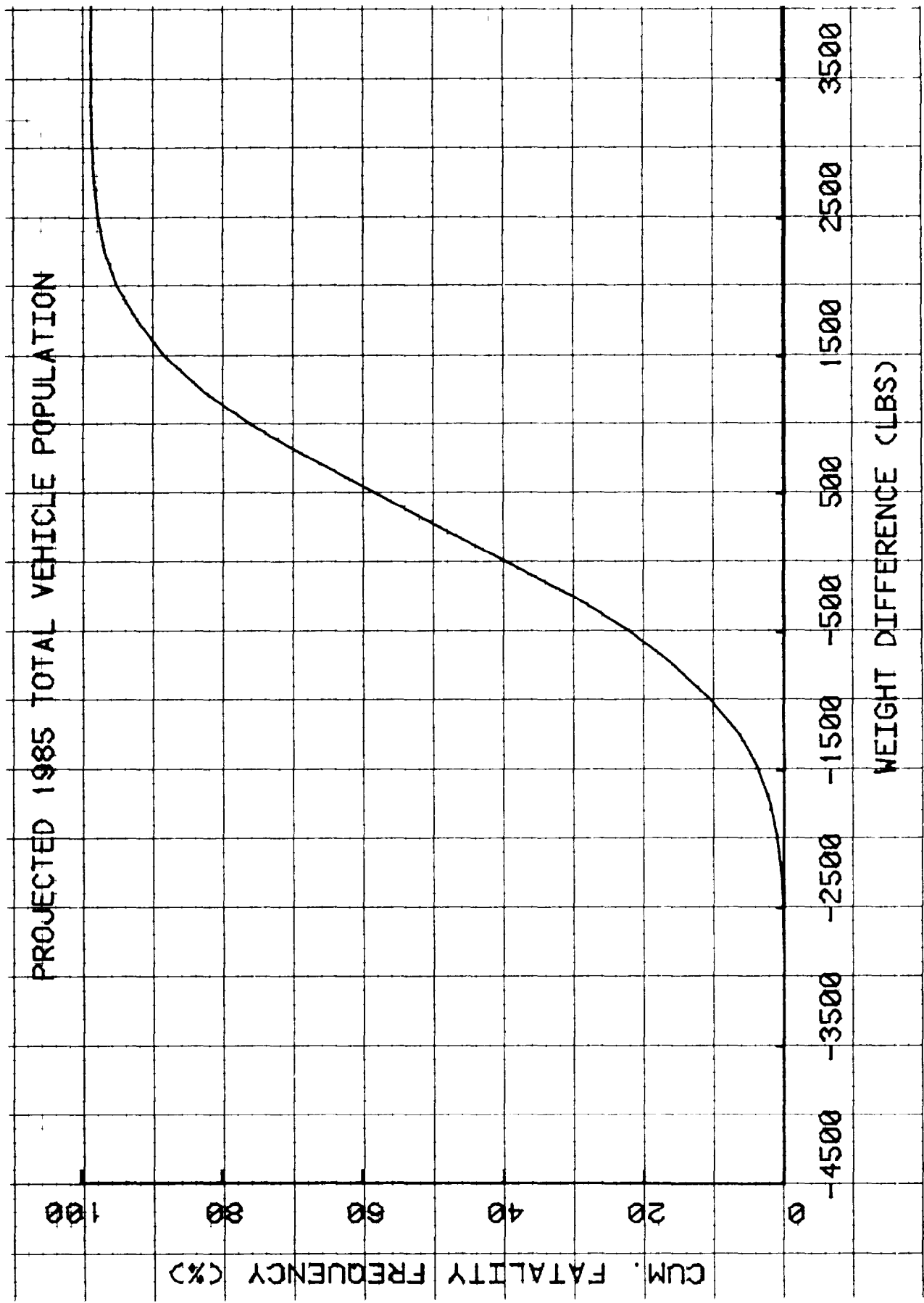


Figure 12 CUMULATIVE RELATIVE FATALITY FREQUENCY BY WEIGHT DIFFERENCE FOR 1985 VEHICLE POPULATION

Note that we believe it appropriate to apply this 300 lb. weight difference to the 1985 car sales population rather than the total population at that time since only the new production would be required to comply with the upgraded side protection standard. A moving barrier weight of between 3400 and 3500 lbs. will then reflect a condition that is characteristic of the more severe side collisions for the 1985 new car population. From Figure 1 it is seen that this weight will be greater than about 82% of the projected new car sales weight.

From Figure 13, it can be seen that a 50% benefit can be achieved for the new car population when tested at about 32 MPH with a barrier weight of 3450 lbs. The actual choice of the test speed, however, must be made considering the practicality of producing safety systems for the vehicles that would reduce injuries to less than the AIS = 4 level for the test conditions.

Applying this methodology to a projected mid 1980's vehicle population should result in test conditions for a side structure compliance test that will significantly increase occupant protection in those vehicles for which compliance is required. As discussed previously, a reasonable level of benefit cannot be chosen solely by this procedure; trade-offs of benefit against practicality (costs) are required. However, we believe that a barrier weight which is representative of the projected population can and has been determined. A second test parameter, impact velocity, can then be chosen to reflect the degree of benefit that is ultimately decided upon.

This study should not be considered to be a final statement of the test conditions for the proposed side structural performance requirement upgrade. Rather, it should be viewed as a development of a methodology which should be continually upgraded both with respect to the assumptions employed in the analysis and with respect to the data employed. In particular, injury data is being continually collected and the projected vehicle mix in the 1985 time period is undergoing continual refinement. As more, and presumably better,

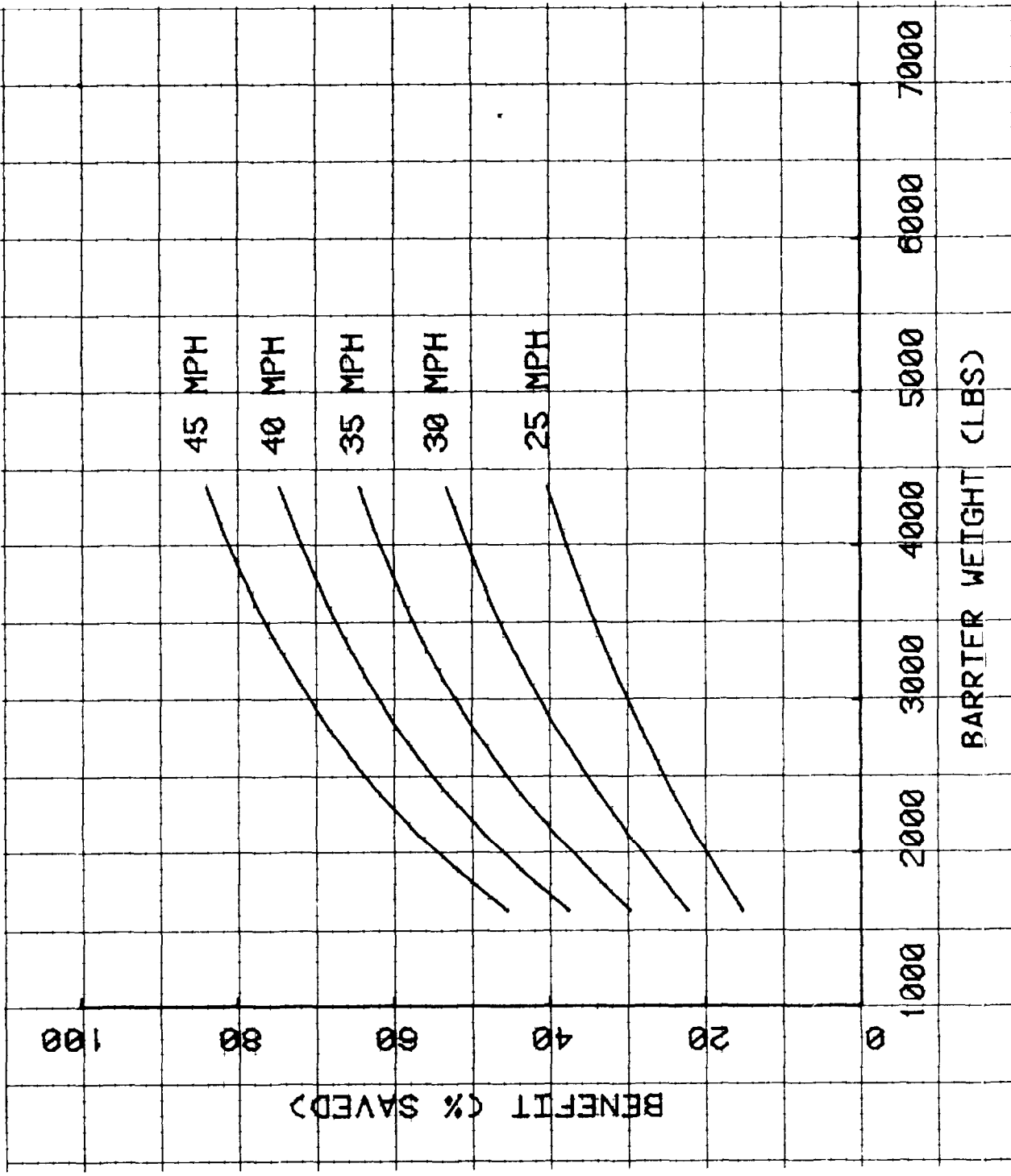


Figure 13 INJURY REDUCTION BENEFIT FOR 1985 VEHICLE SALES POPULATION VS. BARRIER WEIGHT

data become available, their influence on the conclusions of this study should be determined. Furthermore, efforts should be undertaken to extend this analysis to consider other test condition variables, such as impact orientation.

We also believe that it would be desirable to examine a limited number of NCSS accident cases that are representative of the recommended test conditions in order to develop a better understanding of the structural performance of the current car population under those conditions. This would lead to a better understanding of the degree of structural modifications that will be necessary to insure compliance on future vehicles.

4. REFERENCES

1. Hedlund, J., "Update of Distributions for Key Variables in Side Crashes, based on Aggregate NCSS Data," Memorandum to J Hackney, February 2, 1979.
2. Burgett, A., "A Method for Estimating the Effect of Weight of Barrier in Side Impacts," Unpublished
3. Jatras, K. and Carlson, W., "Frequency Distributions of Passenger Cars by Weight and Wheelbase by State - July 1, 1976," Report No. DOT-HS-803 382, June 1978.
4. Data supplied by Carl Ragland, U. S Department of Transportation, National Highway Traffic Safety Administration, September 1979.
5. "Passenger Car Specifications," Report No. DOT-HS-802 435, prepared by the Motor Vehicle Manufacturers Association, June 1977.
6. "Research Safety Vehicle (RSV) Phase I Final Report--Volume II, Automobile Usage Trends, Accident Factors," Ford Motor Company, Contract No. DOT-HS-4-00842, Report No. DOT-HS-801 599, June 1975.
7. Partyka, S., "Incidence of Fatality and Injury in Car-to-Car Side Crashes by Striking Vehicle Weight," National Center for Statistics and Analysis, August 1979.

APPENDIX D  
MGA OCCUPANT INJURY ANALYSIS REPORT

MGA RESEARCH CORPORATION  
58 Sonwil Drive  
Buffalo, New York 14225  
(716) 683-5855

AN ANALYTICAL STUDY  
OF OCCUPANT INJURY  
IN OBLIQUE SIDE COLLISIONS

David J. Segal

November 1981

FINAL REPORT  
MGA Report No. G9-003-V-2

Dynamic Science Purchase Order No. 02668  
Contract No. DOT-HS-8-01933

Prepared for:  
Dynamic Science, Inc.  
1850 West Pinnacle Peak Road  
Phoenix, Arizona 85027

## TABLE OF CONTENTS

	<u>Page No.</u>
1. INTRODUCTION	1
2 CONCLUSIONS	4
3. TECHNICAL APPROACH	7
3.1 Modeling Approach	7
3.2 Parameter Study Plan	9
4. DISCUSSION OF RESULTS	21
4.1 Frontal Force-Crush Characteristics	21
4.2 Simulation Parameter Study	26
5. REFERENCES	44
APPENDIX A SPRING-MASS DYNAMICS SIMULATION (SMDYN)	A-1
APPENDIX B AUTOMOBILE FRONTAL STRUCTURE FORCE-CRUSH CHARACTERISTICS	B-1
APPENDIX C Sample SMDYN Inputs	C-1

## LIST OF FIGURES

<u>Figure No.</u>	<u>Title</u>	<u>Page No.</u>
1	Oblique Side Impact Modeling Approach	8
2	Side Impact Model Schematic	10
3	Comparison of Simulated and Measured Struck Car Lateral Acceleration	11
4	Comparison of Simulated and Measured Struck Door Velocity	12
5	Comparison of Simulated and Measured Occupant Lateral Acceleration	13
6	Projected 1985 Distribution of New Car Sales by Weight	15
7	Simulated Struck Car Upper and Lower Side Force-Crush Characteristics	16
8	Inner Door Panel Padding/Occupant Force-Crush Characteristics	17
9	Simulated Upper and Lower Striking Car Force-Crush Characteristics	19
10	Sample 0 and 30 Degree Force-Crush Characteristics	22
11	Comparison of Static and Dynamic Force-Crush Characteristics	27
12	Struck Door Intrusion vs. Striking Car Stiffness	29
13	Struck Door-Occupant Contact Velocity vs. Striking Car Stiffness	30
14	Struck Door-Occupant Contact Velocity vs. Struck Car Weight	31
15	Occupant Velocity Change vs. Striking Car Stiffness	32
16	Occupant CSI vs. Striking Car Stiffness	34

LIST OF FIGURES (CONTD.)

<u>Figure No.</u>	<u>Title</u>	<u>Page No.</u>
17	Door Padding-Occupant Crush vs. Striking Car Stiffness	35
18	Maximum Struck Door Relative Velocity vs. Striking Car Stiffness	37
19	Maximum Struck Door Relative Velocity vs. Struck Vehicle Weight	38
20	Struck Door-Occupant Contact Velocity vs. Striking Car Stiffness	39
21	Occupant Velocity Change vs. Striking Car Stiffness	40
22	Maximum Struck Door Relative Velocity vs. Striking Car Stiffness	41

LIST OF TABLES

<u>Table No.</u>	<u>Title</u>	<u>Page No.</u>
1	Parameter Study Variations	20
2	Dynamic Force-Crush Summary for Full Frontal Barrier Collisions	24
3	Dynamic Force-Crush Summary for 30° Frontal Collisions	25

SUMMARY OF AN ANALYTICAL STUDY OF OCCUPANT INJURY  
IN OBLIQUE SIDE COLLISIONS

Dynamic Science, Inc., is currently involved in the development of a side impact device and compliance test procedure under Contract No. DOT-HS-8-01933 for the National Highway Traffic Safety Administration. The proposed side impact device will include a deformable front face which would simulate the front end of the striking vehicle more realistically than the rigid side impact device currently used in side impact testing. In order to develop force-deflection characteristics of this deformable face, an analysis of available crash test results was conducted.

Frontal force-crush characteristics were approximated using data obtained from crash tests conducted at Dynamic Science, Inc. and Calspan Corporation. Structural characteristics for both full frontal engagement and loading along a direction 30 degrees to the longitudinal axis were obtained and characterized by an initial structural stiffness and an effective yield strength. The initial stiffness and yield level were chosen to equilibrate the area under the actual curve to the area under the simple fit, up to a point representing 80 to 90% of the maximum deflection.

Results for all the vehicles involving full frontal engagement were averaged to obtain a structural stiffness of 5.3 kips/in and a yield force level of 78 kips. Similarly, results for all the vehicles involving 30° frontal collisions were averaged to obtain a structural stiffness of 2.8 kips/in and a yield force level of 27 kips.

Based on a comparison of the average obtained in the two different test configurations, it appears that the effective stiffness of a vehicle's front structure is reduced by about 45% as the impact direction changes from 0 to 30°. The effective yield force level is reduced by about 55% for the same change in impact direction.

The effects of striking car frontal-crush characteristics on occupant injury exposure were also investigated in this effort, through the use of a one-dimensional lumped-mass, dynamics computer simulation (referred to as SMDYN). Throughout the simulation study, the striking car weight was fixed at 3450 lbs, and the speed and orientation simulated represented a 35 mph, 60 degree oblique side impact. The primary parameters investigated were the weight of the struck car, over a range of 2000-4000 lbs in 500 lb increments, and, the front structural characteristics of the striking car. The baseline level of front structural stiffness approximated the average frontal stiffness of the four cars for which force-crush data was available along a direction 30 degrees to the longitudinal axis. Stiffness levels including 50%, 150%, and 200% of the baseline stiffness level were investigated. Side structural characteristics of the simulated struck cars were then developed from measurements of a modified VW Rabbit side structure. These characteristics were assumed to be the same for all struck vehicles studied.

Several direct and indirect indicators of injury severity were studied in the simulated collisions including, occupant change in velocity, Chest Severity Index (CSI), relative velocity between the occupant and door at contact, maximum door velocity relative to the struck vehicle, door intrusion, and maximum interior door padding crush.

The analytical study results indicated that a moving barrier frontal stiffness can be chosen that is both representative of the vehicle population and capable of providing severe occupant exposure in side impacts. A frontal stiffness of about 3000 lbs/inch as measured along a direction 30 degrees from the longitudinal axis of the test vehicle is recommended for a 60° oblique side collision. However, it is also recommended that additional studies be conducted to clarify and confirm these results.

## 1. INTRODUCTION

Accident studies, particularly the National Crash Severity Study (NCSS), have provided information indicating the serious nature of the current side impact problem. For example, Reference 1 indicates that the side impact accidents contained in the NCSS file constitutes 26% of the vehicles, 27% of the occupants, 53% of the serious (AIS  $\geq$  4) injuries, and 36% of the fatalities.

In response to this problem, the National Highway Traffic Safety Administration (NHTSA) has placed a high priority on reducing the injuries resulting from side impacts. A major effort to upgrade FMVSS 214, "Side Impact Protection" is currently underway. As part of this overall effort, Dynamic Science, Inc., under Contract No. DOT-HS-8-01933, is developing for NHTSA a side impact test device (i.e., impacting barrier) and demonstrating a compliance test procedure. MGA Research Corporation is supporting the Dynamic Science project under a subcontract arrangement.

The proposed side impact test device that is under development will include a deformable front face and thus is expected to be a more realistic simulation of actual side collisions than would be possible by using a rigid moving barrier. Our activities, described in this report, have involved developing information which may be used by NHTSA to select frontal stiffness characteristics of the side impact test device. The test procedure that will be developed by Dynamic Science is intended to be reasonably representative of the more severe actual car-to-car collisions, and thus, knowledge of both frontal force-crush characteristics of existing vehicles and the influence of these characteristics on occupant injury levels was necessary. The specific activities called out in the Statement of Work for which MGA provided support were

"...the Contractor shall determine approximations of frontal force-crush characteristics by vehicle weight category, using the results of Phase II - Task 3 and other sources.

Analytically estimate, if possible, the sensitivity of occupant injury levels to crush characteristics within the range determined above when the following parameters are held constant; weight, speed, and orientation of the striking vehicle. Assume the struck vehicle has modified side structure and reasonable padding. Perform the analysis for five (5) hypothetical weights for struck vehicles. If possible, determine the optimum (in terms of injury reduction in a 1985 mix of new vehicles) force-crush characteristics for a side impact barrier."

Crash tests conducted at Dynamic Science, Inc. and Calspan Corporation provided data from which approximations to frontal force-crush characteristics were obtained. Structural characteristics for both full frontal engagement and loading along a direction 30 degrees to the longitudinal axis were obtained and characterized by an initial structural stiffness and an effective yield strength for ease of comparison. The resulting information is presented and discussed in Section 4 of this report.

An analytical investigation of the effects that striking car frontal force-crush characteristics, or stiffness, have on occupant injury exposure was carried out with a one-dimensional lumped-mass, dynamics computer simulation. An overview of this simulation, referred to as SMDYN, is provided in Appendix A. Throughout the simulation study, weight of the striking car was held constant at 3450 lbs. and the speed and orientation simulated represented a 35 MPH, 60 degree oblique side impact. The primary parameters investigated were weight of the struck car, which ranged from 2000 lbs. to 4000 lbs. in 500 lb. increments, and frontal structural characteristics of the striking car. A baseline level of front structural stiffness was obtained from the compilation of force-crush characteristics. The level used as the baseline condition approximated the average frontal stiffness of the three cars for which force-crush data was available along a direction 30 degrees to the longitudinal axis. Variations of this baseline stiffness studied included 50%, 150% and 200% levels.

Side structural characteristics of the struck cars simulated were developed from measurements made on a modified VW Rabbit side structure which

was considered to be representative of the structural improvements available in the 1985 time frame. These characteristics were assumed to be the same for all struck vehicles studied.

A number of direct and indirect indicators of injury severity were studied in an attempt to establish occupant injury sensitivity to striking car stiffness in the simulated collisions. These included: occupant change in velocity, Chest Severity Index (CSI), relative velocity between the occupant and door at contact, maximum door velocity relative to the struck vehicle, door intrusion and maximum interior door padding crush.

Results from the analytical study indicate that a moving barrier frontal stiffness can be chosen that is representative of the vehicle population and which will provide severe occupant exposure in side impacts. A frontal stiffness of approximately 3000 lbs/inch, as measured along a direction 30 degrees from the longitudinal axis of the test device, is recommended for a 60° oblique side collision. However, it is also recommended that additional studies be conducted to clarify and confirm results obtained.

Conclusions from this study are discussed in the following section of this report. Section 3 provides a description of the modeling methodology employed in the analytical study and a discussion of the data and parameters investigated. Vehicle front structure force-crush data and simulation parameter study results are presented and discussed in Section 4.

## 2. CONCLUSIONS

Conclusions resulting from our activities in support of development of a side impact test device are given in this section. It should be noted that the analytical study conducted represents an initial attempt at simulation of oblique side collisions with a one-dimensional lumped mass model. As such, it has resulted in pointing out many areas which require further study if a more complete understanding of the interrelationships of the many variables associated with the side impact event is to be attained. The conclusions described below reflect some unexpected results and, without a better understanding of the side collision event, should be viewed as tentative subject to confirmation by additional analytical or experimental studies.

1. Of the twenty-one cars involved in full frontal barrier collisions for which data was available, the average front structural stiffness was approximately 5.5 kips/inch. Values obtained from force-deflection characteristics ranged from 2.3 to 7.9 kips/inch. In general, this simplified stiffness representation of force-crush properties was reasonable up to about 5 inches of deformation. Of the four cars for which force-crush data was available along a direction 30° to the longitudinal axis, the average front structural stiffness was 2.8 kips/inch. Minimum and maximum values were 2.3 and 3.2 kips/inch, respectively. For this loading orientation, the simple stiffness representation provided a good fit to the force-crush characteristic up to at least 10 inches of deformation.

2. The modeling approach used in this study to simulate a 60 degree oblique side collision resulted in good agreement of struck vehicle responses, including door and occupant response, with test measurements made on a structurally modified vehicle. However, certain assumptions were made regarding the input data for this comparison as sufficiently detailed data was not available. Consequently, the model may be assumed to result in qualitatively correct predictions of other crash configurations, but caution should be exercised in interpreting results quantitatively.

3. Near side occupant response to lateral impacts is related to the response of the struck door, however, this relationship is not completely understood. There are a number of variables that have a primary effect on door response--striking car stiffness, struck car structural characteristics and the effective door weight. Results indicate that if structural characteristics and effective door weight remain constant, there is little variation of occupant severity exposure as struck car weight varies. However, large variations in severity were obtained as effective door weight was assumed to be proportional to struck car weight. Further investigation of the role played by these variables in analytical studies of side impacts is required.

4. Occupant severity exposure tends to increase as the initial spacing between the occupant and inner door surface decreases. Parameter study results showed that the occupant change in velocity increased with a reduced spacing even through the relative velocity between the door and occupant at initial contact decreased.

5. Direct measures of injury severity, occupant change in velocity and CSI, do not appear to be strongly related to the maximum door panel velocity relative to the struck car. As expected, the peak door velocity increases monotonically with increasing striking car stiffness but severity measures do not necessarily follow this increase. It is not currently known whether this behavior results from a modeling or data limitation. Additional studies should be undertaken to clarify this behavior.

6. Based on the results of this brief study, there appears to be a saturation of occupant injury severity measures at the nominal striking car stiffness. That is, with the assumption that the effective door weight remains constant across the spectrum of struck cars, the change in velocity sustained by the occupant did not increase as the striking car stiffness was increased by 50% above this nominal level. The occupant CSI actually decreased under the same conditions. This nominal striking car stiffness corresponds to a value of about 3000 lb/in (measured at a 30 degree angle relative to the longitudinal

axis of the striking car), approximately the mean of the three cars for which data was available. Subject to further confirmation of the results of this study, a stiffness of the side impact test device of approximately 3000 lbs/in is recommended.

### 3. TECHNICAL APPROACH

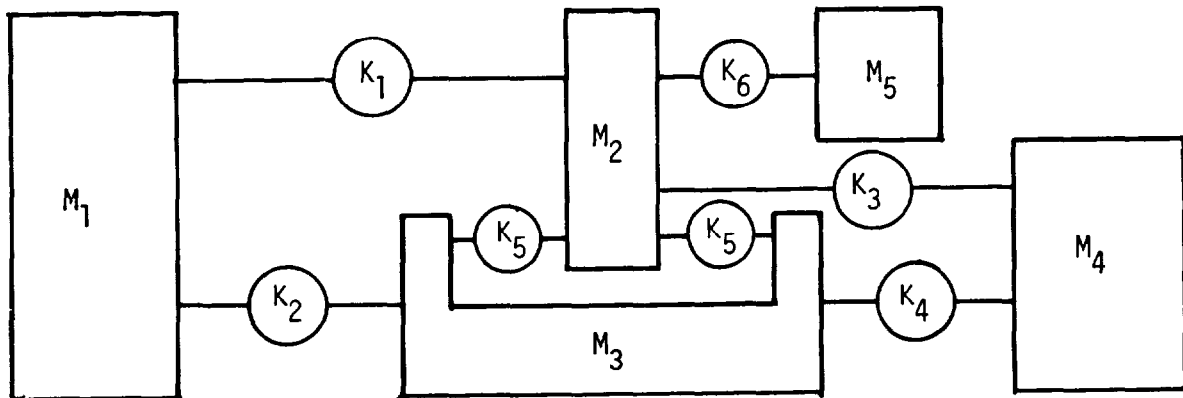
As noted in the Introduction, the objectives of this study were twofold:

- 1) to determine approximations of frontal force-crush characteristics by vehicle weight category and,
- 2) to analytically estimate, if possible, the sensitivity of occupant injury levels to striking car crush characteristics and determine the optimum force-crush characteristics for a side impact barrier.

The first of these two objectives is straightforward to accomplish given the necessary data and the results, in fact, serve to provide input data for accomplishing the second objective. The problem of estimating the sensitivity of occupant injury in side collisions to the range of frontal stiffness is considerably more challenging due to the inherent complexity of the event. Nonetheless, an attempt has been made to evaluate injury sensitivity using various measures of severity with a lumped-mass dynamics model (SMDYN) as described immediately following. A second subsection describes the parameter study performed with the model.

#### 3.1 Modeling Approach

As subcontractor to The Budd Company on the NHTSA sponsored "Lightweight Subcompact Vehicle Side Structure Program," (DOT-HS-7-01588), MGA has been evaluating modeling procedures for the simulation of 60 degree oblique side collisions. Our efforts under that program have resulted in a technique which has successfully duplicated, to a reasonable degree, the response of the struck car and dummy (Ref. 2). In this technique, the direction of interest (i.e., the effective direction of motion of the one-dimensional model) lies along the lateral axis of the struck car. This modeling concept is illustrated in Figure 1



- $M_1$ : Striking car mass
- $M_2$ : Upper load path interface mass (upper door)
- $M_3$ : Lower load path interface mass (lower door/sill)
- $M_4$ : Struck car mass
- $M_5$ : Struck car LF occupant

- $K_1$ : Striking car upper load path resistance
- $K_2$ : Striking car lower load path resistance
- $K_3$ : Struck car upper load path resistance
- $K_4$ : Struck car lower load path resistance
- $K_5$ : Upper/lower door relative motion resistances
- $K_6$ : Combined door padding & dummy compliance

Figure 2 SIDE IMPACT MODEL SCHEMATIC

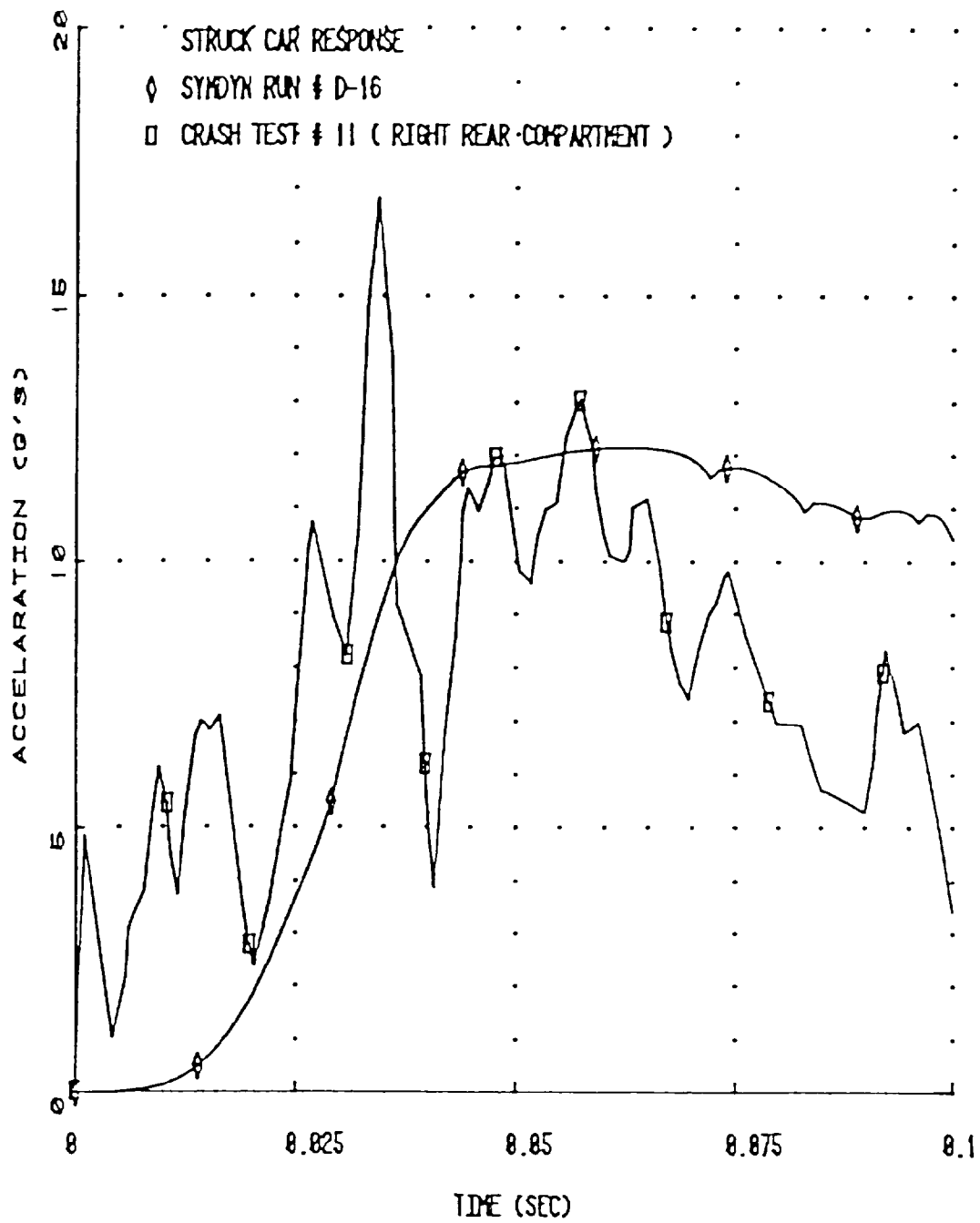


Figure 3 COMPARISON OF SIMULATED AND MEASURED STRUCK CAR LATERAL ACCELERATION

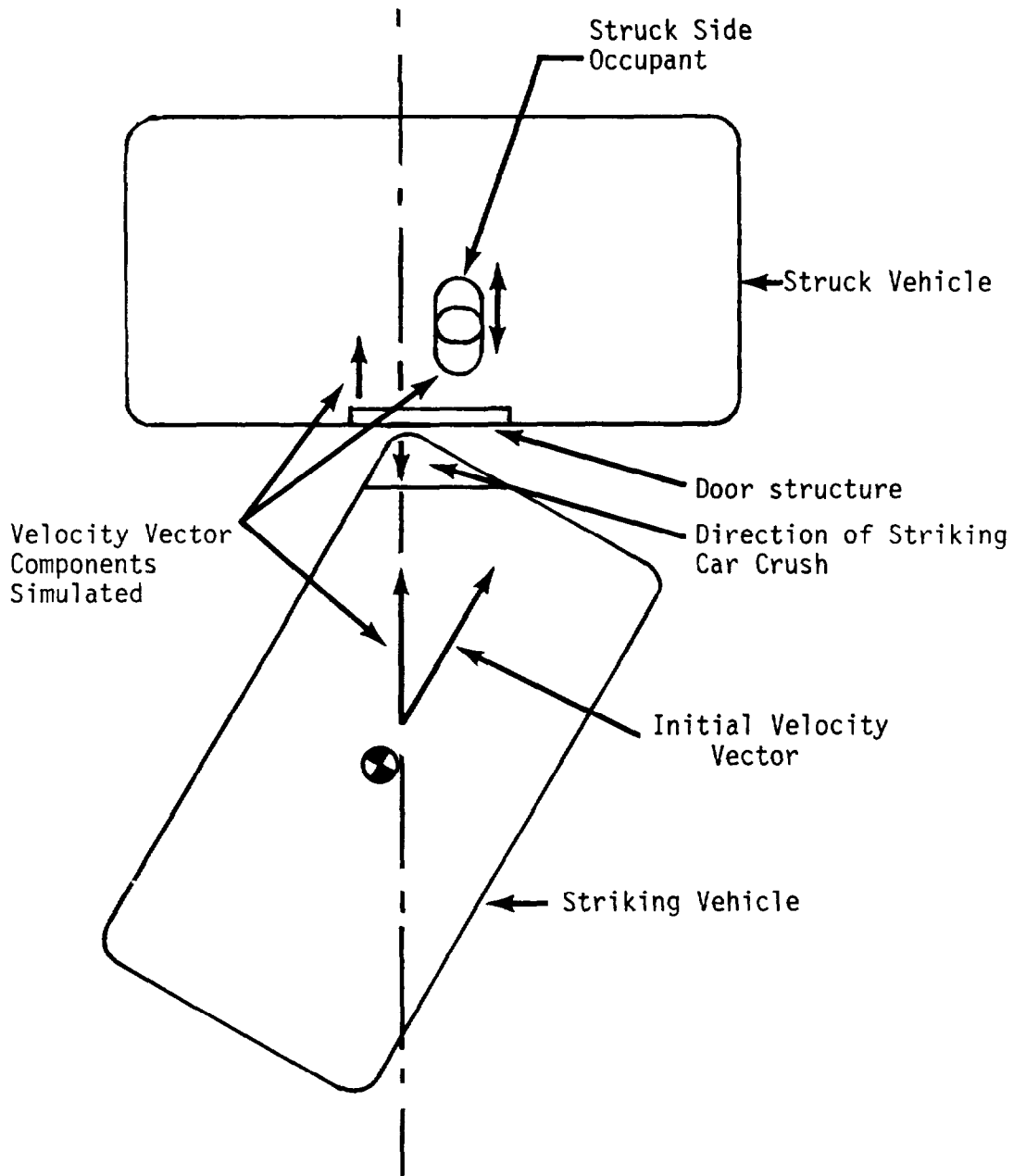


Figure 1 OBLIQUE SIDE IMPACT MODELING APPROACH

A schematic diagram of the lumped mass model used in the subsequent simulation runs is illustrated in Figure 2. Within this model, the striking car is represented as a single mass with an upper and lower load path interacting with the struck car. The struck car is represented by three masses, an upper door mass, a lower door/sill mass, and the remainder of the vehicle mass. A single mass is used to represent the struck side occupant. Two primary load paths are assumed to exist in the struck car structure; one acting between the upper door and the body (representing the force transmission through the A and B posts), the other acting between the lower door/sill mass and the body (representing force transmission through the sill and floor). A force-deflection characteristic representing the resistance to relative motion between the two door masses is included. The resistance acting between the occupant and upper door represents a series combination of dummy compliance and inner door panel crush characteristics.

Limited verification of this modeling approach has been made by comparison of model responses with test measurements. Since this work is being conducted under Contract No. DOT-HS-7-01588, a detailed description is not provided herein. However, it is pointed out that while much of the required input data was available from testing carried out under that contract, assumptions regarding certain struck car force-crush characteristics and effective masses were made based on engineering judgment. Comparisons of selected model predictions and test measurements are shown in Figure 3 through 5 to illustrate the degree of agreement achieved.

### 3.2 Parameter Study Plan

The parameters of primary interest in the analytical investigation included weight of the struck car and frontal stiffness of the striking car. Weight, speed and orientation of the striking car were held constant. The struck car was assumed to have a modified side structure and reasonable interior door padding.

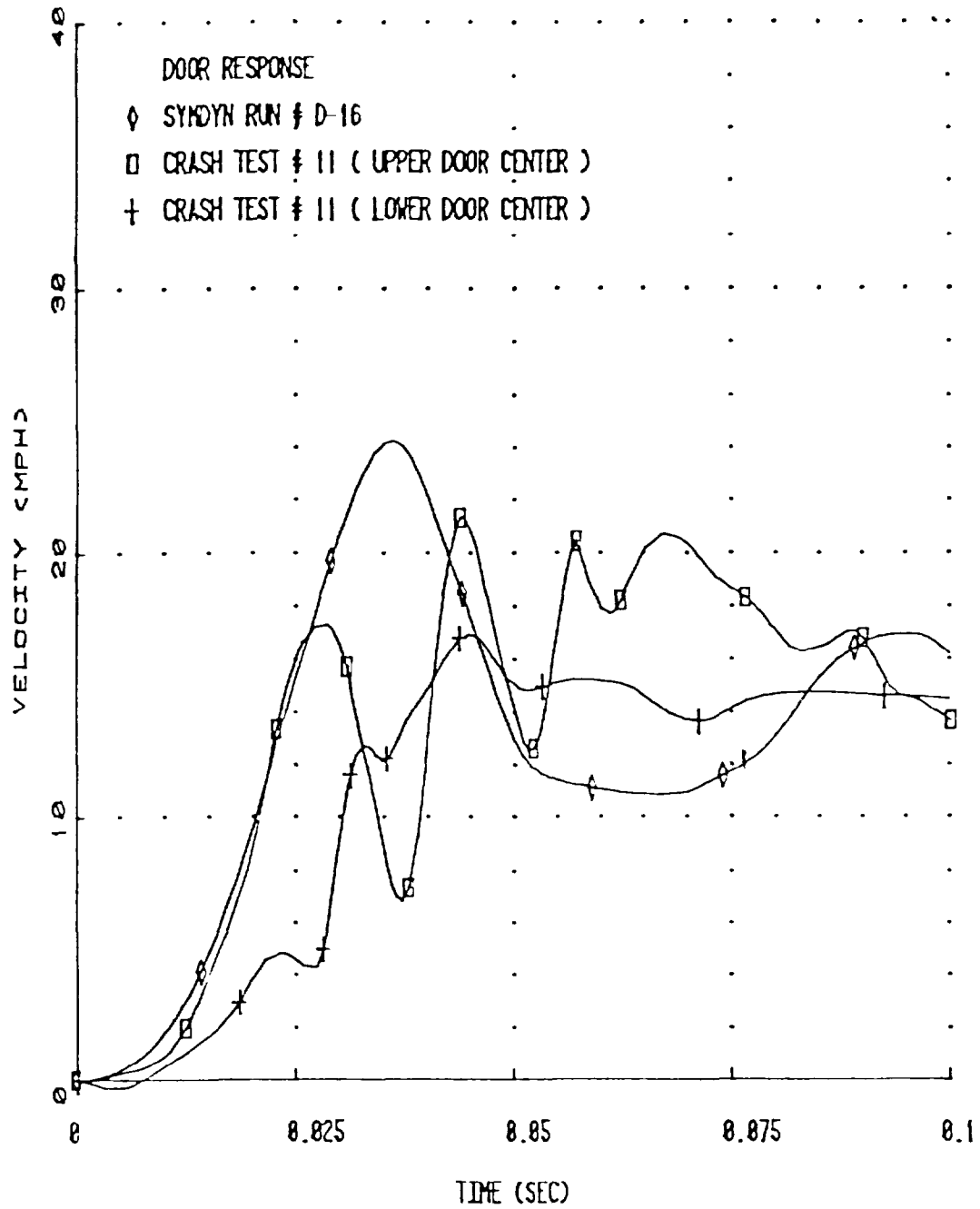


Figure 4 COMPARISON OF SIMULATED AND MEASURED STRUCK DOOR VELOCITY

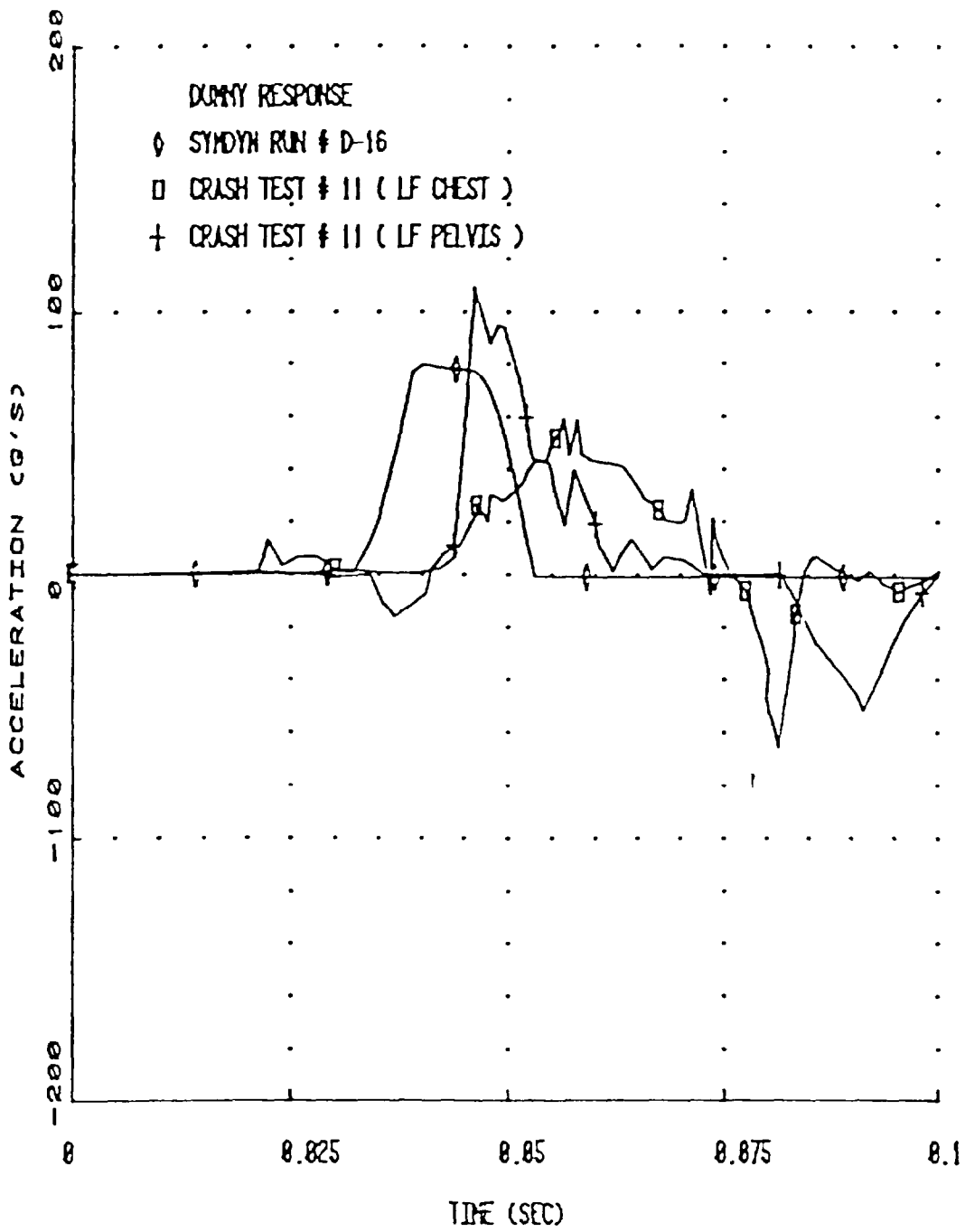


Figure 5 COMPARISON OF SIMULATED AND MEASURED OCCUPANT LATERAL ACCELERATION

Five struck car weights were simulated based on the projected 1985 new car sales weight distribution developed in a companion study (Ref. 3). A distribution of the percentage of new car sales by weight for the 1985 time period is included as Figure 6. Based on this data, struck car weights ranging from 2000 lbs. to 4000 lbs. in increments of 500 lbs. were considered in this simulation parameter study.

Strengthened side structure force-crush data was available only for modified VW Rabbits developed under Contract DOT-HS-7-01588. The middleweight (30 lb.) structural modification was selected as representing structural characteristics that might be available during the 1985 time frame. It was further assumed that the total force-crush characteristic was split between a lower and upper load path according to an 80/20 ratio. These force-crush characteristics are shown in Figure 7 and were assumed to be the same for all struck vehicle weights considered in the study.

A force-deflection characteristic representing a series combination of lateral dummy compliance and yielding door panel padding, shown in Figure 8, was used throughout the parameter study. A basic spacing between the occupant and door padding of 5.0 inches was used; however, a number of runs were made with a 2.5 inch spacing. An effective occupant weight of 50 lbs. was used based on test results from Ref. 4. Initially, the upper and lower door masses were assumed to vary between 80 and 160 lbs. proportional to the struck car weight. However, additional runs were made with these door weights assumed to be 100 lbs. for all struck vehicles.

Striking vehicle information required for the parameter study included vehicle weight and frontal stiffness characteristics. A companion study (Ref. 3) resulted in a suggested moving barrier weight for side impact testing of approximately 3450 lbs. This value was used throughout this study as the striking vehicle weight.

As was noted previously, one of the objectives of this study was to determine approximations of vehicle frontal crush characteristics by weight

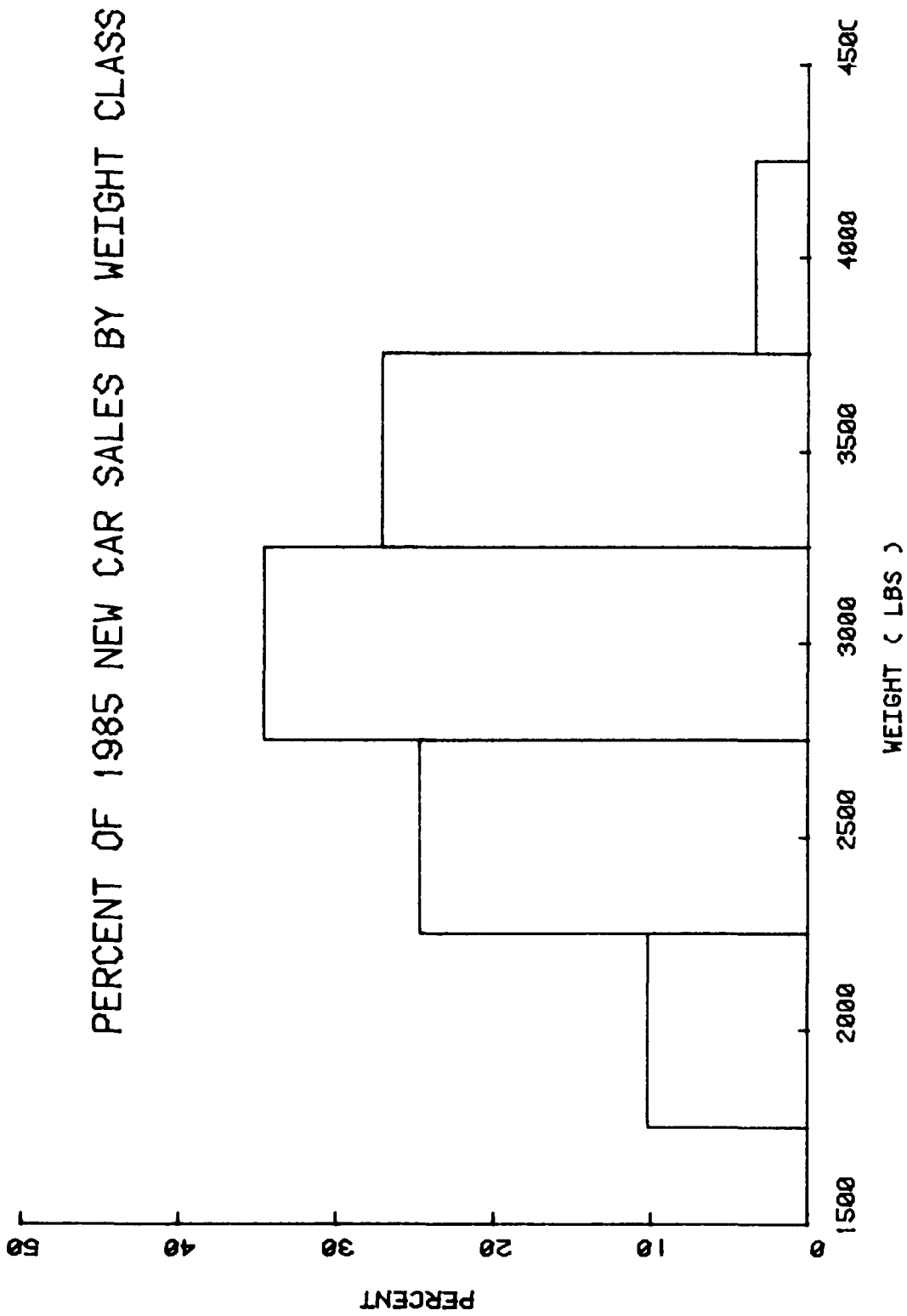


Figure 6 PROJECTED 1985 DISTRIBUTION OF NEW CAR SALES BY WEIGHT

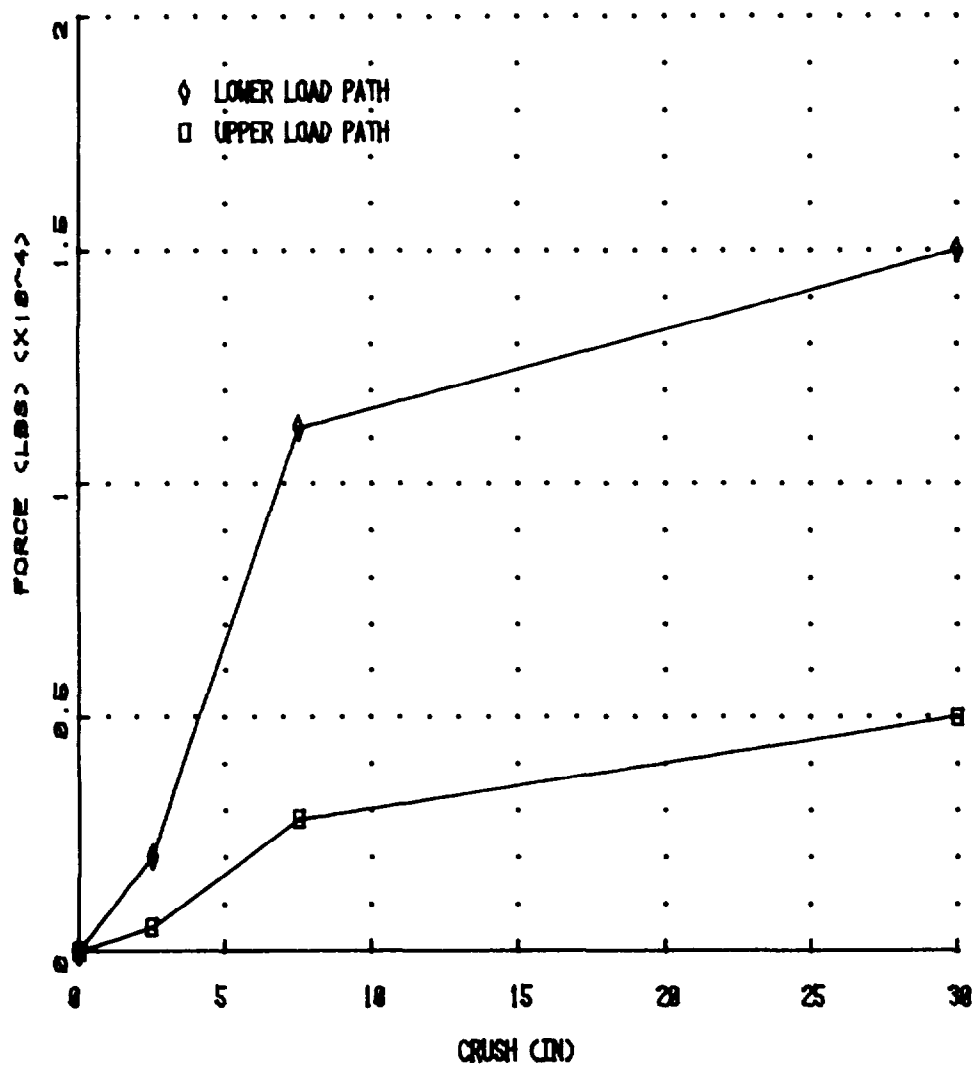


Figure 7 SIMULATED STRUCK CAR UPPER AND LOWER SIDE FORCE-CRUSH CHARACTERISTICS

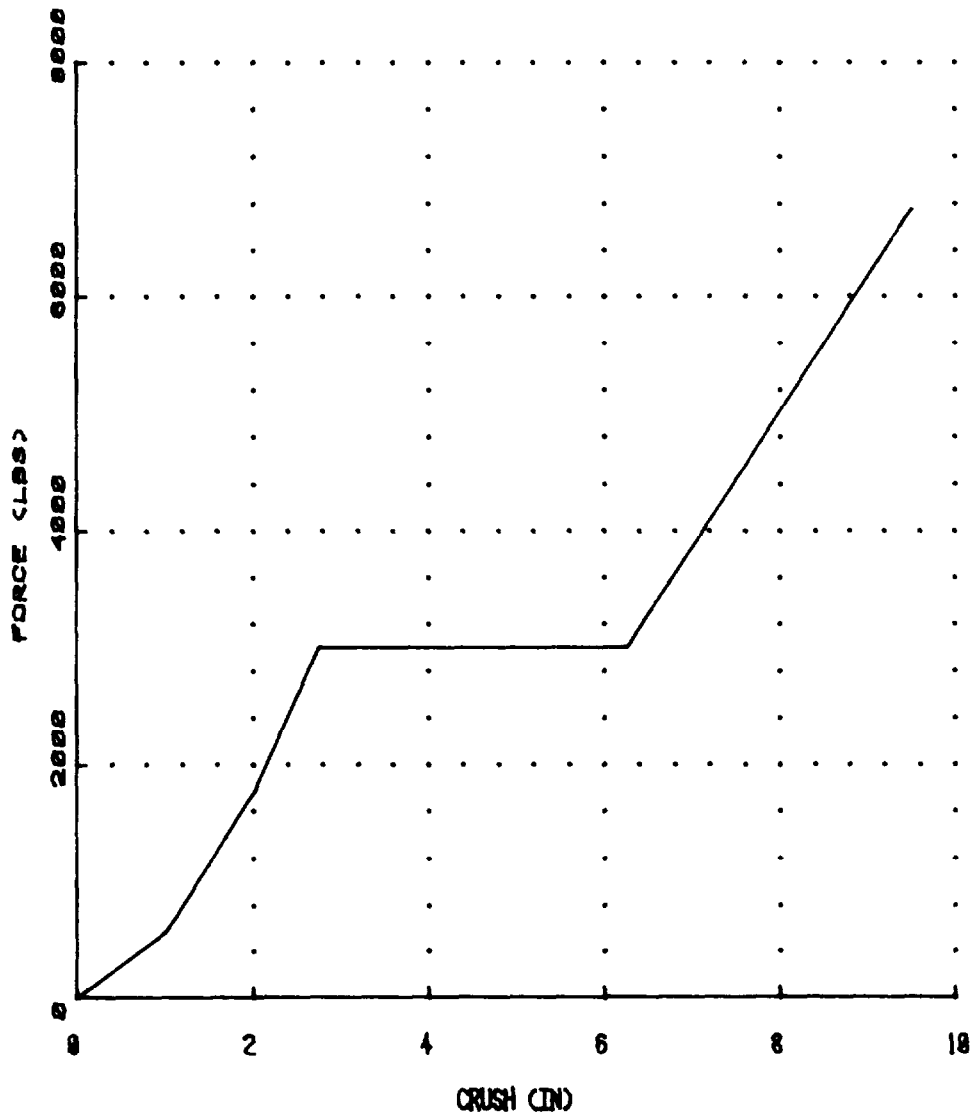


Figure 8 INNER DOOR PANEL PADDING/OCCUPANT  
FORCE-CRUSH CHARACTERISTIC

categories. Crash tests conducted under Contract Nos. DOT-HS-8-01938, DOT-HS-8-01933 and DOT-HS-5-01099 provided the data from which crush characteristics were developed. Frontal barrier crash tests conducted at Calspan Corporation under Contract Nos. DOT-HS-8-01938 and DOT-HS-5-01099 were conducted at 35 or 40 MPH and measurements of barrier load were made. Double integration of the average compartment longitudinal acceleration provided a measure of deflection against which the measured barrier force was plotted.

Tests conducted at Dynamic Science, Inc. under Contract No. DOT-HS-8-01933 were made with the NHTSA moving load cell barrier test device impacting stationary vehicles angled at 30 degrees to the direction of travel of the test device. These tests provided a measure of force-crush characteristics along a direction perpendicular to the initial plane of the side of a struck car in a 60° side impact test.

The frontal stiffness data obtained from these test results is discussed in the following section. For the purpose of defining the simulation parameter study, however, a nominal frontal stiffness was chosen as a baseline condition based on the approximate mean stiffness as determined from the Dynamic Science test results which simulate the effective striking car stiffness in a 60° side collision. Note that since these tests were conducted with a segmented load cell barrier face, upper and lower load path levels were available for the front structure. The nominal front structural force-crush characteristics used in the parameter study and represent the characteristics appropriate for the 60° side collision orientation assumed in the study. Note that the nominal frontal stiffness chosen for the simulation study was approximately 3000 lb/in (total of both upper and lower load paths). Variations in stiffness about this nominal value were then explored to estimate its influence on occupant injury. These variations included a 50% decrease, a 50% increase, and in some cases, a 100% increase in this stiffness.

Striking car speed was assumed to be 35 MPH throughout the study. Note that due to the coordinate system employed, the velocity component along the lateral axis of the struck car, 30.3 MPH, was used in the simulation runs. A matrix of parameter changes investigated is shown in Table 1.

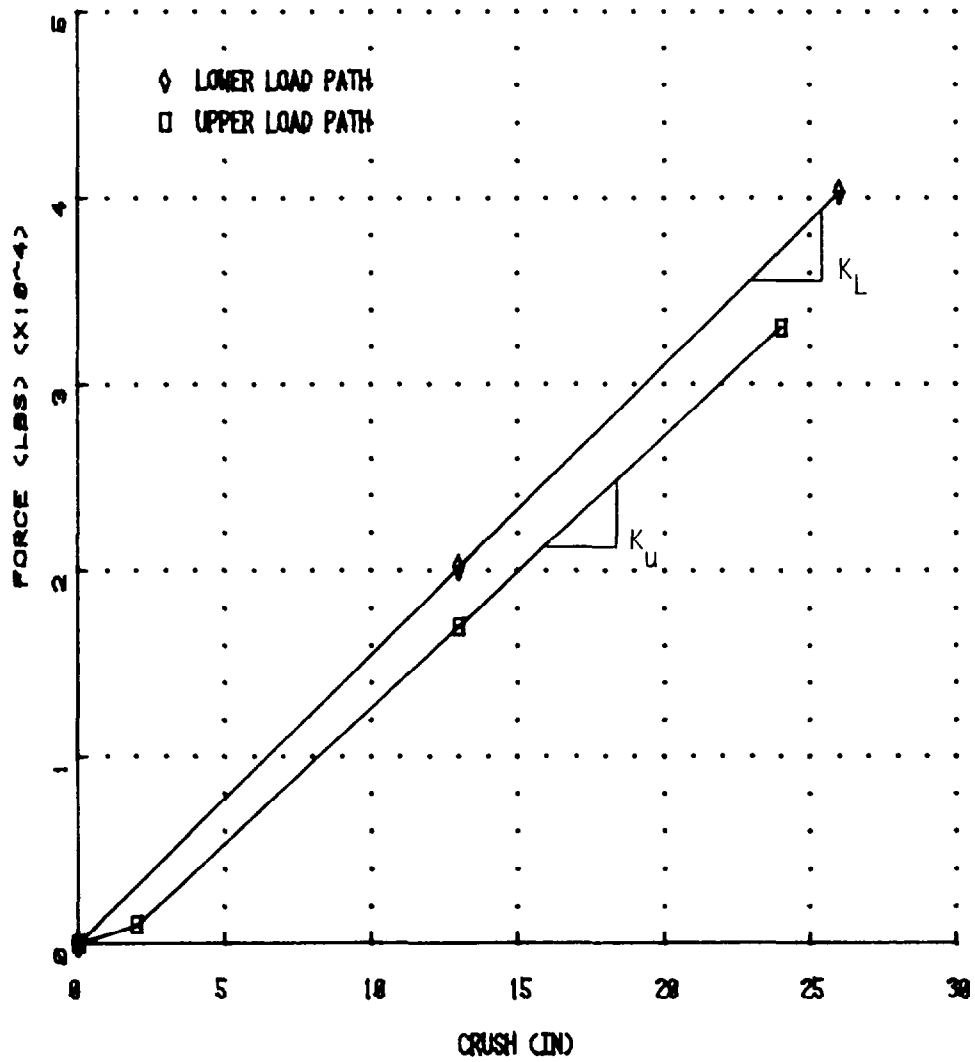


Figure 9 SIMULATED UPPER AND LOWER STRIKING CAR FORCE-CRUSH CHARACTERISTICS

Table 1

PARAMETER STUDY VARIATIONS

Struck Car Weight Lbs.	Struck Car Door Weight Lbs.	Percent of Nominal Striking Car Stiffness			
		50	100	150	200
2000	80	2.5, 5.0*	2.5, 5.0	2.5, 5.0	5.0
	100	5.0	5.0	5.0	
2500	100	2.5, 5.0	2.5, 5.0	2.5, 5.0	5.0
3000	120	2.5, 5.0	2.5, 5.0	2.5, 5.0	5.0
	100	5.0	5.0	5.0	
3500	140	2.5, 5.0	2.5, 5.0	2.5, 5.0	5.0
	100	5.0	5.0	5.0	
4000	160	2.5, 5.0	2.5, 5.0	2.5, 5.0	5.0
	100	5.0	5.0	5.0	

\* Numbers associated with each combination of stiffness and weight represent the initial occupant spacing away from the inner door padding in inches.

#### 4. DISCUSSION OF RESULTS

The results obtained in this study are discussed in this major section of the report. In the subsection immediately following, a discussion of the frontal structure force-crush information reviewed is provided together with a simplified means of categorizing important elements of that data. Following this is a description of the results obtained in the simulation study of selected parameters important in oblique side collisions

##### 4.1 Frontal Force-Crush Characteristics

As noted in the previous section, vehicle crash test data from both Dynamic Science, Inc. and Calspan Corporation were available from which to determine approximations of the frontal force-crush characteristics of a wide range of vehicles. Most of the data available was from frontal barrier tests conducted at speeds of 35 or 40 MPH at the Calspan Corporation crash test facility. In these tests, direct measurements of force were made with a load cell barrier fixture. Crush was determined from a double integration of the average compartment deceleration.

Three tests were conducted at Dynamic Science, Inc. with the NHTSA moving load cell barrier test device for which data was available. These tests involved a moving test device impacting a stationary test vehicle which was oriented at  $30^\circ$  relative to the direction of travel of the test device. Force-crush data from these tests were determined from direct measurement of impact force by the load cells on the face of the test device and from an indirect determination of crush of the test car. This measure of crush as a function of time was obtained from a difference in displacements of the test device and test car which were integrated from accelerometer traces. For these  $30^\circ$  tests, a procedure was developed by Dynamic Science to account for the rotation of the struck car in determining its crush as a function of time. Typical time histories of force vs. crush are shown in Figure 10.

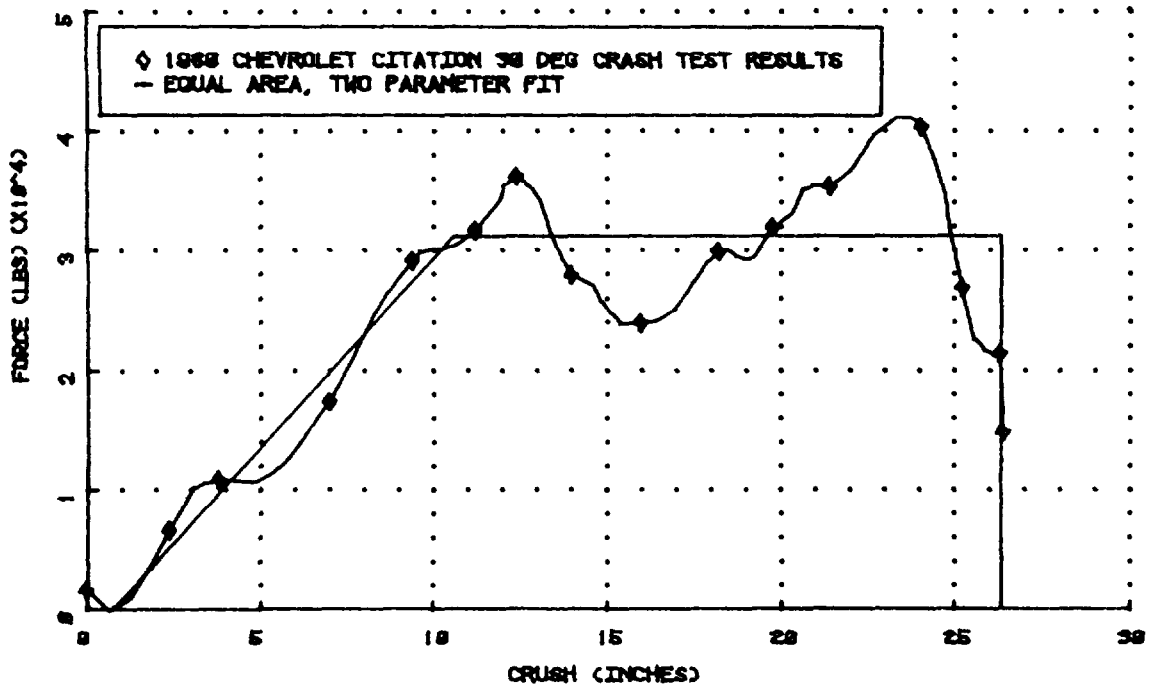
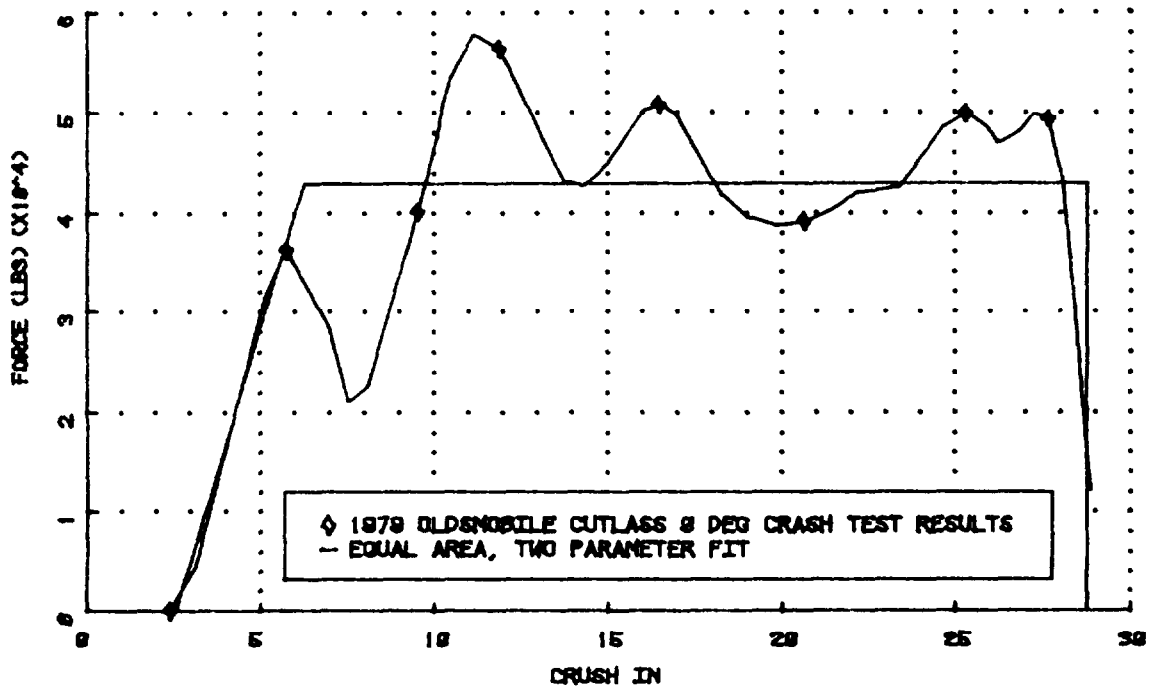


Figure 10 SAMPLE 0 AND 30 DEGREE FORCE-CRUSH CHARACTERISTICS

In order to categorize frontal stiffness characteristics of a substantial number of vehicles, a simple, two parameter fit was made to all force-crush data. This representation consisted of an initial stiffness and a yield force level chosen to equilibrate the total area under the actual curve to the area under the simple fit, up to the point of maximum deflection. Examples of this simplified fit are superimposed on the test data shown in Figure 10. Thus, frontal crush characteristics for all cars were categorized by a stiffness and a yield force level.

Results of this fit procedure for the tests involving full frontal structure are shown in Table 2. The vehicles tested are grouped according to the indicated weight ranges and average values within each weight range together with the total sample average are provided.

Categorizing the 30° frontal collision results in the same manner results in the stiffness and yield force information shown in Table 3. A complete set of force-crush characteristics with the simple fit superimposed is provided in Appendix B for both 0 and 30 degree tests.

Based on a comparison of the overall average values of the two different test configurations, it appears that the effective stiffness of a vehicle's frontal structure is reduced by about 45% as the direction of impact changes from 0 to 30 degrees. The effective yield force level, however, is reduced by about 55%. Ratios of the 30 degree to 0 degree parameters for the three vehicles common to both test conditions are listed below

<u>Vehicle</u>	<u>30°/0° Stiffness Ratio</u>	<u>30°/0° Yield Force Ratio</u>
Citation	0.39	0.53
Fairmont	0.68	0.27
Cutlass	0.64	0.53

Table 2

DYNAMIC FORCE-CRUSH SUMMARY FOR  
FULL FRONTAL BARRIER COLLISIONS

Test Weight Range (lbs.)	Vehicle	Speed (MPH)	Stiffness (KIPS/IN)	Yield (KIPS)
1750-2249	'81 Honda Civic	35	7.0	72
	Toyota Starlet	35	5.3	66
	Average	35	6.2	69
2250-2749	Volkswagen Rabbit	35	4.3	76
	Datsun 310	35	4.1	64
	Fiat Strada	35	3.8	64
	Subaru GLF	35	5.9	68
	Chevrolet Chevette	35	6.5	68
	Plymouth Horizon	35	2.3	60
	'80 Toyota Tercel	35	5.9	58
	Average	35	4.7	65
2750-3249	Volvo	35	4.2	93
	Chevrolet Citation	35	7.9	51
	Mazda 626	35	6.1	75
	Average	35	6.1	73
3250-3749	Toyota Cressida	35	6.1	104
	AMC Concord	35	5.7	94
	'79 Ford Fairmont	35	3.4	86
	Mercedes 240D	35	6.2	112
	Average	35	5.4	99
3750-4249	Plymouth Volare	35	5.7	64
	Chrysler LeBaron	35	6.4	112
	Oldsmobile Cutlass*	35	3.9	43
	Average	35	5.3	73
4250	Chrysler Imperial	35	4.6	102
	Cadillac Seville	35	6.0	114
	Average	35	5.3	108
OVERALL AVERAGE		35	5.3	78.4

\* Valid for up to 24" crush

Table 3

DYNAMIC FORCE-CRUSH SUMMARY FOR  
30° FRONTAL COLLISIONS WITH LCMB\*

Test Weight Range (lbs.)	Vehicle	Stiffness (KIPS/IN)	Yield (KIPS)
2750-3249	Chevrolet Citation	3.1	27
	Average	3.1	27
3250-3749	Ford Fairmont	2.3	23
	Average	2.3	23
3750-4249	Oldsmobile Cutlass	2.5	23
	Chevrolet Impala	3.2	35
	Average	2.9	29
OVERALL AVERAGE		2.8	27

\* Force is in direction of LCMB

Results from a 30 degree angled Impala crush test (Ref. 5) allowed an additional comparison to be made. Figure 11 compares the dynamic force-crush results from the Dynamic Science angled crash test, the static force-crush characteristic, and an estimated dynamic force-crush curve. The estimated curve was developed from the static data by applying a constant rate factor of 1.35. As is seen on the figure, this dynamic factor results in good agreement with the dynamic test results.

#### 4.2 Simulation Parameter Study

An analytical evaluation of the sensitivity of the struck car and occupant responses to striking car stiffness was carried out with the SMDYN program which is described in Appendix A. Over fifty simulation runs were made investigating striking car frontal stiffness effects as well as certain other struck car parameters that were found to be of interest. Consistent with the Statement of Work, weight, speed and orientations of the striking car were held constant and reasonable assumptions were made regarding struck car structural characteristics and padding.

The simulation runs discussed in this section were made under two different assumptions regarding the effective impacted door weights. In the first category, door weights (upper and lower) were assumed to be 100 lbs. for all struck vehicle weights considered. Within this category, an initial occupant to door spacing of 5 inches was simulated. The second category of runs was made with the assumption that the upper and lower door weights were proportional to the total struck car weight, ranging from 80 lbs. to 160 lbs. for the 2000 lb. and 4000 lb. vehicles, respectively. Within this category, initial occupant to inner door surface spacings of both 2.5 inches and 5.0 inches were considered. A sample of the SMDYN input data for a typical run is shown in Appendix C.

Although Figures 3 through 5 indicated that the predicted responses agreed quite well with the measurements for a single test condition, uncertainty

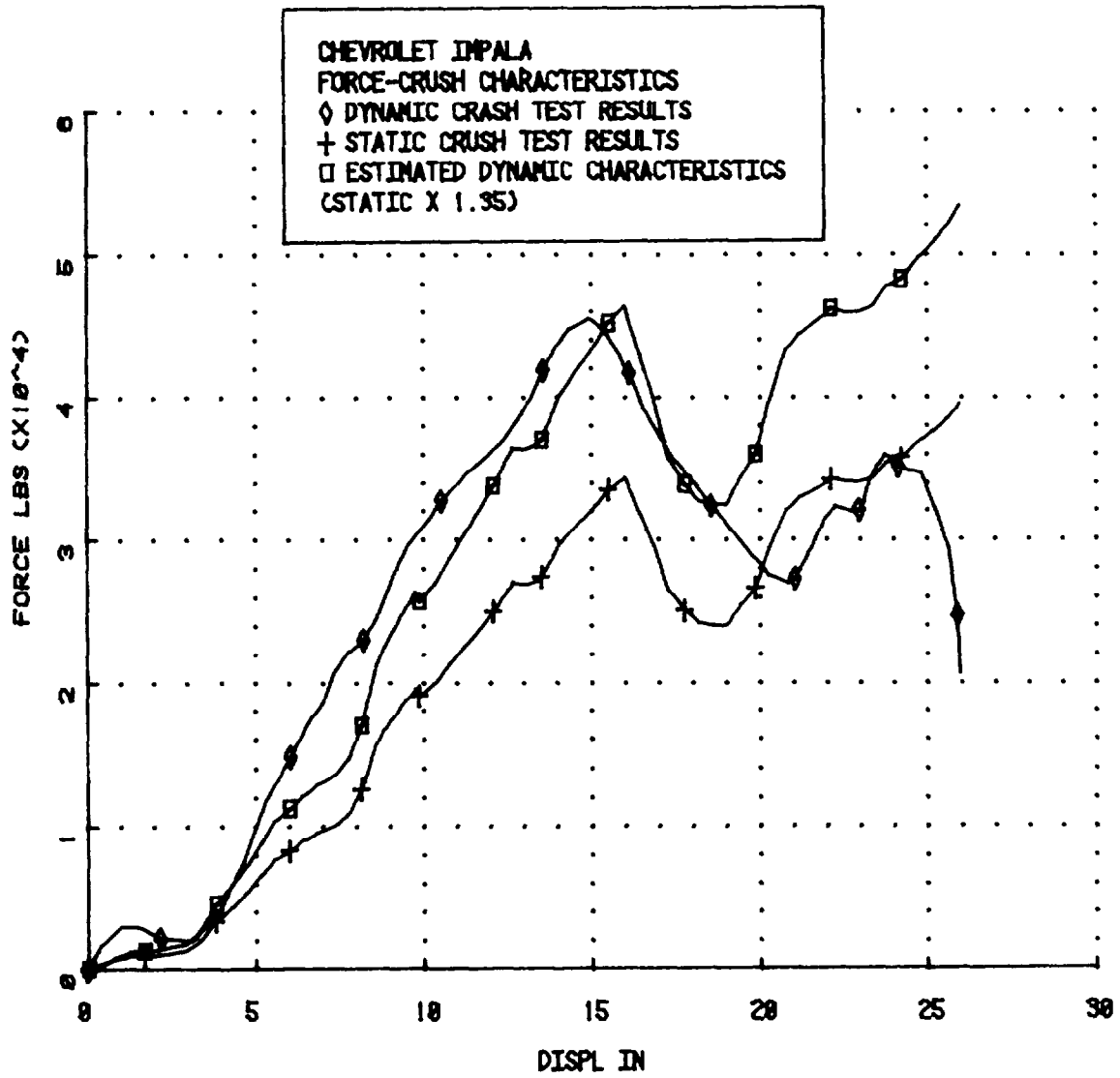


Figure 11 COMPARISON OF STATIC AND DYNAMIC FORCE-CRUSH CHARACTERISTICS

of the validity of the predictions of occupant response under other conditions led to the consideration of a number of different "severity" measures. These measures included not only occupant CSI and change in velocity but also door intrusion, relative velocity between the door and occupant at first contact, mutual door padding/occupant crush and maximum upper door velocity relative to the struck vehicle.

Predicted door intrusion\* as a function of relative striking car stiffness for all struck car weights considered are shown in Figure 12. This figure includes results from both the constant door weight and proportional door weight categories, both with a five inch initial spacing between the occupant and the door. In both cases, a tendency for the intrusion levels to saturate at the nominal striking car stiffnesses is seen. A similar tendency is seen in Figure 13 where the rate of change of relative velocity between the door and occupant at contact decreases with increasing stiffness. Note that for many of the individual runs indicated on the figure, this velocity exceeds the initial velocity of the striking car (30.3 MPH). The relative door to occupant velocity at contact with the occupant also appears to be a function of the effective door weight. That is, the range of relative velocities at a given stiffness is considerably larger for the case where this weight varied with struck car weight than where it was held constant. This is further illustrated in Figure 14 where the relative velocity decreases with increasing struck car (and door) weight in the one case but remains relatively constant when the door weight was assumed constant.

Figure 15 illustrates the effects of striking car stiffness on occupant change in velocity for the constant weight door and proportional weight door cases, both with 5 inches of initial occupant spacing. For the constant

---

\* Note that the intrusion values were taken at the end of the simulated event, 0.075 seconds. Had longer event times been simulated, maximum intrusion values would likely have been larger; however, struck car rotation begins to occur after this time which would invalidate results.

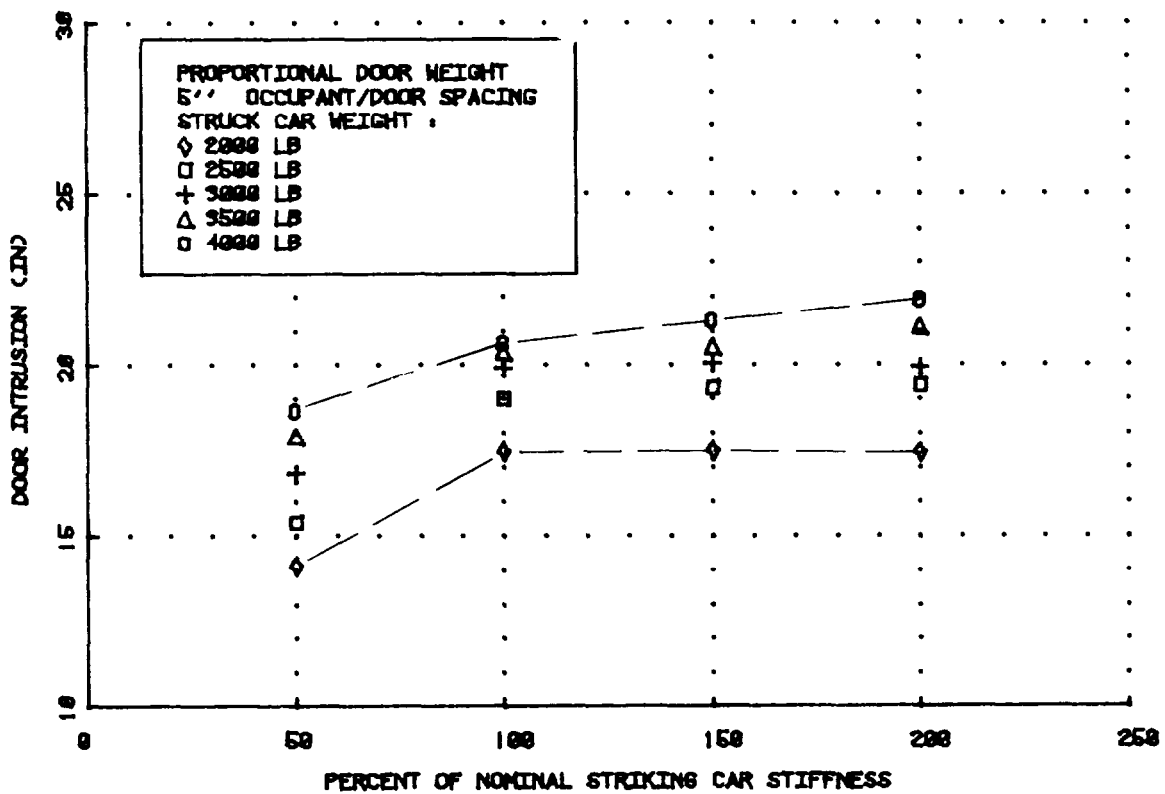
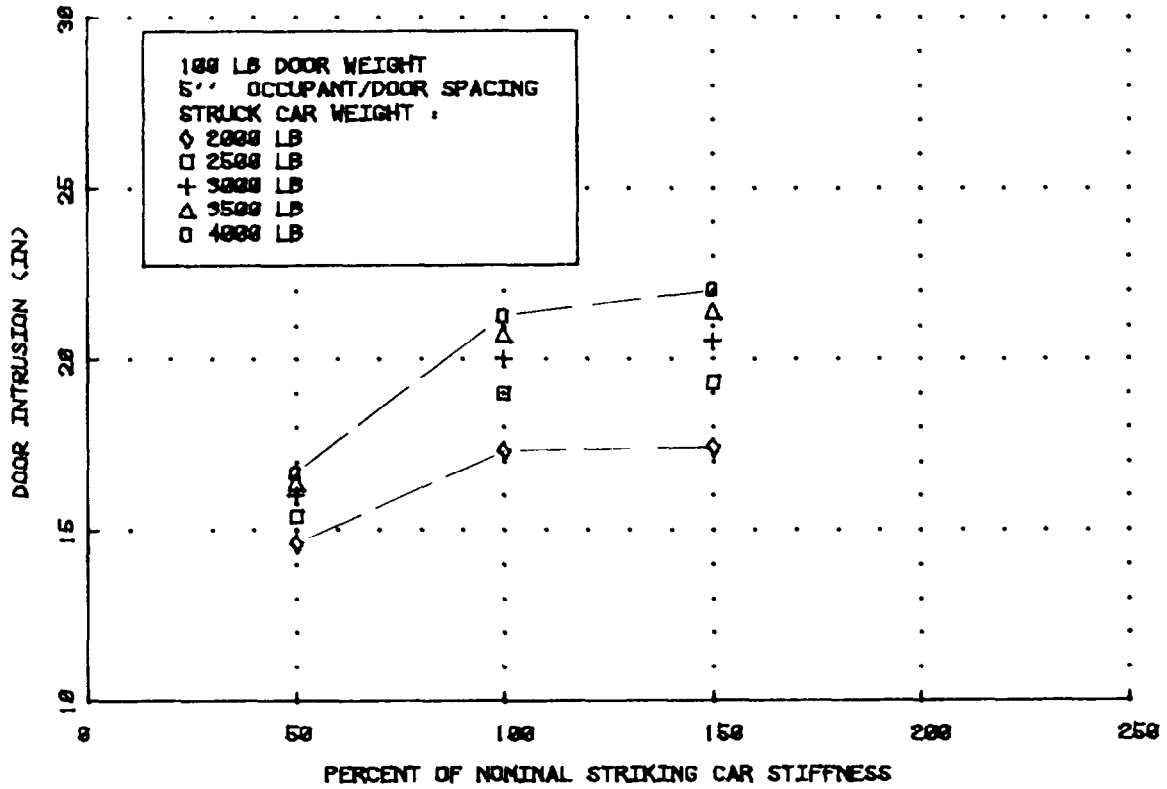


Figure 12 STRUCK DOOR INTRUSION VS. STRIKING CAR STIFFNESS

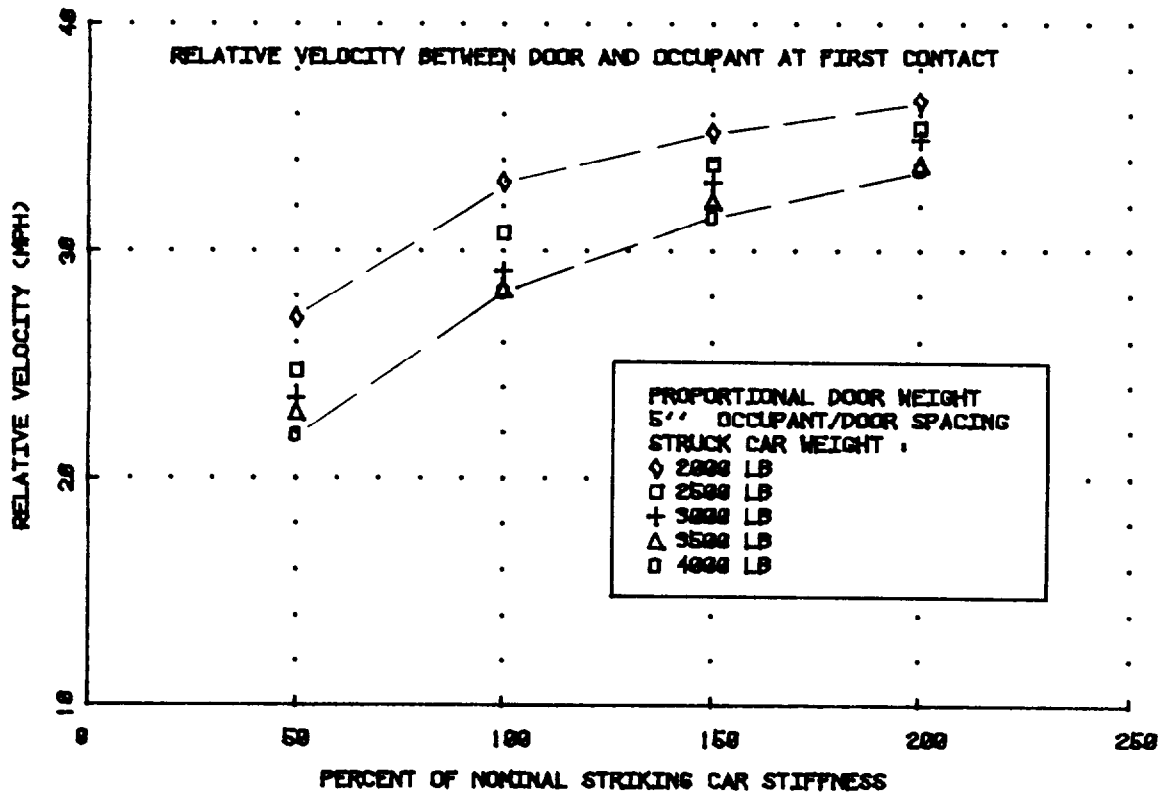
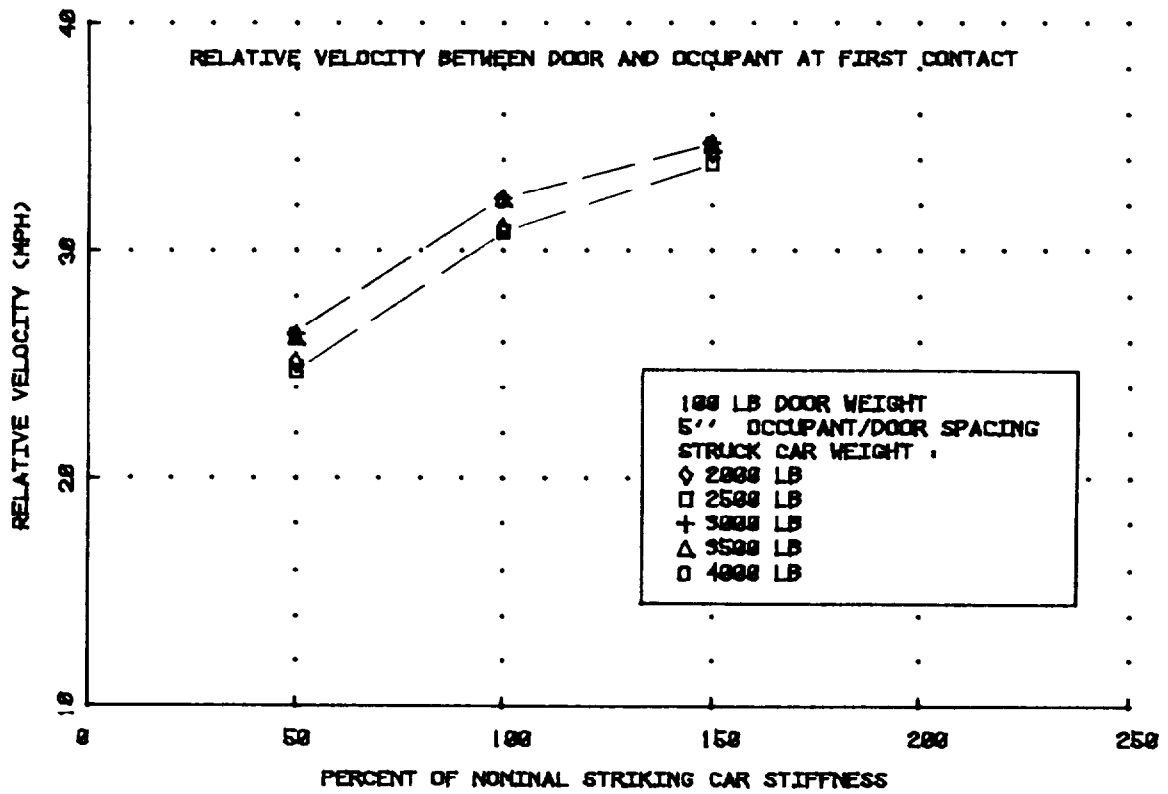


Figure 13 STRUCK DOOR-OCCUPANT CONTACT VELOCITY VS. STRIKING CAR STIFFNESS

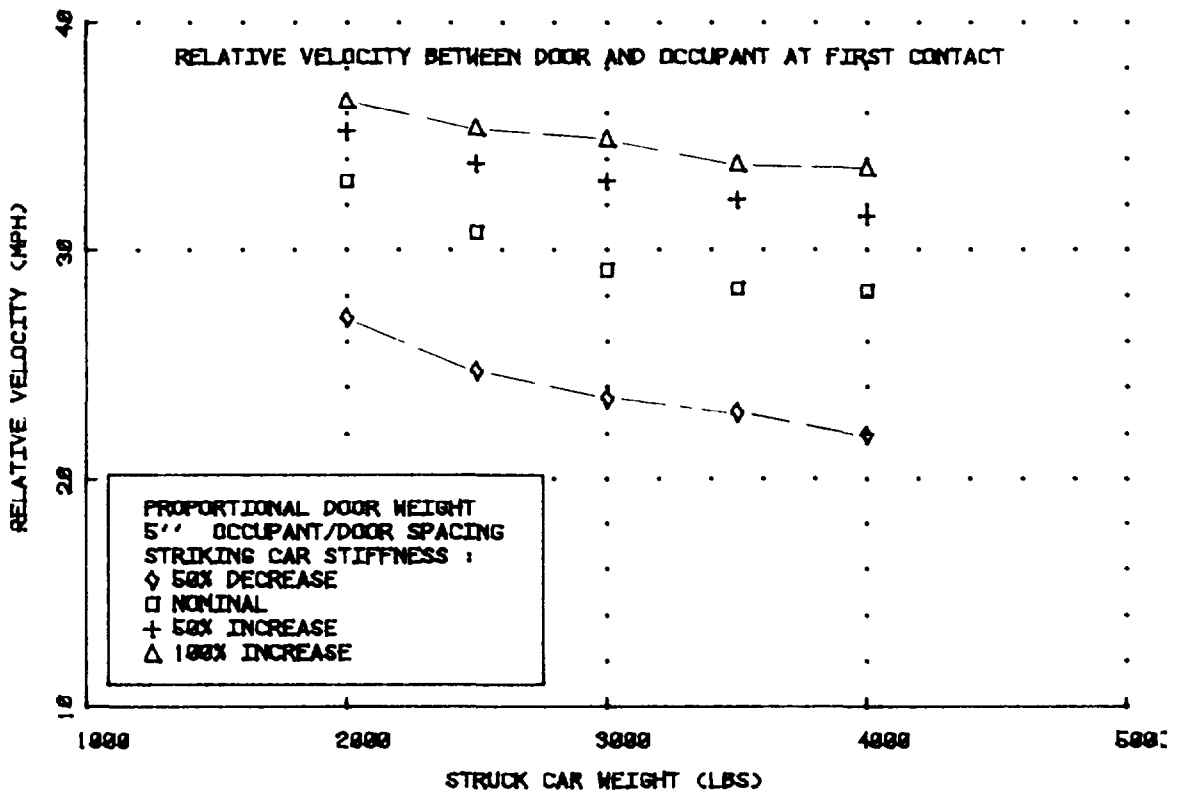
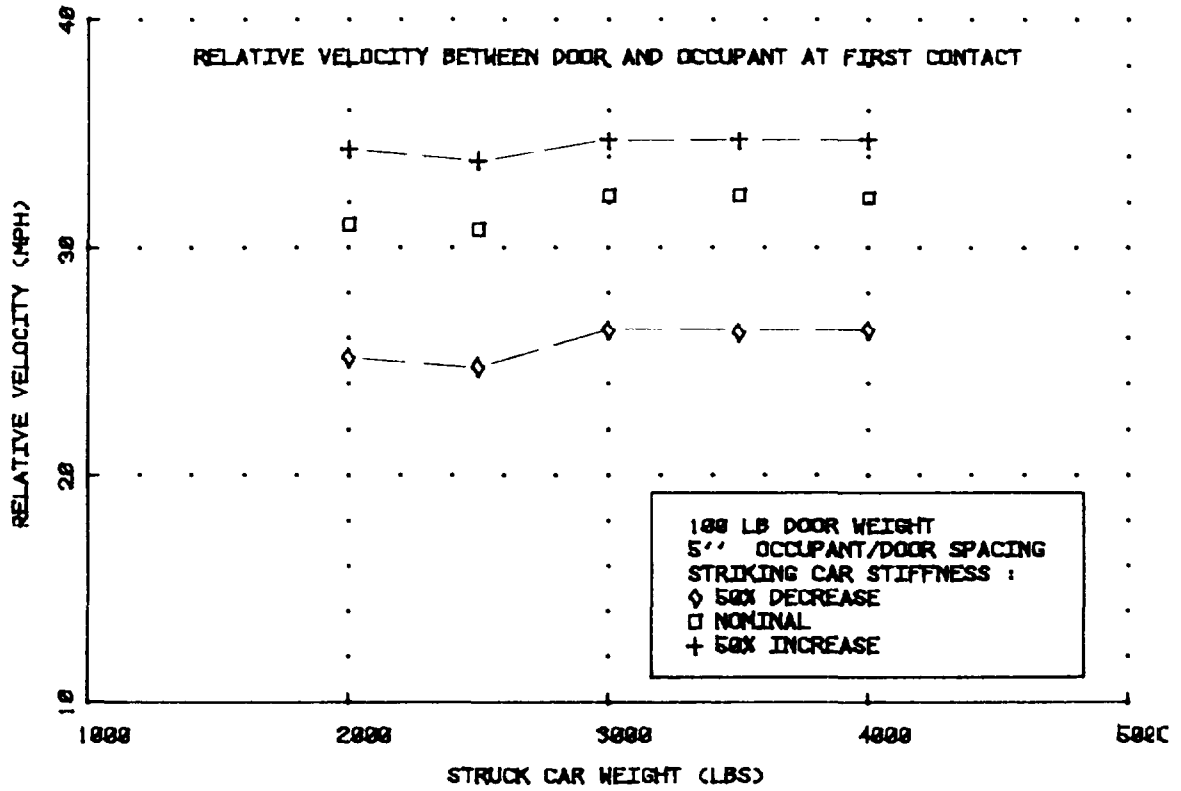


Figure 14 STRUCK DOOR-OCCUPANT CONTACT VELOCITY VS. STRUCK CAR WEIGHT

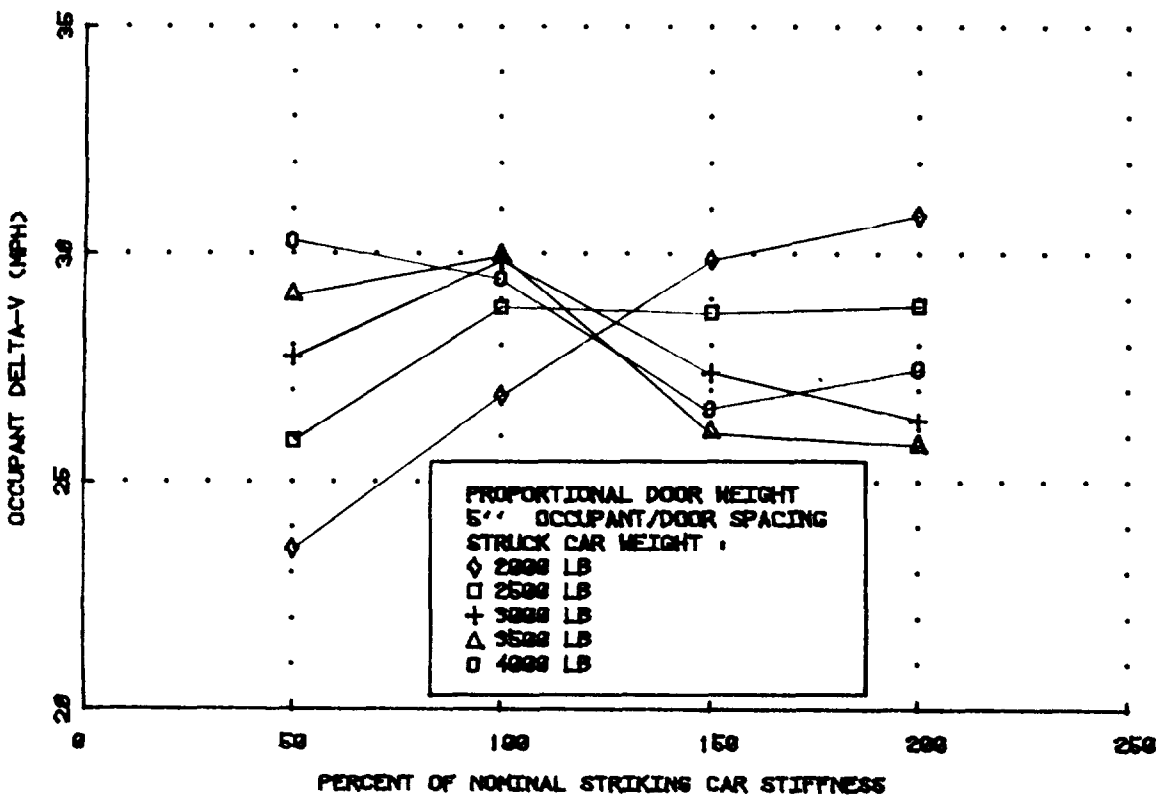
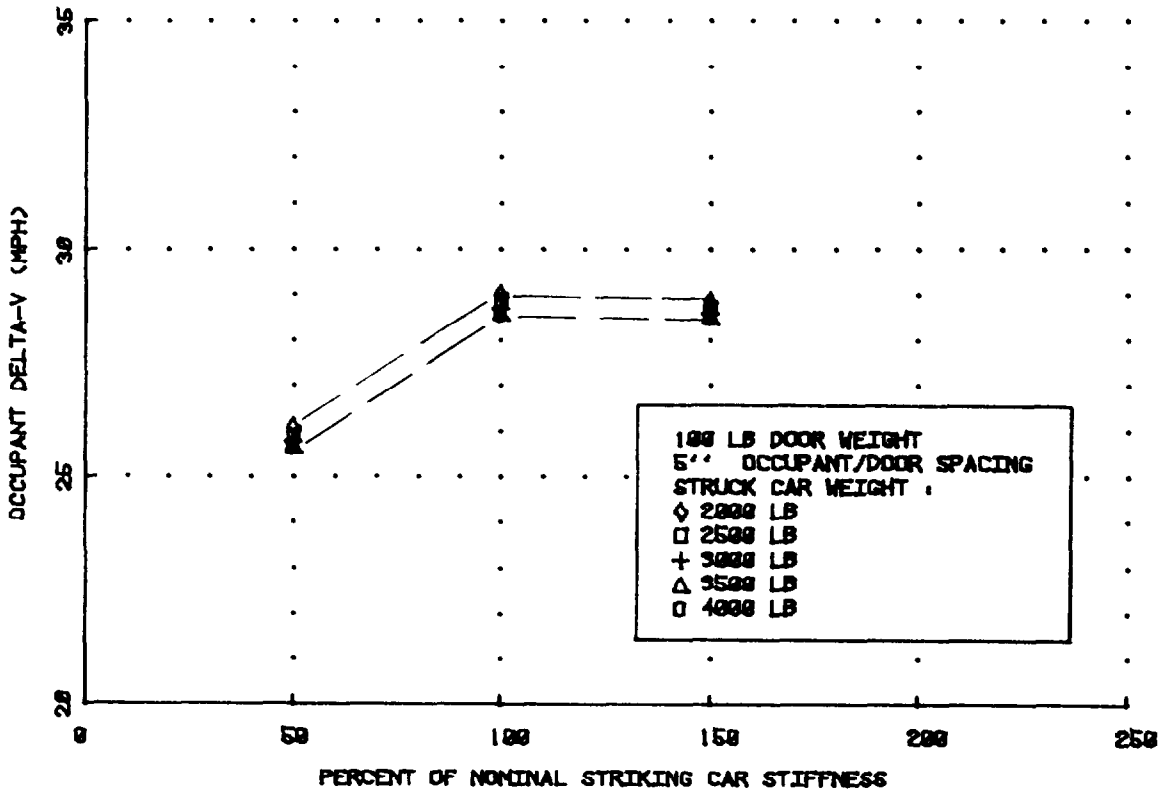


Figure 15 OCCUPANT VELOCITY CHANGE VS. STRIKING CAR STIFFNESS

weight door case, it is again seen that a response saturation occurs at the nominal striking car stiffness. That is, increasing the striking car stiffness beyond the nominal value of 3000 lbs/in does not result in an increase in occupant velocity change. However, when door weight proportional to the struck car total weight is assumed, the results do not follow a consistent pattern. It is seen that, with this modeling approach, the occupant response is clearly a function of the assumed effective door weight. This is one area that deserves considerably more attention if results from side impact analytical studies are to be properly interpreted. A complete explanation for this behavior is not available at this time; however, it is believed that the combination of stiffnesses acting on the upper door and the door mass result in different kinematics of the system as individual parameters are varied which, in turn, have a strong effect on occupant response.

Figure 16 illustrates another example of response variations resulting from changes in effective door weight. With constant weight doors assumed, the calculated CSI is seen to peak at the nominal value of striking car stiffness. In the proportional weight door case, there is also a tendency for the CSI to peak at the nominal stiffness value except in the case of the 4000 lb. struck car. There is also considerably more scatter in the predicted CSI values than with the constant weight door assumption.

The effect of striking car stiffness on combined interior door padding/occupant crush, is shown in Figure 17. For the constant weight door case, door padding crush is seen to be independent of stiffness. When proportional weight doors are assumed, the change in crush with stiffness is quite small. These results indicate that door padding deformation is not likely to be an effective measure of occupant injury if the assumed properties are representative.

Figure 18 shows the peak upper door velocity relative to the struck car as a function of striking car stiffness for both constant weight and proportional weight doors. Note that with both door weight assumptions, this peak velocity increases monotonically with striking car stiffness,

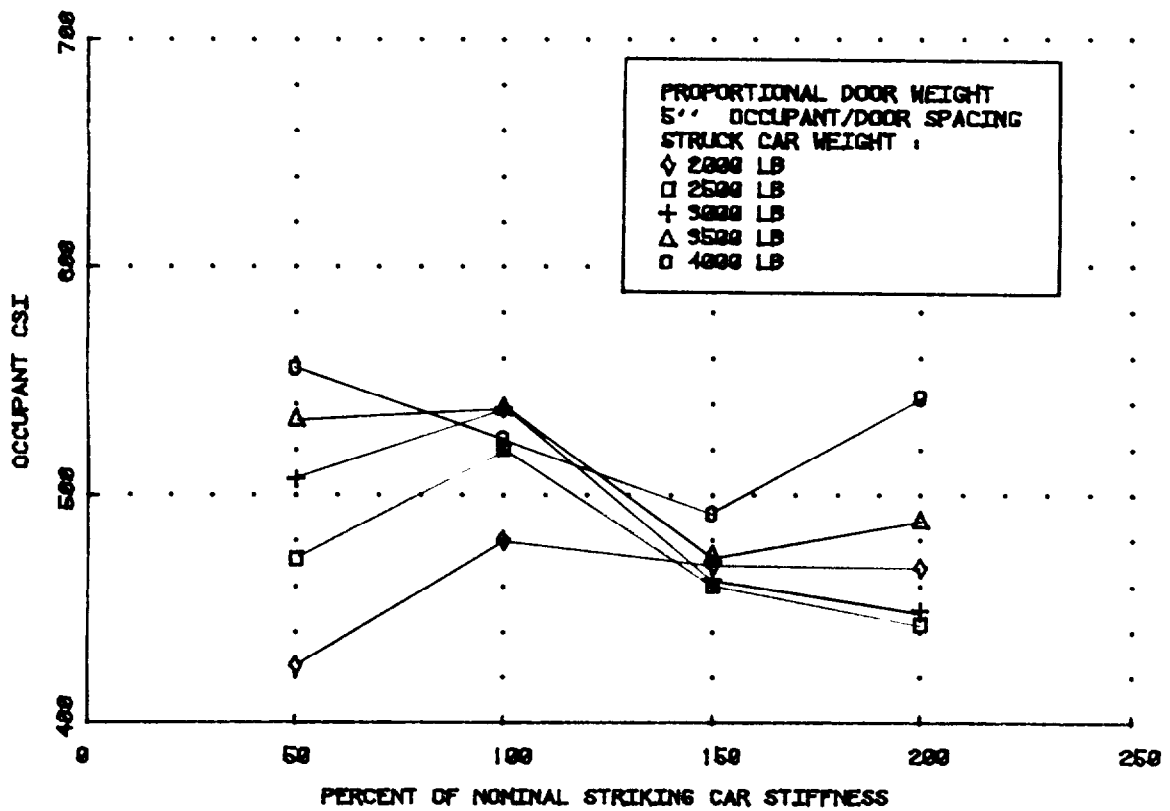
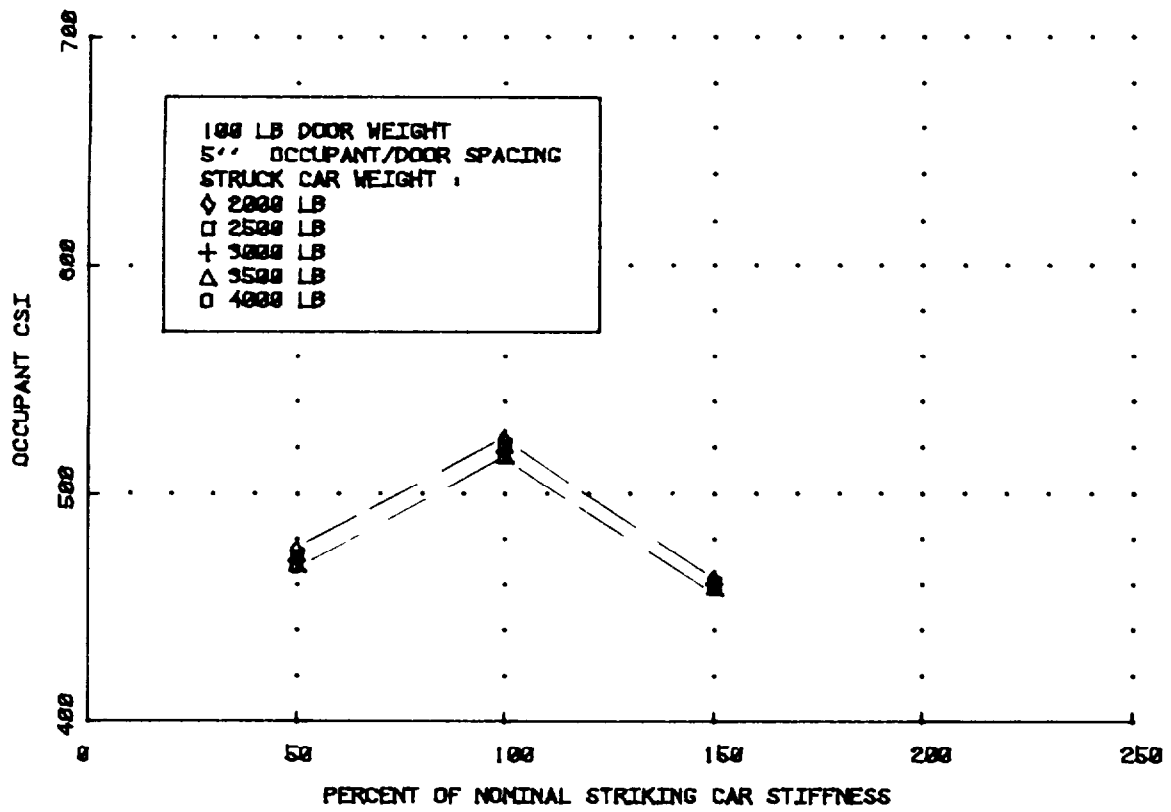


Figure 16 OCCUPANT CSI VS. STRIKING CAR STIFFNESS

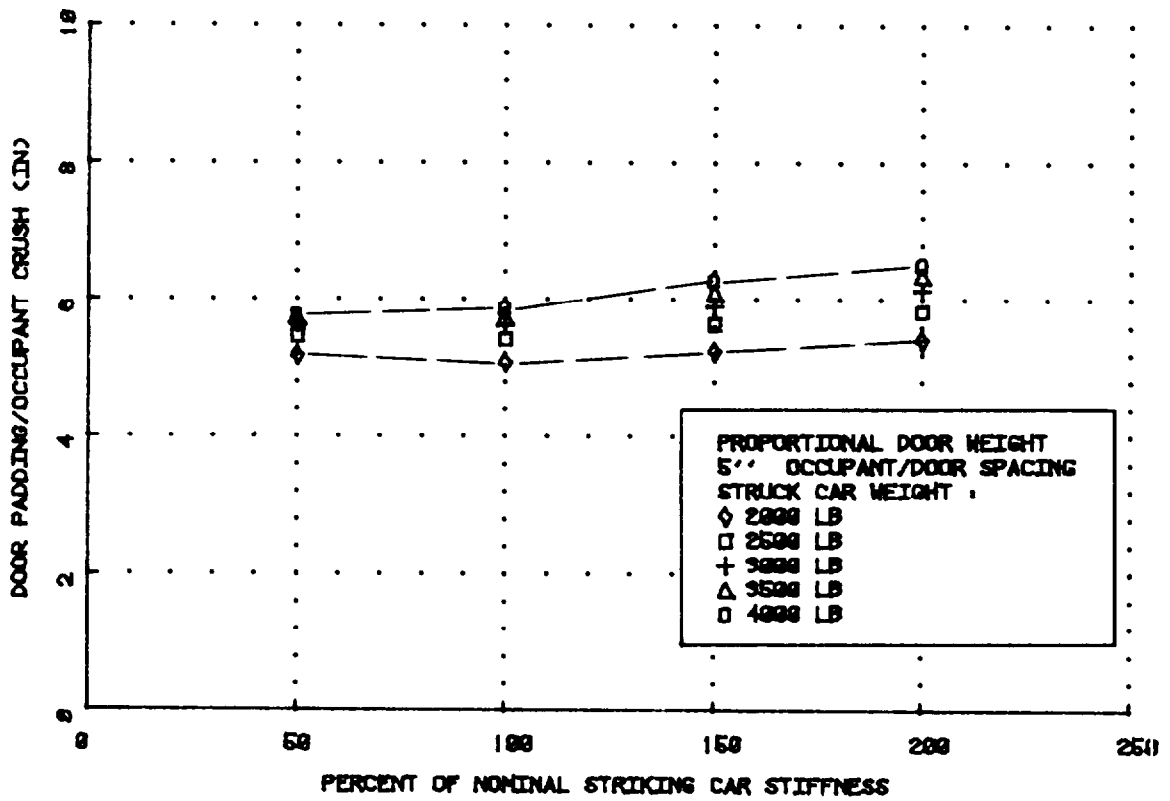
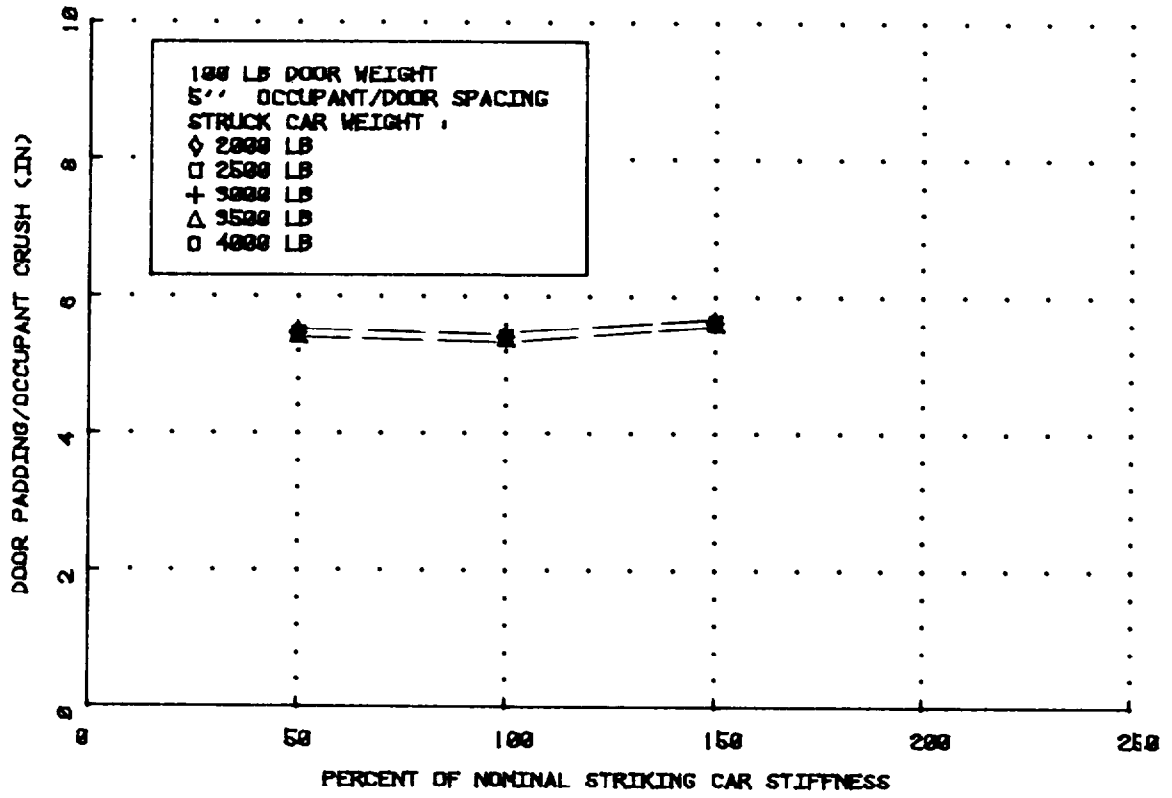


Figure 17 DOOR PADDING-OCCUPANT CRUSH VS. STRIKING CAR STIFFNESS

although the rate of increase decreases with stiffness. Previously presented results indicated that two measures of occupant injury severity, change in velocity and CSI, did not necessarily increase monotonically with striking car stiffness. This leads to the possibility that peak door velocity relative to the struck car, by itself, may not be a valid indicator of exposure severity. It is not, at this time, known whether this result is an artifact of the model or data used in the study or if, in fact, it is a result that might be confirmed through additional investigation.

Replotting peak door velocity data as a function of struck car weight, Figure 19, further illustrates the effects of door weight on its response. In the case of constant weight, 100 lb. doors, the peak door velocity relative to the struck car increases slightly as struck car weight increases. On the other hand, as door weight increases (proportional to total struck car weight), the peak relative velocity decreases.

While not directly required by the Statement of Work, additional runs were made with the relative spacing between the occupant and interior door surface reduced to 2.5 inches in an attempt to learn more about the interaction between various parameters in the dynamic event. These runs were made with the assumption that struck car door weights were proportional to the total struck car weight and thus are directly comparable to the corresponding runs made with a 5.0 inch spacing. Figure 20 illustrates the change in relative velocity between the door and occupant at initial contact as a result of the spacing change. With the reduced spacing, this relative velocity is reduced by a significant amount, apparently due to the fact that contact occurs before the door velocity has had sufficient time to reach the higher levels. The total occupant change in velocity is, however, larger with the reduced spacing as is seen in Figure 21. This is believed to result from a longer duration of contact between the door and occupant at the reduced spacing. The effect of occupant/door spacing on the maximum door/vehicle relative velocity is illustrated in Figure 22. Note that with reduced spacing, the maximum relative velocity decreases somewhat, apparently due to the effects of occupant/door contact occurring earlier in the event.

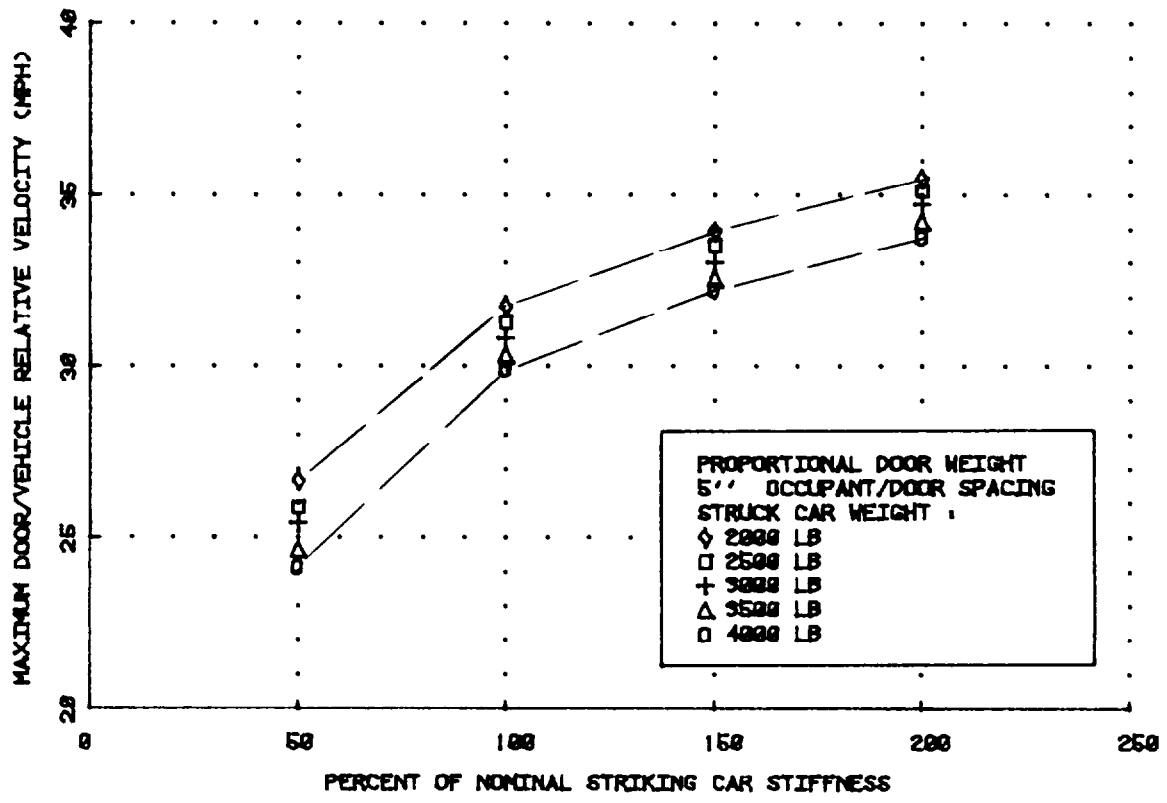
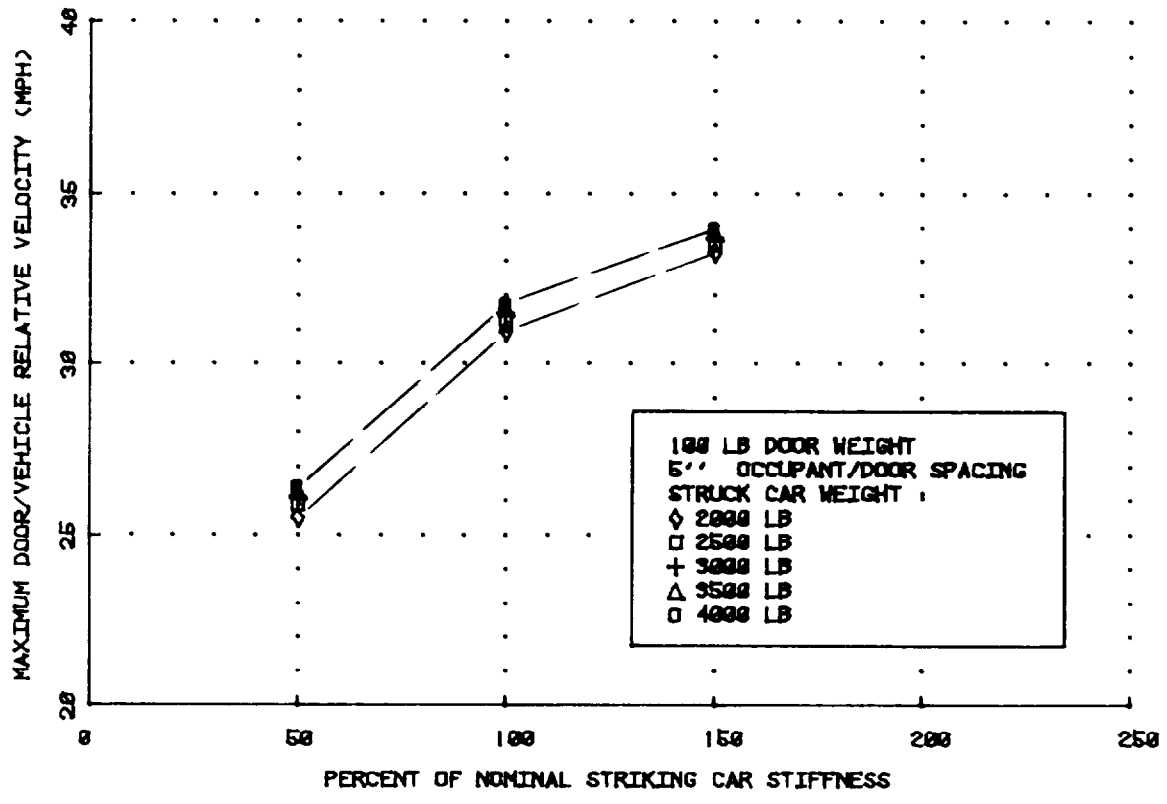


Figure 18 MAXIMUM STRUCK DOOR RELATIVE VELOCITY VS. STRIKING CAR STIFFNESS

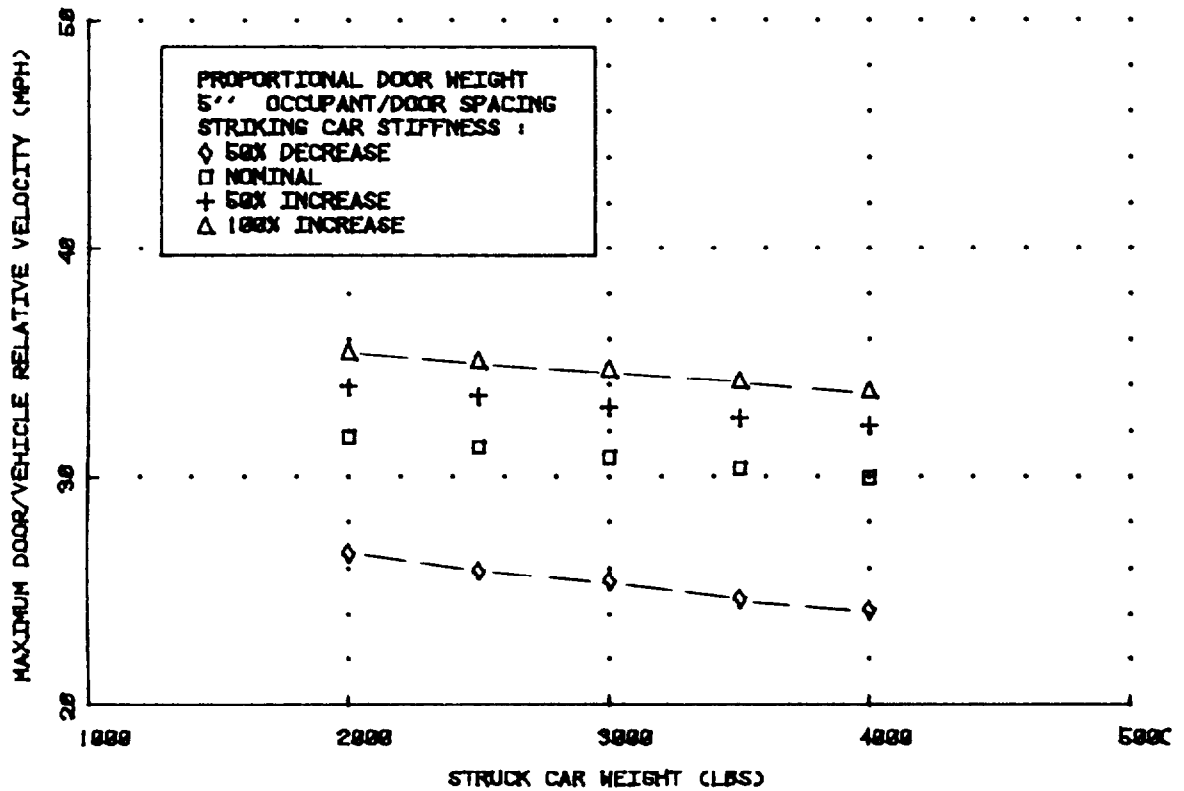
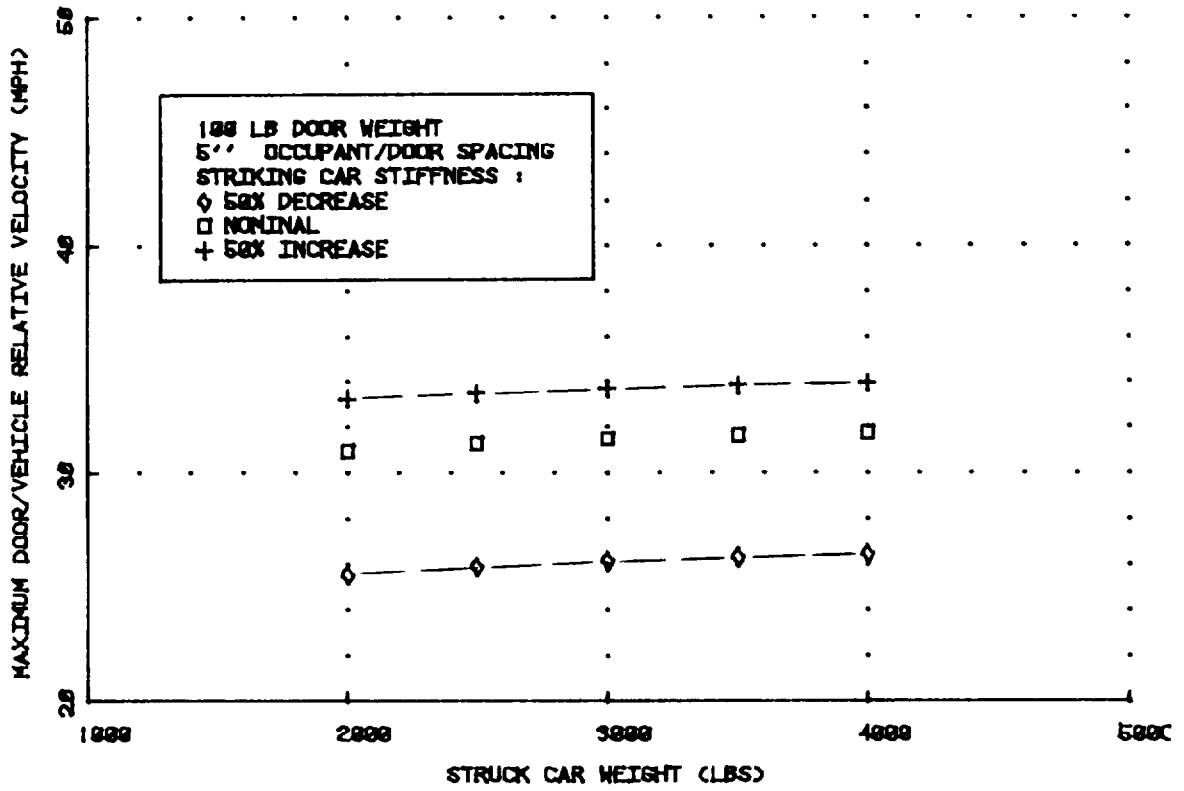


Figure 19 MAXIMUM STRUCK DOOR RELATIVE VELOCITY VS. STRUCK VEHICLE WEIGHT

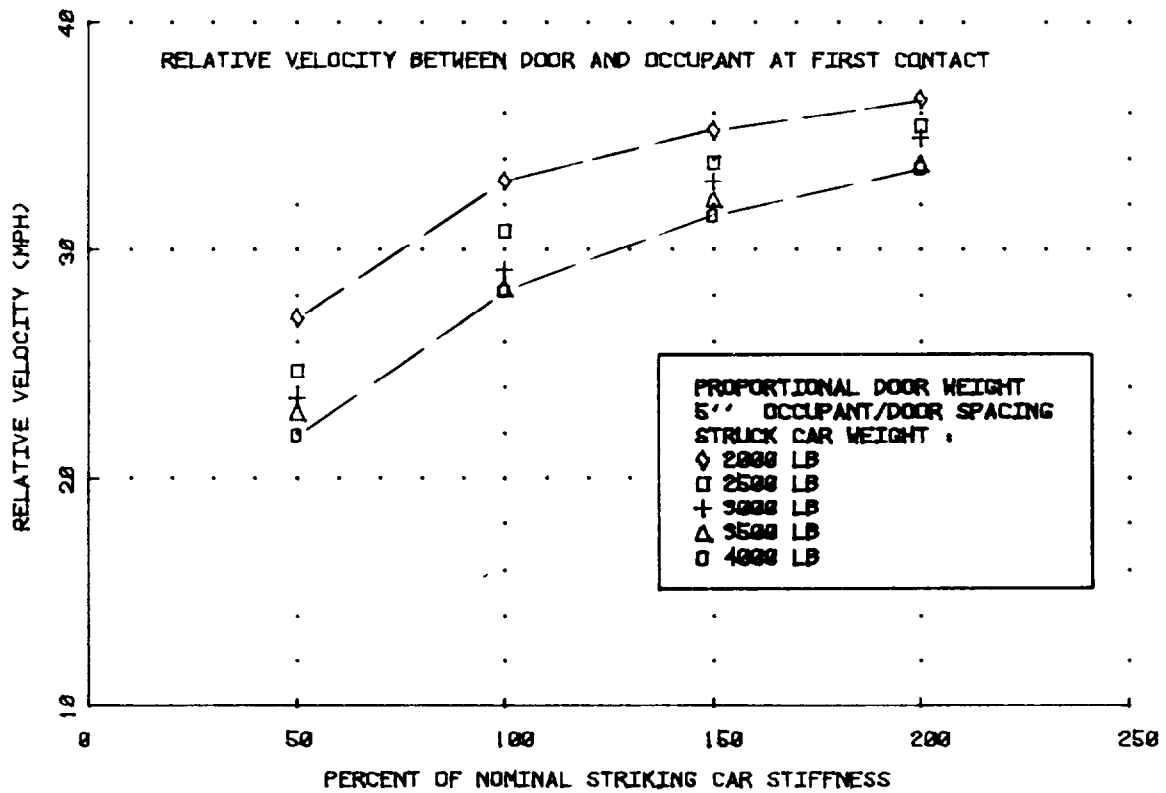
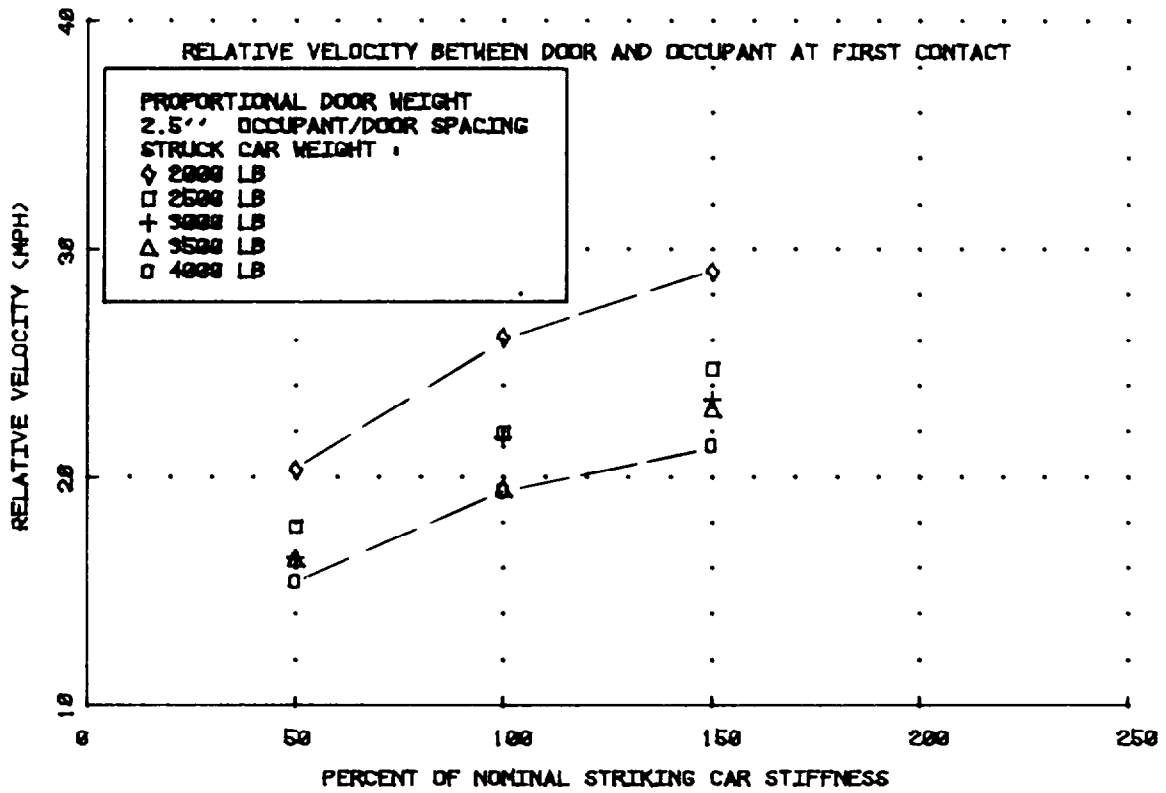


Figure 20 STRUCK DOOR-OCCUPANT CONTACT VELOCITY VS. STRIKING CAR STIFFNESS

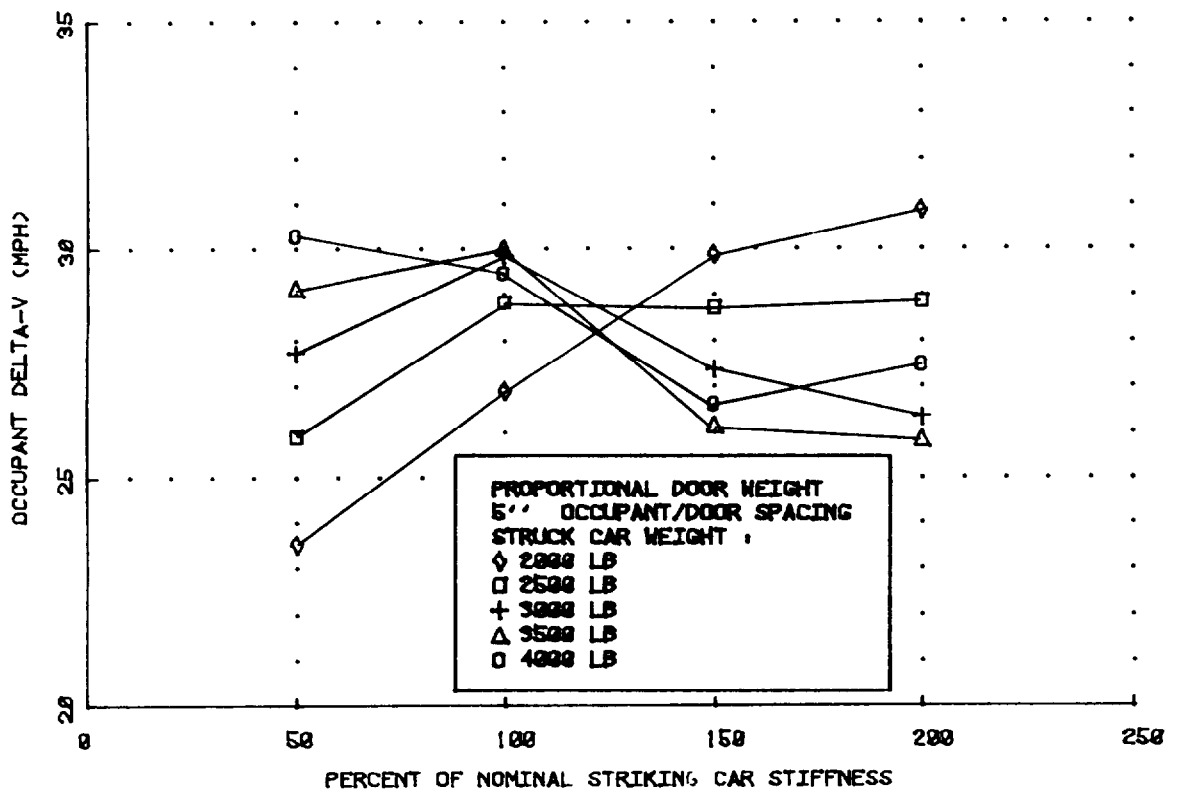
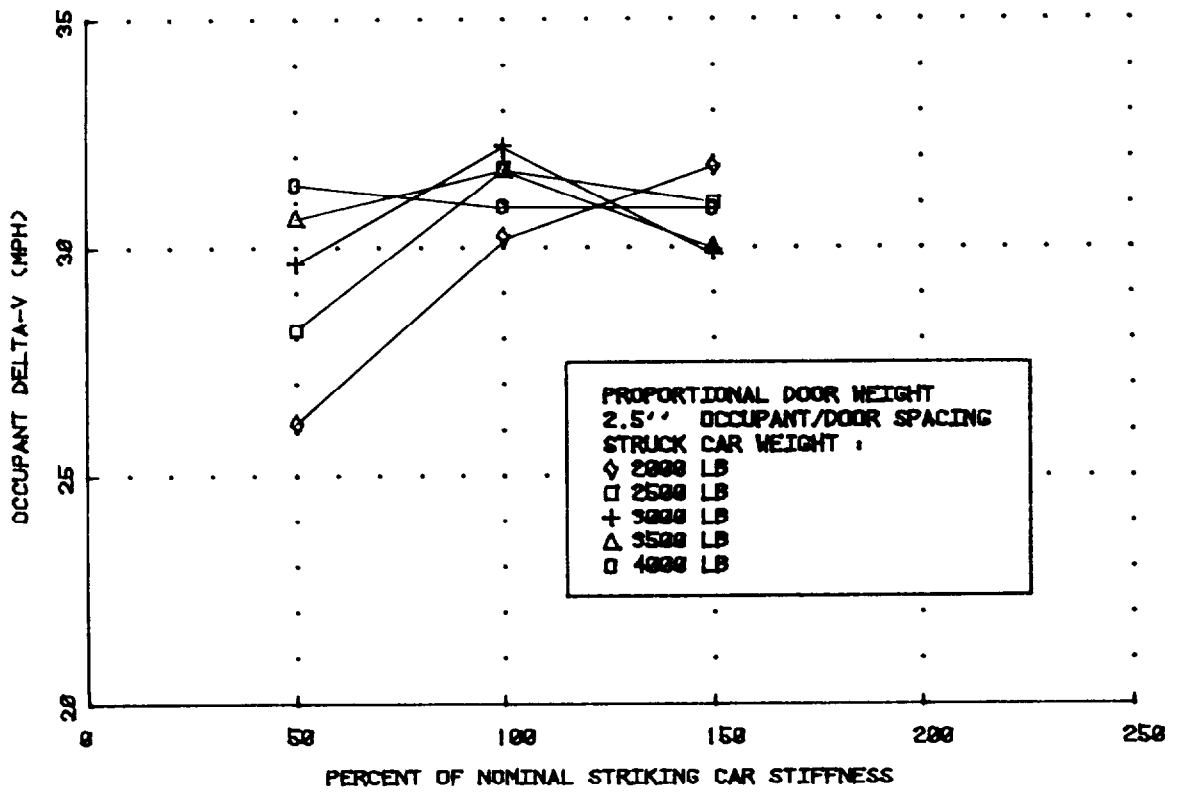


Figure 21 OCCUPANT VELOCITY CHANGE VS. STRIKING CAR STIFFNESS

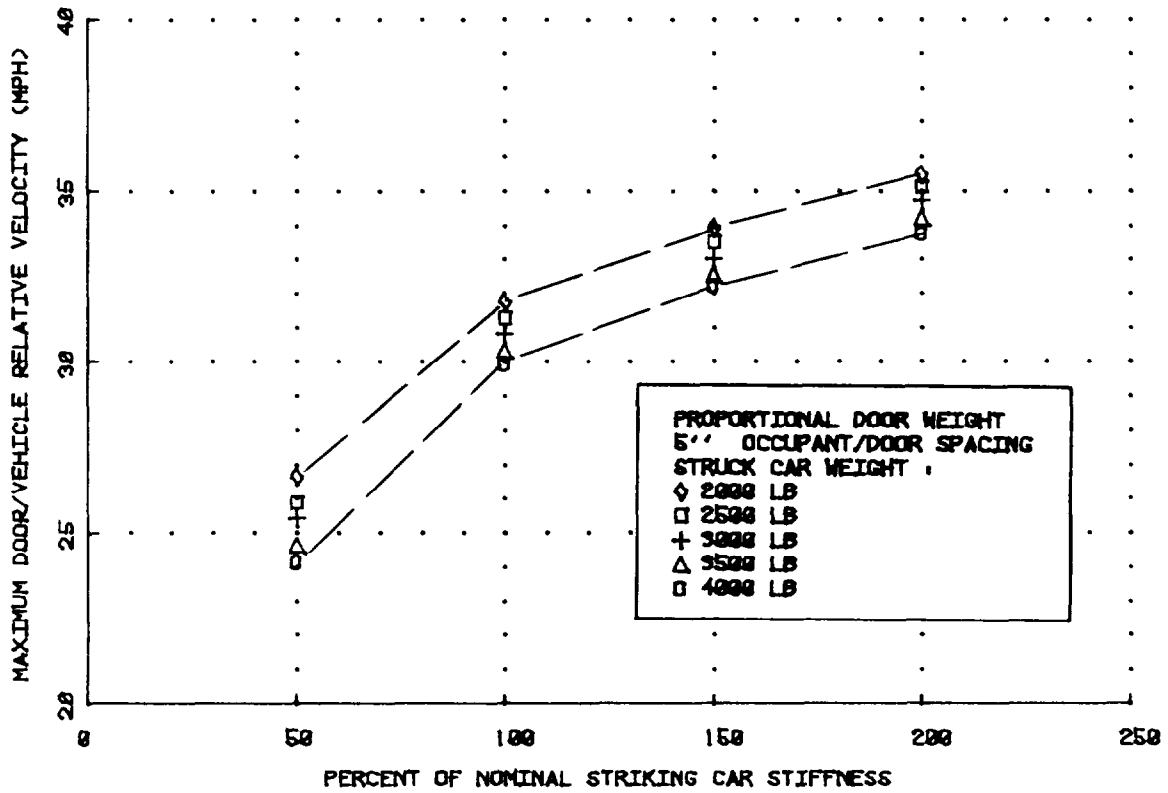
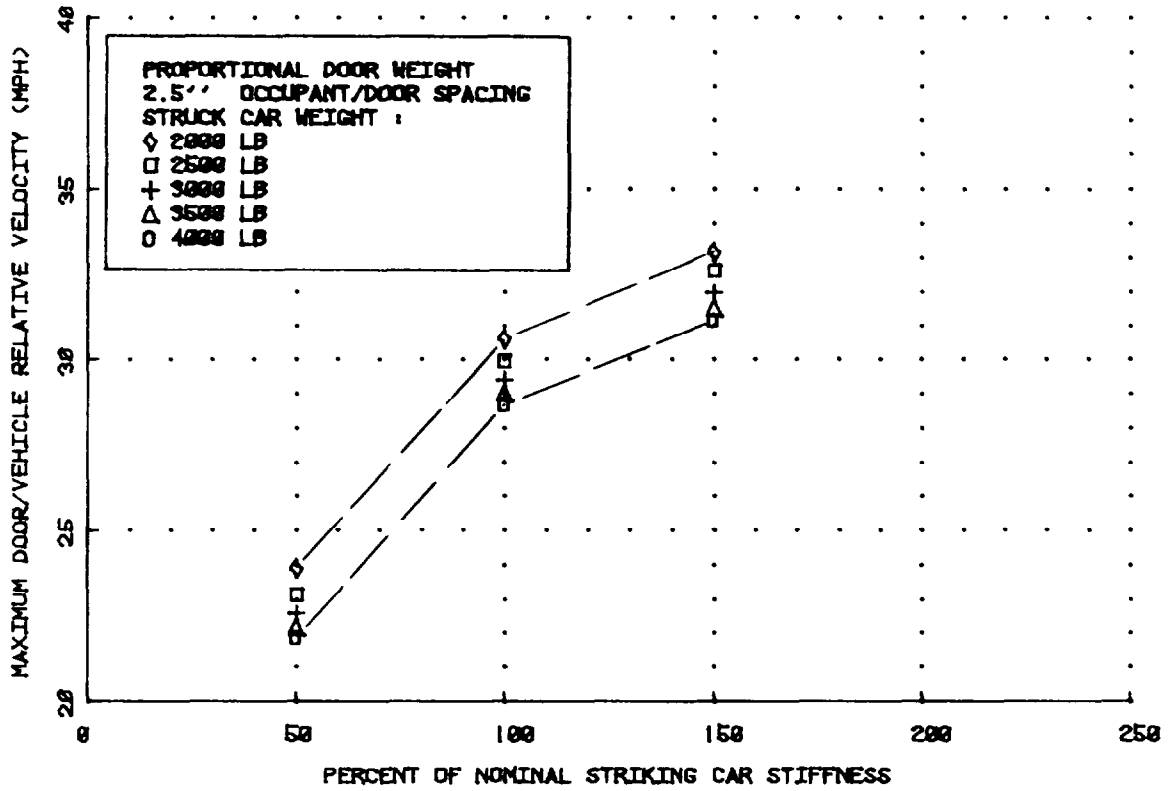


Figure 22 MAXIMUM STRUCK DOOR RELATIVE VELOCITY VS. STRIKING CAR STIFFNESS

The simulation parameter study reported above was made with the primary objective of determining the frontal stiffness characteristics of the NHTSA side impact test device that would maximize the benefits associated with an upgraded FMVSS 214 test procedure. Since side impact simulation techniques have not been developed to a high level at this point, the absolute validity of the results obtained must be viewed in the context in which they were obtained--that of exploratory procedural development of a mechanism for studying a very complex dynamic event. In view of this context, we have not attempted to assign a benefit (in terms of probability of a reduction in injury associated with complying with an upgraded standard) for each frontal stiffness impacting a spectrum of struck vehicle weights. We feel that the number of unsubstantiated assumptions (reasonable in our view but nonetheless unsubstantiated by test data) regarding the side structure model used and the data applied to it do not justify such an extrapolation.

Furthermore, some of the results obtained in this study require further investigation for proper interpretation. Obviously, the assumed effective mass of the impacted door plays a major role in both its response and the response of the simulated occupant. Direct measures of occupant injury (change in velocity and CSI) are apparently not strongly related to indirect measures (e.g., peak door velocity relative to the struck car, door padding crush). These results should be studied further to determine whether they result from deficiencies in the modeling procedure or data used in this study.

Results do show, however, that occupant injury severity does not continually increase as striking car stiffness increases. This trend was most clearly demonstrated under the assumption that effective door weights were constant across the struck vehicle spectrum where it was seen that the change in velocity sustained by the simulated occupant increased as the striking car stiffness increased from 50% to 100% of the nominal level but did not increase as the stiffness was increased beyond the nominal level of 3000 lbs/in. Since this value of frontal, 30 degree stiffness was the approximate average stiffness

of the three cars for which data was available, and is thus reasonable in terms of the automobile population, it is suggested that this value of stiffness is appropriate for use on the moving side impact barrier. Additional analytical studies should be undertaken in order to evaluate if the effects of assumptions made in this study have a strong influence on the stiffness level at which injury response saturation occurs. Consideration should also be given to empirical verification of this result.

5. REFERENCES

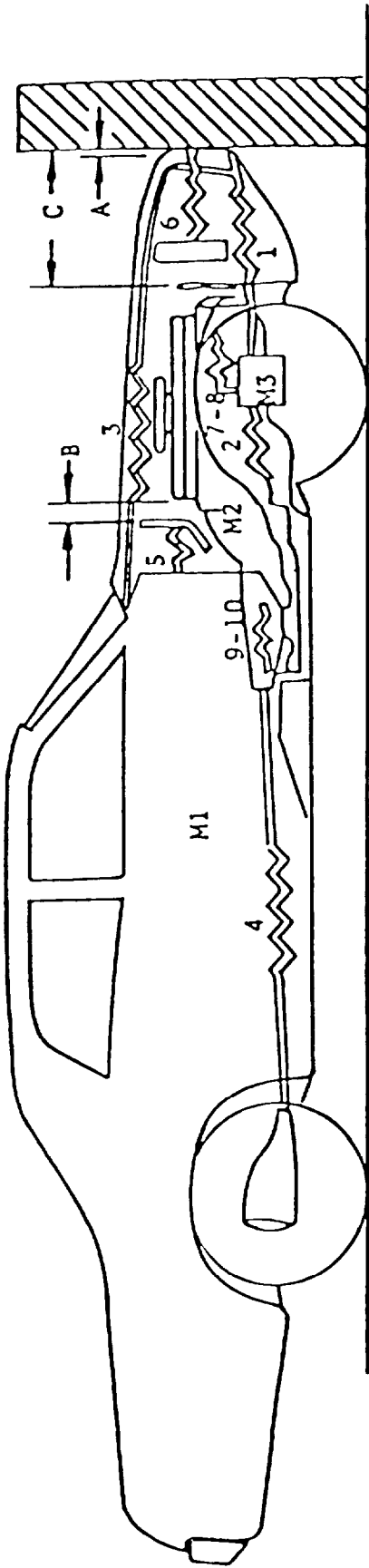
1. Hedlund, J., "Update of Distributions for Key Variables in Side Crashes, based on Aggregate NCSS Data," Memorandum to J. Hackney, February 2, 1979.
2. "Lightweight Subcompact Vehicle Side Structure Program--Progress Report for October 1979," MGA File No. G7-002, Prepared for The Budd Company, P. O. No. TC-17649, Contract No. DOT-HS-7-01588, November 1979.
3. D. J. Segal and P. M. Miller, "Methodology for Recommending Side Impact Moving Barrier Weight," MGA Report No. G9-003-V-1, October 1979.
4. "Research Safety Vehicle - Phase II - Fifth Status Report," Contract No. DOT-HS-5-01214, 16 March to 15 May 1976.
5. D. A. Alianello, "Improved Lightweight Subcompact Side Structure Test Report - Baseline Static Crush Test No. 5," Calspan Report No. 6225-V-5, April 1978.

## APPENDIX A

### SPRING-MASS DYNAMICS SIMULATION (SMDYN)

SMDYN is a rather simple (in concept) computer program that treats a physical automobile structure as a one-dimensional representation, idealized in the form of discrete (lumped) masses interconnected by massless, deformable elements characterized by force-deflection properties. The model is general in nature allowing a large number of discrete masses with totally flexible connectivity. Each specific application requires the definition of lumped masses and resistive elements to approximate the physical characteristics of the structural system under consideration. Figure 1, for example, illustrates a typical modeling approach for simulation of an automobile impacting a rigid barrier.

The program is implemented in the BASIC computer language and inputs required include the magnitude, initial displacement and velocity of each discrete mass, and a definition of the connectivity and force-deflection properties (for both loading and unloading) of each resistive element. Schematic diagrams of various collision models typically studied are shown in Figure 2.



MASSES

- M1 - TOTAL CAR LESS M2 AND M3
- M2 - ENGINE AND TRANSMISSION
- M3 - FRONT CROSSMEMBER, TIRES, SUSPENSION, AND WHEELS

DIMENSIONS

- 1 - FRONT OF RAILS
  - 2 - REAR OF RAILS
  - 3 - FRONT SHEETMETAL
  - 4 - DRIVELINE
  - 5 - DASH
  - 6 - RADIATOR
  - 7 - ENGINE MOUNTS - FWD.
  - 8 - ENGINE MOUNTS - RWD.
  - 9 - TRANS. MOUNTS - FWD.
  - 10 - TRANS. MOUNTS - RWD.
- A - FRONT SHEETMETAL TO BARRIER
  - B - REAR OF ENGINE TO DASH PANEL
  - C - FRONT OF ENGINE TO BARRIER

Figure 1 SCHEMATIC OF FRONT STRUCTURAL MODEL

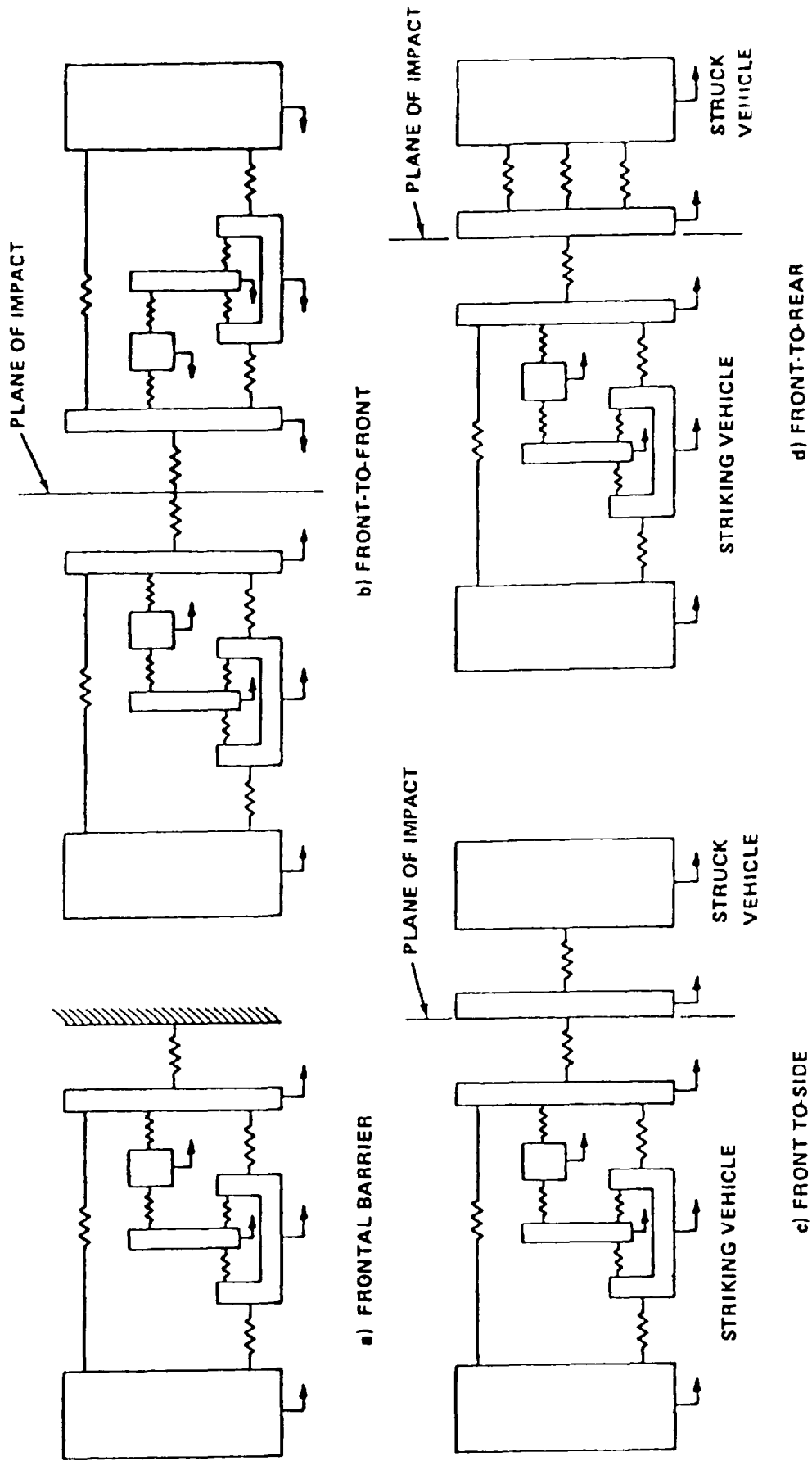


Figure 2 SCHEMATIC OF ONE-DIMENSIONAL VEHICLE STRUCTURE COLLISION MODELS

Force-deflection properties of specific resistive elements can be obtained by static crush testing of the corresponding physical structures. Crush testing techniques have been developed that facilitate isolation, proper collapse mode control and measurement of the force-deflection properties of various automotive structural elements

The program itself accepts such empirically developed force-deformation characteristics in a tabular format, thus allowing a general loading curve consisting of a number of force-deflection coordinates. An unloading curve is also specified for each resistive element in the form of three unloading slopes (Figure 3). The unloading path is automatically constructed based on the point at which unloading is initiated. If reloading takes place, the unloading curve is retraced back to the primary loading curve which is then used thereafter. Cyclical loading/unloading is also considered. If this does occur, the unloading path shifts parallel to the deflection axis consistent with the most recent point of zero deflection rate. The general nature of the unloading path allows consideration of elements that allow only compression (e.g., the bumper structure) or elements that are physically capable of developing tension forces (e.g., the frame rails).

Since automobile collisions are obviously dynamic events and automotive structural materials are known to be strain rate sensitive, methods of accounting for dynamic overstress are incorporated into the model. Based on the work of kamal and others, overstress (rate) factors in the neighborhood of 1.3 or 1.4 have been found to produce reasonable correlation between static and dynamic test data for collision velocities around 30 MPH.

The SMDYN program provides the user with a choice of 5 dynamic load factors which are consistent with the nominal overstress magnitudes indicated above. A description of each load factor is given below.

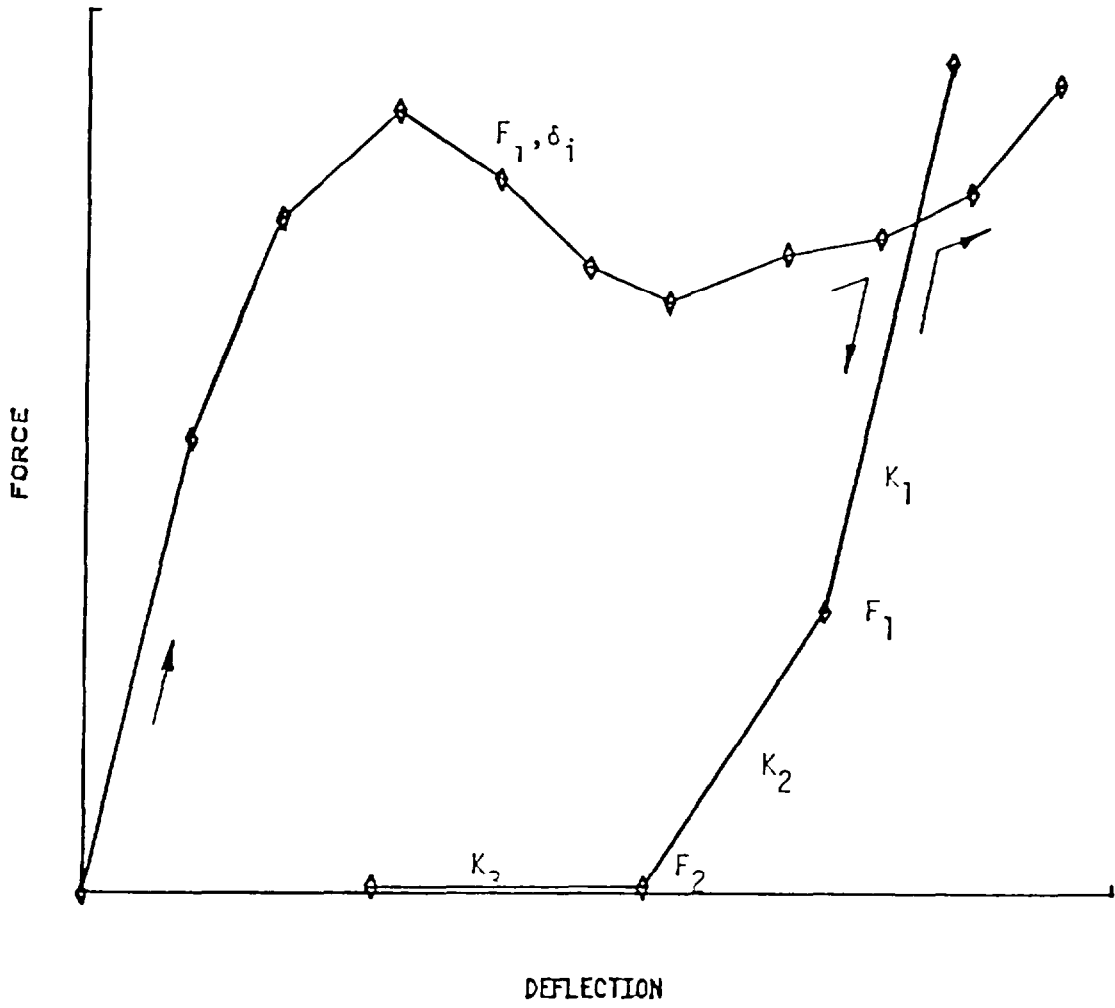


Figure 3 ILLUSTRATION OF RESISTIVE ELEMENT INPUT PROPERTIES

TYPF 1 - Logarithmic

The dynamic load factor is calculated using the following relationship

$$DLF = 1.27228 + .0197119 \times \text{LOG (INSTANTANEOUS CRUSH RATE)}$$

TYPL 2 - Logarithmic

This logarithmic load factor is calculated using the following relationship

$$DLF = 1.0957 + .075 \times \text{LOG (MAX. CRUSH RATE ENCOUNTERED)}$$

Due to the fact that the maximum crush rate encountered is used to calculate the DLI, this load factor can only increase or remain constant.

TYPI 3 - Quartic

The general quartic equation shown below can be used to calculate this dynamic load factor

$$DLF = A + B (\text{CRUSH RATE}) + C (\text{CRUSH RATE})^2 \\ + D (\text{CRUSH RATE})^3 + E (\text{CRUSH RATE})^4$$

The 5 coefficients are specified by the user and the crush rate used is the absolute value of the instantaneous crush rate of the energy absorber. Modification of the force deflection curve by a fixed amount can be accomplished by setting "A" to the desired magnification, and setting the remaining constants to zero.

TYPE 4 - Dynamic Load Factor Based on Material Properties  
and Test Strain Rate

Research for this load factor was performed at Ford Motor Company. Material properties and strain rate effects are used in calculating this factor as shown below

$$DLF = A + KR * \ln (CR/SCR)$$

where A is constant, usually 1.0

KR is a material factor

CR is the absolute value of the instantaneous crush rate

SCR is the crush rate of the test specimen, usually  
.03333"/sec.

TYPE 5 - Quartic DLF with Different Crush Rate

This DLF is identical to Type 3, but the crush rate is determined from the velocity difference between two selected masses.

An example of the Type 1 dynamic load factor is shown in Figure 4

Output from the simulation consists of a) a concise listing of all input parameters, b) acceleration, velocity and displacement time histories for each discrete mass, c) force and deflection time histories for each resistive element, d) maximum value of acceleration for each mass, and e) maximum value of deflection for each resistive element.

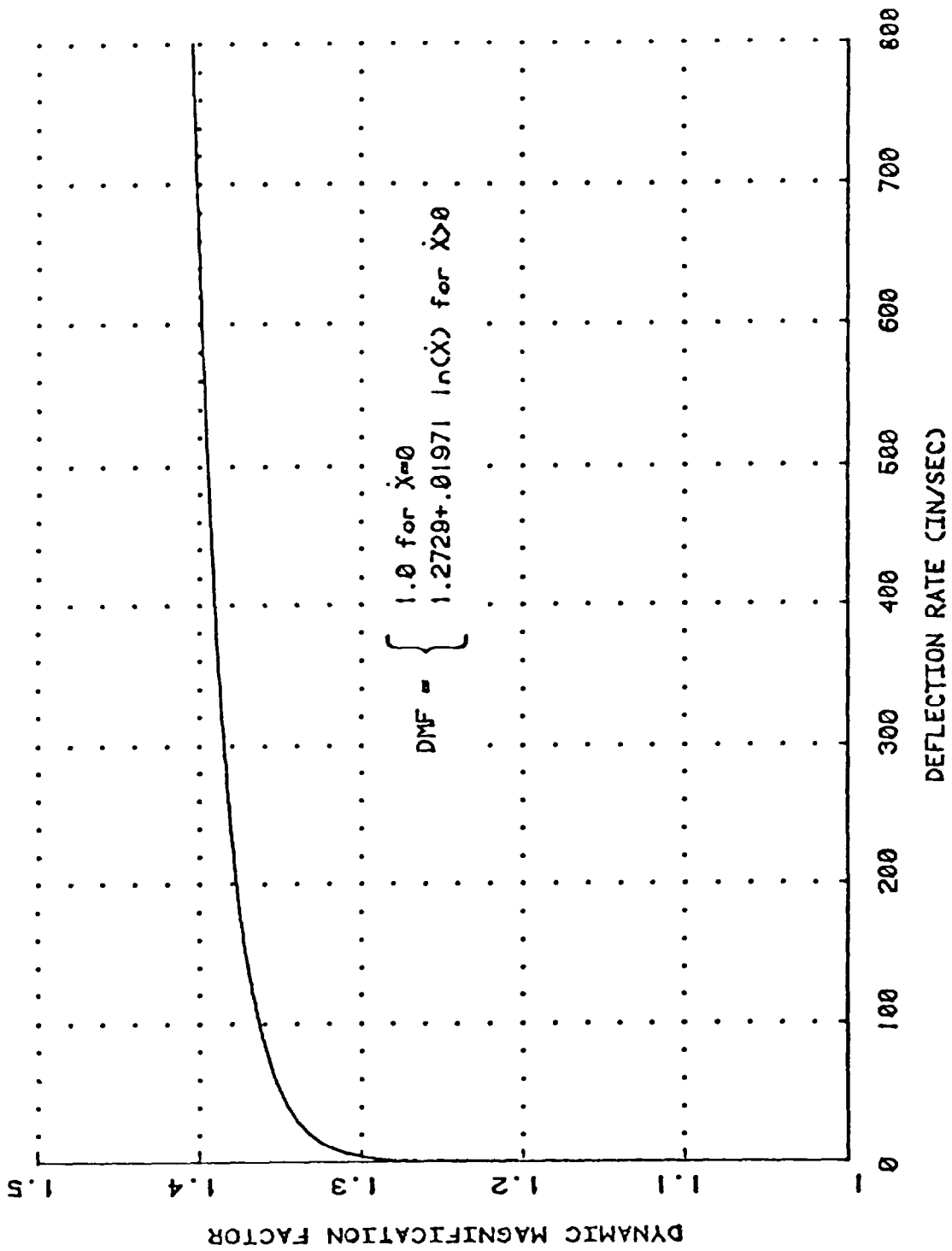


Figure 4 DYNAMIC OVERSTRESS FACTOR USED IN MODEL

## APPENDIX B

### AUTOMOBILE FRONTAL STRUCTURE FORCE-CRUSH CHARACTERISTICS

Structural information compiled under this program is presented in this Appendix. Unless otherwise noted, impact tests were made at 35 MPH into a rigid, perpendicular barrier. In the 30 degree tests, the test vehicle was oriented at the indicated angle to the direction of motion of force measuring moving barrier. Included on the following plots are simple two parameter fits to the force-crush information. Coefficients for these fits were given previously in Tables 2 and 3 of this report.

